Mineral. Deposita (Berl.) 9, 339—356 (1974)

U—Th—Pb Isotope Systematics Related to Igneous Rocks and Ore Pb, Mount Isa, Queensland

R. B. FARQUHARSON
University of Calgary, Calgary, Alberta, Canada

J. R. RICHARDS
Research School of Earth Sciences, Australian National University, Canberra, A.C.T., Australia

This study is a search for a genetic relationship between Pb sulphide ore and igneous rocks in the region of Mount Isa, Queensland. The approach involves derivation of Pb isotope initial ratios by the whole-rock isochron method, and comparison of the initial ratios (Pb^{206}/Pb^{204}, Pb^{207}/Pb^{204} and Pb^{208}/Pb^{204}) with the isotopic composition of the ore Pb. Data are reported for four igneous units; Kalkadoon granodiorite, Kalkadoon adamellite, Sybella granite and Eastern Creek volcanics. The results display considerable scatter for each of the units, and reveal the effects of recent surficial loss of U. The positioning of isochrons is aided by previous Rb—Sr geochronological data wherever possible. Comparison of initial ratios and ore Pb suggests that none of the igneous rock units is co-genetic with the ore deposit. Both phases of the Sybella Granite are more radiogenic and are apparently younger than the ore Pb. The Kalkadoon Granite is possibly related to the ore through some post-emplacement process of extraction and transport of Pb (e.g. by erosion or by anatectic magma generation) to the present site of the orebodies.

Introduction

Over the years the lead-zinc-silver mineralization at Mount Isa, Queensland, has supported considerable geological enquiry and controversy over such matters as mode of origin, source of metals, and time of mineralization. KNIGHT (1953), FISHER (1960), MURRAY (1961), HEWETT and SOLOMON (1964) and BENNETT (1965) typify the consensus which holds that the orebodies are syngenetic. If this is true, the question of time of the mineralization converts to one of stratigraphy, and as such is actively being pursued by a number of workers.

The source of the metals is an elusive problem which has been attacked largely through conjecture based on geological inferences and temporal variations in philosophy In a search for measurable constraints, we find some potential in Pb isotopes used as geochemical tracers. An isotopic match between Pb-in-ore and the Pb of a geologically suitable source unit lends credence to a proposed relationship. Conversely and perhaps more strongly, an isotopic mismatch contributes by the process of elimination to a narrowing of alternatives.

Mount Isa ore-Pb was one of the set of world-wide volcanic-associated sulphide deposits used by STANTON and RUSSELL (1959) in the presentation of their "single-stage" isotope development model, which has generally been taken to invoke the mantle as the immediate source of the Pb. On this basis the calculated model age for Mount Isa Pb comes to 1600 m.y. (RICHARDS 1963), or 1500 m.y., according to the parameters more recently suggested by COOPER *et al.* (1969). Subsequent appraisal of regional structural deformation in relation

to the timing of plutonic events suggested that the strata enclosing the orebodies are at least 150 m.y. older than the Pb model age (FARQUHARSON and WILSON 1971). This observation was one of the arguments used by RICHARDS (1971) to question both the single-stage model and the mantle origin hypothesis for many orebodies, including Mount Isa. We must then entertain the possibility that the ore-Pb development was much more complicated than envisaged by STANTON and RUSSELL, and that the process has involved rocks which are now accessible to observation

The aim of this study has been twofold. We have attempted to measure the ages of several igneous rock units in the region of Mount Isa, by the method of U-Pb and Th-Pb isochrons We have then compared the initial Pb ratios, estimated from the isochrons, with ore-Pb values in a search for possible linkages between them. We must emphasize the preliminary nature of the conclusions which we have been able to draw. As indicated in the next section, the minimal number of samples has been analyzed, from locations which often are widely spaced, and where the correlations are based on mapping which leaves ample room for uncertainty. Under these circumstances the search must be for the broad outlines of discernible trends.

Background

The geology of the Mount Isa region is described in detail by CARTER *et al.* (1961) and has recently been summarized by FARQUHARSON and WILSON (1971). The lead-zinc-silver orebodies are contained in the Urquhart Shale formation of the Mount Isa Group, a sequence of shales and siltstones which form the youngest unit in the local (?) Lower Proterozoic section (BENNETT 1965). The base of the section is the Leichhardt Metamorphics, a unit which comprises moderately to highly metamorphosed dacitic and rhyolitic lavas, plus large quantities of schist and gneiss. Progressing upwards, the section includes the Argylla Formation, a sequence of acid metavolcanics; Mount Guide Quartzite; Eastern Creek Volcanics, a sequence of basic volcanics with intercalated lenses of quartzite; Myally Beds and equivalent Judenan Beds, comprising siltstones, sandstones and conglomerates; and the Mount Isa Group and equivalent Mingera Beds and Surprise Creek Beds. Fig. 1 is a generalized geologic map with sample locations.

The three units investigated in this study are the Kalkadoon Granite, the Sybella Granite and the Eastern Creek Volcanics. Both granitic units are composite batholiths which regrettably have not yet been described petrologically or structurally in detail. Random and widely-spaced sampling, with the optimistic hope of co-genesis and original isotopic homogeneity, has led to derivation of Rb-Sr isochron ages by FARQUHARSON and WILSON (1971), and to the results reported herein. So far, the Rb-Sr data indicate that the Kalkadoon Granite could be as much as 1930 m.y. old, and that a western marginal adamellite phase which includes the Ewen Granite is about 1785 m.y. old. The Sybella Granite is about 1655 m.y. old, and contains subsequent microgranite and pegmatite phases dated at about 1550 m.y. (FARQUHARSON and RICHARDS 1970a and 1970b).

It is not easy to place the plutonic events correctly within the volcano-sedimentary sequence. Attempts to assign an approximate time of deposition of the Mount Isa Group (and hence the ore bodies) have been frustrated by structural complexities in the region, and by lack of contact exposures between the sedimentary host and datable igneous rock units. The few exposed contacts between batholiths and other units are ambiguous, deemed variously to be intrusive or unconformable (eg. Sunday Gully — location GA 379, CARTER *et al.* 1961). The recent suggestion by FARQUHARSON and WILSON (1971) that the Mount Isa Group may be pre-Kalkadoon Granite has been rescinded in the light of recent (unpublished) observations by Australian Bureau of Mineral Resources geologists (WILSON 1973). Evidence from newly mapped unconformities and from granitic boulders in conglomerates, suggests that the Mount Guide Quartzites and overlying strata have a maximum age of about 1785 m.y., the time of intrusion of Kalkadoon adamellite. Based on truncation of regional foliation in the Mount Isa Group by the Sybella Granite, the minimum age for the Mount Guide Quartzite — Mount Isa Shale sequence

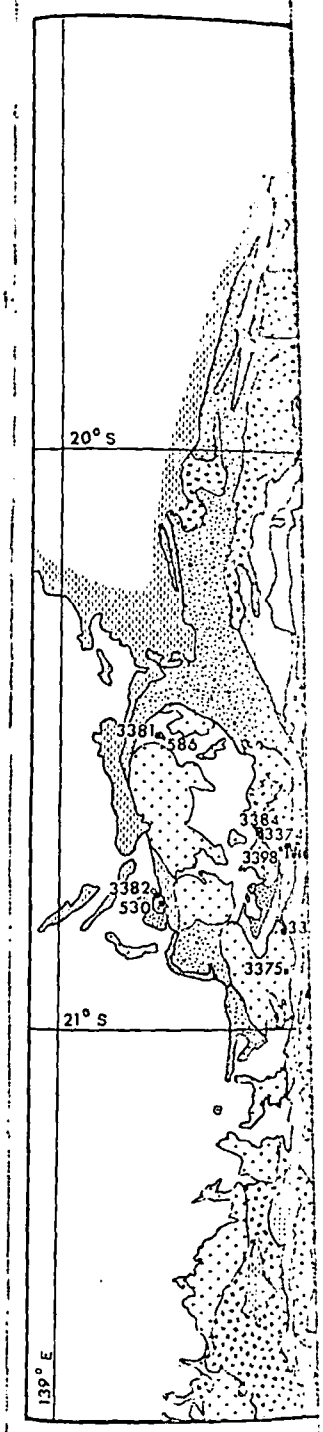

Fig. 1. General geology of t
sample locations. Broadly equ

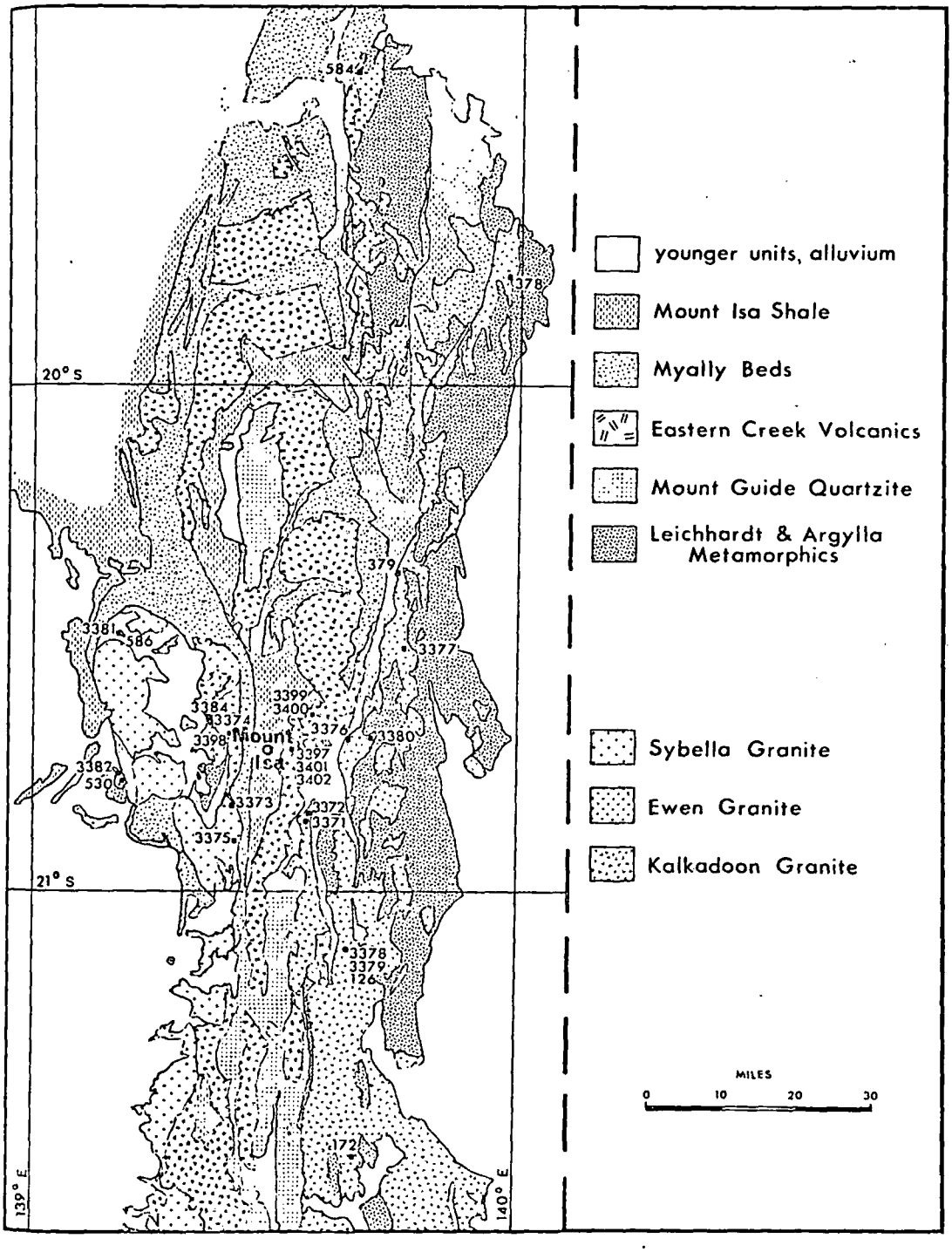

Fig. 1. General geology of the Mount Isa region, adapted from Carter, *et al.*, 1961. Black dots mark sample locations. Broadly equivalent units are grouped under the formation names in the legend (see text)

is 1655 m.y. (WILSON and FARQUHARSON 1972). Accordingly, the Eastern Creek Volcanics and the Mount Isa orebodies appear to have been deposited some time in the interval, 1785 m.y. to 1655 m.y.

Whole-rock Isotopic Studies

The application of the whole-rock isochron method to the Rb-Sr decay system has proved to be a very successful approach to the dating of rocks. After an initial lag caused in part by the much greater experimental difficulties, the U-Pb and Th-Pb analogues have recently been gaining increased attention (ROSHOLT *et al.* 1973; GALE 1973). The evidence is that these systems can yield what appears to be valid ages (ULRYCH and REYNOLDS 1966; ROSHOLT *et al.* 1970; FARQUHARSON and RICHARDS 1970), but with what seems to be a greater susceptibility to open-system behaviour (ROSHOLT *et al.* 1969; BLACK and RICHARDS 1973).

Previous whole-rock isotopic results from the Mount Isa region are summarized as follows. RICHARDS (1966) reported Rb-Sr ages of 1760 m.y. for the Kalkadoon Granite and 1600 m.y. for the "old phase" of the Sybella Granite, respectively (no uncertainty limits given). FARQUHARSON and WILSON (1971) subsequently revised these ages to 1930 ± 51 m.y. for the Kalkadoon granodiorite and 1656 ± 21 m.y. for the main Sybella Granite. MCDOUGALL *et al.* (1965) derived an age of 1780 ± 20 m.y. for a single sample of Ewen Granite, and FARQUHARSON and WILSON (1971) suggested that the Ewen Granite may be related to western marginal Kalkadoon adamellite on an isochron of 17.88 ± 8 m.y. FARQUHARSON and RICHARDS (1970a) reported concordant Rb-Sr and U-Th-Pb isochrons for the Sybella microgranite and pegmatite, as follows:

(a) Rb^{87}-Sr^{87}; 1554 ± 29 m.y.
(b) U^{238}-Pb^{206}; 1573 ± 161 m.y.
(c) U^{235}-Pb^{207}; 1576 ± 343 m.y.
(d) Th^{232}-Pb^{208}; 1555 ± 146 m.y.

Thus the evidence is that this small section of crust may have experienced up to four intrusive episodes; the Sr initial ratios (see FARQUHARSON and WILSON 1971) provide evidence for considerable reworking of upper-level material. In contrast then to magmas generated in the deep crust or mantle, it seems possible that a strictly homogeneous initial ratio for each intrusive may not be obtained.

Experimental Method

Samples of approximately 1 to 5 kilograms were hammered from surface outcrop with the exception of three; GA 3381, GA 3378 and GA 3379 which were selected from sites previously blasted by the Bureau of Mineral Resources. The samples were reduced in a jaw crusher and "Sieb" mill, and from each, 10 to 12 grams of powder was dissolved by the conventional HF-$HClO_4$ treatment. U and Th were separated by the hexone solvent extraction method (TILTON *et al.* 1955) and Pb was isolated by the barium-nitrate co-precipitation and dithizone extraction method of TATSUMOTO (1966). Measured U and Th blanks were negligible, whereas the Pb blank was high (2.1 micrograms, of isotopic composition, $204 : 206 : 207 : 208 = 1 : 17.80 : 1577 : 37.60$). Pb contamination ranged from about 0.6 to 2.7 percent of sample Pb.

Concentrations of U, Th and Pb were measured by isotope dilution, using isotopically enriched U^{235} and Th^{230} tracers and a Pb^{207}-Pb^{204} double-spike (COMPSTON and OVERSBY 1969). U and Th were loaded together as phosphates on the side filaments of a rhenium triple-filament assembly, and Pb was loaded as oxalate on a single rhenium filament (COOPER and RICHARDS 1966). All analyses were performed in the Department of Geophysics and Geochemistry, Australian National University on a N.A.A. "Nuclide", 12-inch radius of curvature, 60° sector single-focusing spectrometer with a modified Craig-type source; peaks were switched by magnet current selection. At the time the work was done, the Pb calibrations were being normalized to the "Kollar values" of the U.B.C. No. 1 Broken Hill Pb standard (COOPER and RICHARDS 1966). The results presented here have not been normalized to the equal-atom Pb standard of CATANZARO *et al.* (1968).

Although the Pb double-spike is intended to provide a correction for isotopic fractionation during analysis, we encountered difficulties. For reasons not entirely apparent, some "corrected" Pb isotope analyses were sufficiently far removed fr values, to be obviously causes include accidental casional poor spectrom hydrocarbon interference. of subjective evaluation "corrected" values are va be disqualified. The scatte improved by the use of corrected values. They h rejected *in toto*, and the unc been used, with due allow in fractionation. An u analysis of the C.I.T. s follows: 204:206:207:20 37.02, which is in good mean of 5 measurements (1 reported by COOPER and COOPER and RICHARDS' (1 oxalate method yielded (95% confidence) of ab 206/204 ratio, and isotopic order of 0.25 percent for t 0.5 percent for the 208/ isolated from rock samples purify. Thus for our grai measured 2σ of the 206/20 percent, ranging from 0. For the volcanic rocks the ment was generally lower. In assigning uncertainty to in Figs. 2, 3 and 4, a frac percent was added to the measurement precision. was multiplied by 1.5 uncertainty estimates for 2 respectively. The uncert ratios was arbitrarily take value, and of the Th/Pb duplicate analysis of 337 within these error limits,

Results

Analyses for twenty whol one mineral separate (337 Table 1. The data are plot for the Kalkadoon Gran and Eastern Creek Volca each figure, the lower h laysen" diagrams (NICO three parent-daughter sys

:p crust or mantle, it seems
ictly homogeneous initial
sive may not be obtained.

hod

ıately 1 to 5 kilograms were
urface outcrop with the
GA 3381, GA 3378 and
were selected from sites
by the Bureau of Mineral
nples were reduced in a
ieb" mill, and from each,
wder was dissolved by the
ClO_4 treatment. U and
by the hexone solvent
(TILTON *et al.* 1955) and
he barium-nitrate co-preci-
ne extraction method of
Measured U and Th blanks
ereas the Pb blank was
, of isotopic composition,
= 1 : 17.80 : 1577 : 37.60).
nged from about 0.6 to
e Pb.

Th and Pb were measured
, using isotopically en-
230 tracers and a Pb^{207}-
(COMPSTON and OVERSBY
were loaded together as
de filaments of a rhenium
ply, and Pb was loaded as
henium filament (COOPER
). All analyses were per-
tment of Geophysics and
alian National University
lide", 12-inch radius of
single-focusing spectro-
ified Craig-type source;
ed by magnet current
the work was done, the
being normalized to the
ıe U.B.C. No. 1 Broken
PER and RICHARDS 1966).
d here have not been
ual-atom Pb standard of
8).
ıble-spike is intended to
or isotopic fractionation
encountered difficulties.
ntirely apparent, some
ope analyses were suf-

ficiently far removed from the uncorrected values, to be obviously in error. Possible causes include accidental contamination, occasional poor spectrometric resolution, or hydrocarbon interference. It is thus a matter of subjective evaluation to decide which "corrected" values are valid and which are to be disqualified. The scatter in the data is not improved by the use of these double-spike corrected values. They have therefore been rejected *in toto*, and the uncorrected values have been used, with due allowance for uncertainties in fractionation. An uncorrected isotopic analysis of the C.I.T. shelf standard is as follows: 204:206:207:208 = 1:16.79:15.71:37.02, which is in good agreement with the mean of 5 measurements (1:16.78:15.71:36.99) reported by COOPER and RICHARDS (1966). COOPER and RICHARDS (1966) found that the oxalate method yielded measurement error (95% confidence) of about 0.1% for the 206/204 ratio, and isotopic fractionation on the order of 0.25 percent for the 206/204 ratio and 0.5 percent for the 208/204 ratio. The Pb isolated from rock samples is more difficult to purify. Thus for our granitic rocks the mean measured 2σ of the 206/204 ratio was about 0.25 percent, ranging from 0.06 to 0.67 percent. For the volcanic rocks the precision of measurement was generally lower.

In assigning uncertainty to the values as plotted in Figs. 2, 3 and 4, a fractionation error of 0.5 percent was added to the 2σ value of 206/204 measurement precision. The resulting value was multiplied by 1.5 and 2.0 to obtain uncertainty estimates for 207/204 and 208/204, respectively. The uncertainty of the U/Pb ratios was arbitrarily taken to be $\pm 3\%$ of the value, and of the Th/Pb ratio, $\pm 5\%$. The duplicate analysis of 3374 (see Table 1) falls within these error limits, for all ratios.

Results

Analyses for twenty whole-rock samples plus one mineral separate (3375M) are presented in Table 1. The data are plotted in Figs. 2, 3 and 4 for the Kalkadoon Granite, Sybella Granite and Eastern Creek Volcanics respectively. In each figure, the lower half exhibits "Nicolaysen" diagrams (NICOLAYSEN 1961) for the three parent-daughter systems; the upper half shows the corresponding Pb–Pb diagrams. (Pb^{208}/Pb^{204} and Pb^{207}/Pb^{204} versus Pb^{206}/Pb^{204}. The linear (isochron) regressions reported in the text are based on the Model I treatment of MCINTRYE *et al.* (1966) for parent-daughter isochrons, and on the Model II treatment of YORK (1969) for the Pb–Pb isochrons. Confidence limits are reported as one standard deviation; decay constants are those recommended by STIEFF *et al.* (1959).

Kalkadoon Granite

The Kalkadoon Granite samples can be categorized as follows:

a) coarse granodiorite — probably the best representative of the main intrusive phase; samples 3377, 3378 and 3379,

b) gneissic granodiorite; 3380,

c) marginal adamellite; 3371 and 3376,

d) sheared marginal granodiorite; 3372,

e) hybrid chloritized marginal granodiorite; 379.

In the ensuing discussion we follow the results of the Rb–Sr analysis of these samples (FARQUHARSON and WILSON 1971) in treating the marginal rocks (c, d and e; age 1785 m.y.) as distinct from, and younger than the remainder (a and b; age 1930 m.y.). This leads us to expect two isochrons on each diagram of Fig. 2, each of slope appropriate to one of the ages. Departures from this are the likely result of open system behaviour (the depth of the weathering profile suggests that recent disturbance of the system is distinctly possible).

As an added constraint, and aid in the assessment of what is believable, we note that the initial ratios should not be too different from values which fit a lead growth curvey similar to that observed for major orebodies (Ostic *et al.* 1967) and which we, by extrapolation, would wish to ascribe to an average terrestrial system (RICHARDS 1971). For such a system the average U^{238}/Pb^{204} (μ) should be close to 9 (KANASEWICH and FARQUHAR 1965), and hence a Kalkadoon Granite which is not abnormally deviant from terrestrial average should yield intercepts on the Nicolaysen diagram within the vicinity of $Pn^{206}/Pb^{204} = 16$, $Pb^{207}/Pb^{204} = 15.5$, and $Pb^{208}/Pb^{204} = 36$.

Table 1. U—Th—Pb *analyses for Kalkadoon granite, Sybella granite and Eastern Creek Volcanics, Mount Isa*

G. A. No.	U[a]	Th[a]	Pb[a]	U^{238}/Pb^{204}	U^{235}/Pb^{204}	Th^{232}/Pb^{204}	Pb^{206}/Pb^{204}	Pb^{207}/Pb^{204}	Pb^{208}/Pb^{204}
Kalkadoon granite									
3371	0.02482	0.1289	0.1547	13.70	0.0994	71.71	23.77 ± 0.14	16.40 ± 0.14	41.06 ± 0.48
3372[b]	0.00332		0.06671	3.46	0.0251		16.88 ± 0.10	15.59 ± 0.14	37.45 ± 0.44
3376	0.01825	0.06931	0.09973	15.11	0.1096	57.79	24.74 ± 0.29	16.49 ± 0.29	41.84 ± 0.98
3377	0.00698	0.07543	0.07389	7.65	0.0555	83.24	20.53 ± 0.12	16.21 ± 0.15	45.03 ± 0.54
3378	0.02101	0.08943	0.1502	10.82	0.0785	46.38	20.26 ± 0.24	16.15 ± 0.28	41.29 ± 0.97
3379	0.03923	0.2886	0.2319	14.14	0.1026	104.8	20.81 ± 0.13	16.30 ± 0.15	47.01 ± 0.57
3380	0.04446	0.1742	0.2770	14.89	0.1081	58.77	32.81 ± 0.34	17.62 ± 0.28	43.05 ± 0.90
379	0.01281	0.06888	0.06115	16.95	0.1232	91.94	22.49 ± 0.15	16.10 ± 0.15	43.25 ± 0.56
Sybella granite									
3373	0.03035	0.1054	0.1677	14.12	0.1025	49.41	21.24 ± 0.13	16.14 ± 0.15	41.42 ± 0.52
3374(i)	0.03086	0.1531	0.1564	15.84	0.1149	79.13	21.51 ± 0.13	16.15 ± 0.15	43.42 ± 0.52
3374(ii)	0.03080	0.1551	0.1587	15.68	0.1138	79.50	21.65 ± 0.15	16.23 ± 0.17	43.71 ± 0.61
3375	0.02640	0.1366	0.1365	15.86	0.1151	82.68	21.58 ± 0.15	16.44 ± 0.17	44.81 ± 0.61
3375M[c]							16.74 ± 0.10	15.67 ± 0.14	36.94 ± 0.43
3381	0.03250	0.1135	0.1326	20.08	0.1457	70.74	22.77 ± 0.19	16.35 ± 0.20	43.77 ± 0.72
3382	0.01785	0.1166	0.08106	18.82	0.1366	123.9	23.30 ± 0.24	16.37 ± 0.26	46.73 ± 0.98
3384	0.03099	0.09948	0.1434	17.25	0.1252	55.79	21.84 ± 0.13	16.28 ± 0.14	42.18 ± 0.49
586	0.02589	0.09602	0.1796	11.14	0.0808	41.61	20.82 ± 0.19	16.36 ± 0.22	40.83 ± 0.73
Eastern Creek Volcanics									
3397	0.01230	0.03793	0.1050	8.61	0.0624	26.93	19.26 ± 0.44	16.04 ± 0.55	38.79 ± 1.78
3399	0.00589	0.02544	0.2043	2.00	0.0145	8.70	16.82 ± 0.10	15.76 ± 0.14	37.31 ± 0.45
3400	0.00581	0.02050	0.2027	1.97	0.0143	5.37	16.74 ± 0.12	15.59 ± 0.17	36.82 ± 0.52
3401	0.00343	0.02035	0.05667	4.39	0.0318	26.23	18.35 ± 0.28	15.81 ± 0.36	38.68 ± 1.17
3402	0.01814	0.07089	0.07894	18.64	0.1353	73.37	22.07 ± 0.26	16.35 ± 0.28	43.17 ± 1.00

[a] micromoles/gram. [b] Th run failed. [c] acid-washed microcline separate.

All trends in Fig. 2 show
The regression line is
very poor approximation
have chosen therefore
ratios by drawing a line
by the Rb—Sr age, thro
seem to be the least
attempt to defend our c
paragraphs.

1. Kalkadoon Granodiorite

The material, dated by
is represented by the

Fig. 2.
Isochron
then pro
(μ = 9;
for refer

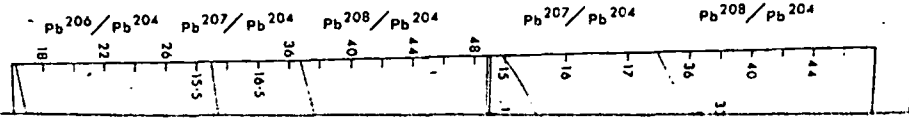

Eastern Creek Volcanics								
3397	0.01230	0.03793	0.1050	8.61	0.0624	26.93	19.26 ± 0.44	16.04 ± 0.55	38.79 ± 1.78
3399	0.00589	0.02544	0.2043	2.00	0.0145	8.70	16.82 ± 0.10	15.76 ± 0.14	37.31 ± 0.45
3400	0.00581	0.02050	0.2027	1.97	0.0143	5.37	16.74 ± 0.12	15.59 ± 0.17	36.82 ± 0.52
3401	0.00343	0.02035	0.05667	4.39	0.0318	26.23	18.35 ± 0.28	15.81 ± 0.36	38.68 ± 1.17
3402	0.01814	0.07089	0.07894	18.64	0.1353	73.37	22.07 ± 0.26	16.35 ± 0.28	43.17 ± 1.00

[a] micromoles/gram. [b] Th run failed. [c] acid-washed microcline separate.

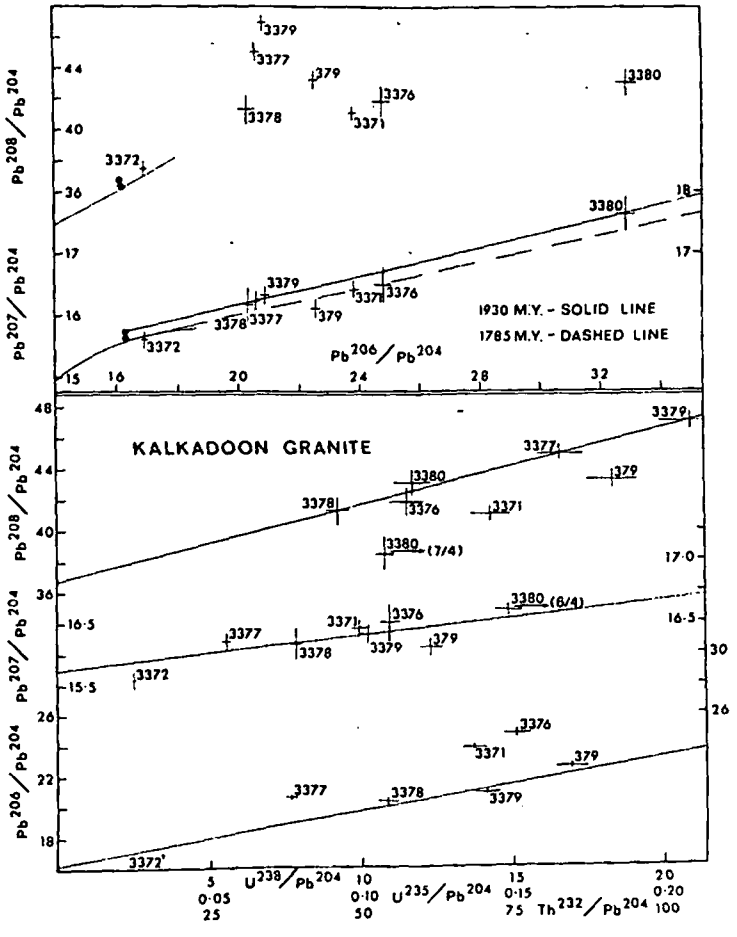

Fig. 2. U–Th–Pb isotopic plot for Kalkadoon Granite data. Isochrons in the „Nicolaysen" diagrams yield initial ratios which then provide the origin for the Pb–Pb isochron. Growth curves ($\mu = 9$; $K = 3.95$) and the Mount Isa ore Pb values are shown for reference

All trends in Fig. 2 show considerable scatter. The regression line is probably therefore a very poor approximation to the isochron. We have chosen therefore to estimate the initial ratios by drawing a line, of slope determined by the Rb–Sr age, through the points which seem to be the least perturbed. We shall attempt to defend our choice in the following paragraphs.

1. *Kalkadoon Granodiorite*

The material, dated by Rb–Sr at 1930 m.y., is represented by the three granodiorite samples 3377, 3378 and 3379, and the gneissic granodiorite 3380. Support for this age is provided by the regression line on the lower Pb–Pb diagram (upper half of Fig. 2). Treated as a secondary isochron, its slope yields an age 1914 ± 47 m.y. It might be argued that this result depends heavily upon sample 3380, which as we see below is somewhat suspect. However essentially the same age may be deduced, independently of this sample, from the Th–Pb Nicolaysen diagram (upper line, bottom half of Fig. 2). In this, the three granodiorite samples alone yield an isochron of

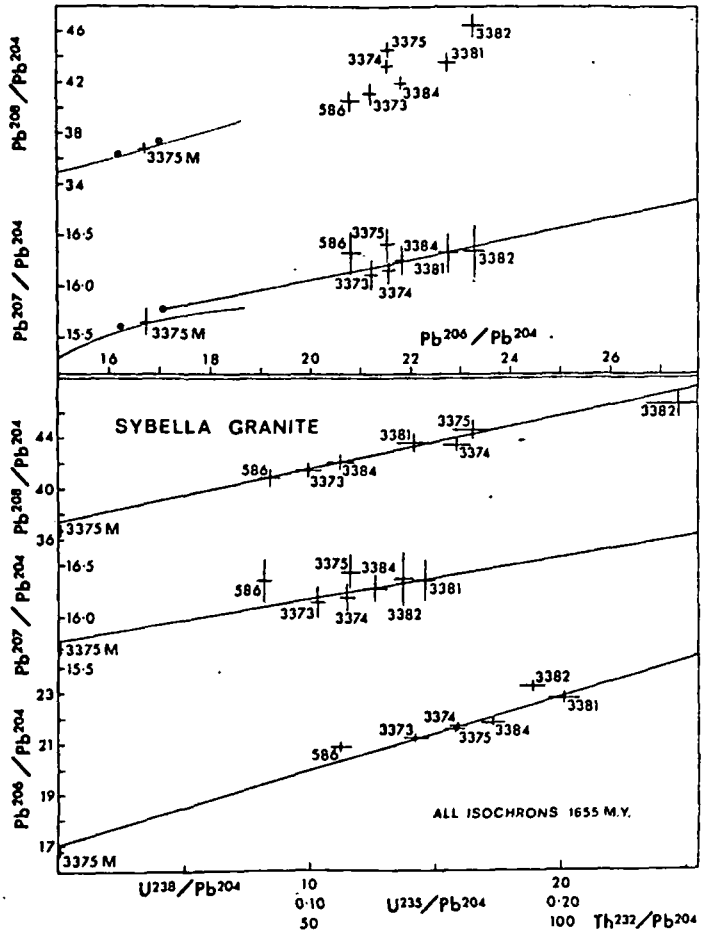

Fig. 3. U—Th—Pb isotopic plot for Sybella Granite data. Isochrons in the "Nicolaysen" diagrams yield initial ratios which then provide the origin for the Pb—Pb isochron. Growth curves ($\mu = 9$; K = 3.95) and the Mount Isa ore Pb values are shown for reference

slope 1923 ± 114 m.y., with a "reasonable" initial ratio 36.75 ± 0.45. This older age therefore merits its place in the provisional timescale.

Turning now to the two U—Pb Nicolaysen diagrams, we note that sample 3380 is excessively deviant, and must be excluded from the process of fitting a 1930 m.y. isochron. This deviance is most easily ascribed to loss of U, which must have occurred recently, since the isotopic composition of the Pb seems to have been little affected (c.f. GRAY and OVERSBY 1972). Note too that this extreme loss of U must have been accompanied by a small degree of Th loss; 3380 deviates slightly also from the Th—Pb isochron. By the same token, 3377 plots abnormally high on the two U—Pb diagrams, and may therefore also have lost some U. For this reason we choose to draw our lines of slope 1930 m.y. through the 3378 and 3379 points. The initial ratios thus derived are $^{206}Pb/^{204}Pb = 16.20$; $^{207}Pb/^{204}Pb = 15.75$. These initial ratios appear to be near correct because they satisfy our criteria for an acceptable result. It is difficult to determine whether, or to what degree, U-loss has affected

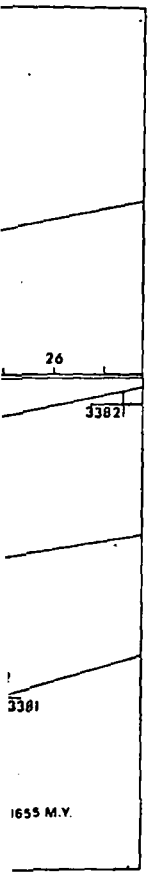

. Isochrons
hen provide
= 9; K =
eference

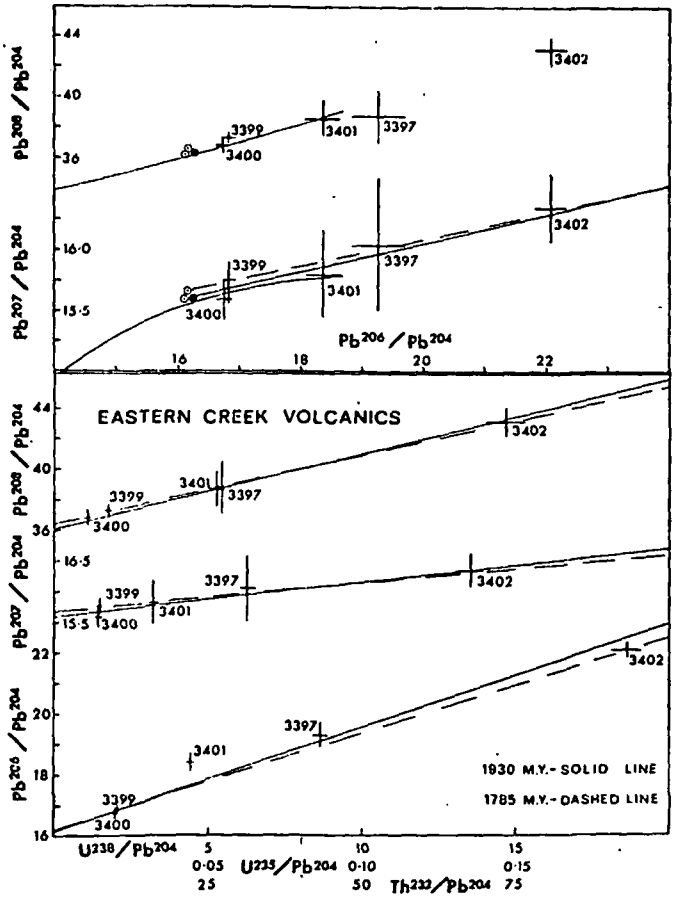

Fig. 4. U–Th–Pb isotopic plot for Eastern Creek Volcanies data. Isochrons in the "Nicolaysen" diagrams yield initial ratios which then provide the origins for isochrons in the Pb–Pb diagram. Growth curves ($\mu = 9$; $K = 3.95$) and the Mount Isa ore Pb values are shown for reference

ompanied by a small degree viates slightly also from the By the same token, 3377 high on the two U–Pb therefore also have lost eason we choose to draw 030 m.y. through the 3378 e initial ratios thus derived 6.20; $^{207}Pb/^{204}Pb = 15.75$. appear to be near correct our criteria for an ac- is difficult to determine degree, U-loss has affected even samples 3378 and 3379. We expect that the deficiency is small, but the initial ratio values must be considered upper limits. Very little can be deduced from the upper Pb–Pb diagram, except that disproportionation between U and Th in the various parts of the batholith is evident from the considerable Pb isotopic variation.

2. *Kalkadoon Marginal Adamellite*

Analogous treatment of the four samples from the western margin of the batholith is more difficult. At least three of them display anomalous behaviour, in both U and Th. Once again, the lower Pb–Pb diagram appears least affected. A line of slope 1785 m.y. (derived from the Rb–Sr data) drawn through 3371 and 3376 points, passes close the Mount Isa ore-Pb value, and close to 3372. In the U–Pb diagrams, the previous arguments would lead us to suspect that sample 3372 has been least affected by U-loss. Extrapolation from this sample along a line of slope 1785 m.y. leads to initial ratio estimates $Pb^{206}/Pb^{204} = 15.75$; $Pb^{207}/Pb^{204} = 15.46$;. These must be considered minimal. The result is questionable,

however, because this rock is sheared, and because of some uncertainty about its classification.

379 has suffered the complications of assimilation at the margin of the batholith and may therefore have had initial ratios different from average Kalkadoon adamellite (3371 and 3376). Notwithstanding that possibility, the U^{238}—Pb^{206} values project to an aberrantly high initial ratio which may be atributable to loss of U. The low Pb^{207}/Pb^{204} value may reflect mixing with more primitive Pb, as was suggested in explanation of the low Sr^{87}/Sr^{86} value (FARQUHARSON and WILSON 1971).

Sybella Granite

The Sybella Granite samples can be categorized as follows:

a) coarse-grained, main phase granite; 3373, 3374, 3375, 3384,

b) "old-phase" granite; 586, 3381,

c) marginal adamellite; 3382.

As was the case for the Kalkadoon Granite, there is significant scatter in the data. Further, the range in values is even more restricted, and meaningful regression is impossible. Once more, therefore, the slopes of the Nicolaysen isochrons (Fig. 3 lower) have been determined by the Rb—Sr data (age 1655 m.y.; FARQUHARSON and WILSON 1971) and the location of the isochron decided by a qualitative choice of what seem to be the least-perturbed data points. Initial ratios thus derived are $Pb^{206}/Pb^{204} = 17.00$; $Pb^{207}/Pb^{204} = 15.75$; $Pb^{208}/Pb^{204} = 37.40$.

In the lower Pb—Pb plot, the 1655 m.y. isochron originating from these estimated initial ratios passes centrally through all data points except for samples 586 and 3375. These latter have an apparent excess of Pb^{207}, evident in both the lower Pb—Pb and in the U^{235}/Pb^{207} diagrams. This anomaly is difficult to explain, except perhaps as an analytical error.

Support for these initial ratio estimates is provided by the microcline concentrate from 3375. In all cases the somewhat arbitrarily-chosen isochron extrapolates quite close to, but slightly above, the microline data points. If 3375 whole rock is corrected for the fractionation apparent in the Pb—Pb diagram, the whole rock — microcline tie-lines in all three parent-daughter diagrams are approximately parallel to the 1655 m.y. isochrons. Thus if we assume there has been no metamorphic resetting, it seems reasonable to regard the microcline Pb as providing a minimum estimate for the initial ratios of the Sybella Granite.

Attempts at deriving isochron ages from linear regressions are not so successful. The error limits are large because of the combination of scatter and narrow range, and the spread of apparent ages is also large, even when obviously aberrant samples are rejected. One observation is worth making in this context, in that it exemplifies the interpretational problems in this study. The preceeding discussion has perforce, for lack of data, treated all Sybella Granite samples as belonging to the one isotopic system. This is undoubtedly not correct. An extreme example is 3382, from the western flank of the batholith. It is not typical of the main Sybella Granite; its divergence from the main isotopic trend in two out of the three Nicolaysen diagrams could be interpreted as arising from a different initial ratio. The Sr system (FARQUHARSON and WILSON 1971) does not show this effect, but this may be because of its lower overall sensitivity. Particularly in the Th—Pb diagram, a regression involving 3382 would almost certainly be erroneous.

Eastern Creek Volcanics

The Eastern Creek Volcanics suite are samples of basaltic flows which have undergone low-grade regional metamorphism. When plotted (Fig. 4) the data again display significant scatter, although this time the Th—Pb diagram yields a Model 1 isochron of age 1807 ± 78 m.y., initial ratio, 36.36 ± 0.14.

In this case we do not have a Rb—Sr age, so that estimation of the other initial ratios involves a somewhat more tortuous argument. Current consensus (see RUSSELL 1972) suggests that the Eastern Creek Volcanics are younger than the Kalkadoon granodiorite, for which we suggest an age of 1930 m.y., and are probably younger than the marginal adamellite (WILSON 1973) and the Ewen Granite (1785 m.y.). Support for the younger age, which is in virtual agreement with the Th—Pb isochron, may be derived from selective treatment of the

238—Pb206 diagram; a 17
s through the extreme p
d 3402. The resulting init
en are: Pb206/Pb204 = 16.
3.68, Pb208/Pb204 = 36.41
930 m.y., drawn for compa
tio which are not so very
3.60, 36.11). The results i
as remained virtually und
ast 1800 m.y. Accordingly,
397 have lost U.
On the Pb—Pb diagram, the
nd the results so few that r
ust be regarded as unsuc
n age which appears to be
n the light of current geo
n conclusion, the data in t
ermit any firm decision
ge of the Eastern Creek
Ewen Granite, except that t
reat.

Discussion

Loss of Uranium

The results suggest that
most of the samples to vary
of the rock units. BLA
(1972) suggested that, in
circumstance, granites furth
and had lost U, possibly in
event. ROSHOLT *et al.* (19
from data on Wyoming
removal of as much as 8
original U by weathering
PLILER and ADAMS (1962)
mobility of U (and Th) in
of Boulder Batholith gra
that considerable loss was
stages of weathering.
The Mount Isa region wa
very close to the present
Late Precambrian time.
unconformably on Sybella
of Mount Isa. This leaves
about 600 m.y. ago the
could have been influenced
and isotopic remobilizatio
extreme loss of U exhibite
is not reflected in the Pb
lie on the "primary"

in all three parent-daughter
oximately parallel to the
s. Thus if we assume ther
iorphic resetting, it seems
rd the microcline Pb as
um estimate for the initial
Granite.
g isochron ages from linear
so successful. The error
use of the combination of
range, and the spread of
so large, even when ob-
mples are rejected. One
making in this context, is
e interpretational problems
preceeding discussion has
f data, treated all Sybella
belonging to the one iso-
undoubtedly not correct.
is 3382, from the western
h. It is not typical of the
e; its divergence from the
in two out of the three
s could be interpreted as
rent initial ratio. The Sr
N and WILSON 1971) does
but this may be because of
sitivity. Particularly in the
regression involving 3382
ily be erroneous.

anics

olcanics suite are samples
ich have undergone low-
morphism. When plotted
again display significant
time the Th—Pb diagram
ochron of age 1807 ± 78
.36 ± 0.14.
ot have a Rb—Sr age, so
the other initial ratios
more tortuous argument.
e RUSSELL 1972) suggests
k Volcanics are younger
ranodiorite, for which we
0 m.y., and are probably
ginal adamellite (WILSON
n Granite (1785 m.y.).
nger age, which is in
th the Th—Pb isochron.
selective treatment of the

U^{238}—Pb^{206} diagram; a 1785 m.y. isochron
s through the extreme points, 3399, 3400
d 3402. The resulting initial ratio estimates
en are: $Pb^{206}/Pb^{204} = 16.18$, $Pb^{207}/Pb^{204} = 15.68$, $Pb^{208}/Pb^{204} = 36.41$. Isochrons for
930 m.y., drawn for comparison, yield initial
tio which are not so very different (16.11,
5.60, 36.11). The results indicate that 3402
s remained virtually undisturbed for the
st 1800 m.y. Accordingly, samples 3401 and
397 have lost U.
In the Pb—Pb diagram, the scatter is so great
nd the results so few that regression attempts
ust be regarded as unsuccessful. They yield
n age which appears to be unreasonably old
n the light of current geological reasoning.
In conclusion, the data in this section do not
ermit any firm decision about the relative
ge of the Eastern Creek Volcanics and the
ewen Granite, except that the difference is not
reat.

Discussion

Loss of Uranium

The results suggest that U-loss has affected most of the samples to varying degree, in each of the rock units. BLACK and RICHARDS (1972) suggested that, in a similar isotopic circumstance, granites further east in Queensland had lost U, possibly in a recent weathering event. ROSHOLT *et al.* (1973) argue cogently from data on Wyoming granitic rocks, for removal of as much as 80 to 90 percent of original U by weathering during the Cenozoic. PLILER and ADAMS (1962), reporting on the mobility of U (and Th) in a weathered profile of Boulder Batholith granodiorite, indicated that considerable loss was apparent in the first stages of weathering.
The Mount Isa region was exposed at a level very close to the present land surface during Late Precambrian time. Cambrian strata lie unconformably on Sybella Granite to the west of Mount Isa. This leaves the possibility that about 600 m.y. ago the rocks now exposed could have been influenced by deep weathering and isotopic remobilization. However, since the extreme loss of U exhibited by 3380 (see Fig. 2) is not reflected in the Pb isotope values (these lie on the "primary" 1930 m.y. isochron), such loss should logically be a recent event, and probably the result of weathering. The Mount Isa region exhibits no evidence of instability, since Middle Proterozoic time, so that any orogenic remobilization of U, if such occurred, was restricted to the early stage in the history of the rocks; i.e. to the time of the Sybella microgranite/pegmatite intrusion. Such remobilization is not evident within the scatter of the data, particularly the Pb-isotope data. Therefore, although the effects of early isotopic remobilization, late Precambrian weathering and recent weathering may all to varying degree be reflected in the scatter of the data, it is possible to discern only the recent weathering effect. The Th—Pb isotopic system yields reasonably consistent isochrons for all three units, which suggests that there has been minimal redistribution of Th during weathering.
The following argument based on internal consistency refines the initial ratio estimate for the Kalkadoon Granodiorite. Previous reference has been made (see Results) to the observation that visually adjusted U—Pb isochrons provide a maximum estimated initial ratio because of the effects of U-loss in even the least-affected samples. If, in Fig. 2, the U^{238}—Pb^{206} isochron had been projected through GA 3379 the initial ratio would be 15.92. Horizontal projection of the points 3377, 3378, 3380 to this line would yield revised U^{238} concentrations which in turn lead to the revised values for $K(=Th^{232}/U^{238})$. As previously noted, 3380 is displaced also toward the Th-loss side of the Th—Pb isochron, so that a revised Th^{232} concentration has been estimated by lateral projection to the isochron of Fig. 2.
If the "true" K-values are known, then Pb^{208}/Pb^{204}—Pb^{206}/Pb^{204} isochrons can be determined for each sample. With samples of different K which are cogenetic and which originally shared a common Pb isotope composition (initial ratio), the individual isochrons should intersect at a point which defines the initial Pb^{208}/Pb^{204} and Pb^{206}/Pb^{204} ratios. Fig. 5 shows the intersections of the four isochrons, which lie closely scattered about the values, $Pb^{208}/Pb^{204} = 36.72$ and $Pb^{206}/Pb^{204} = 15.90$. This consistency indicates that the Th—Pb isochron is well-placed and suggests that the U^{238}—Pb^{206} isochron should project through

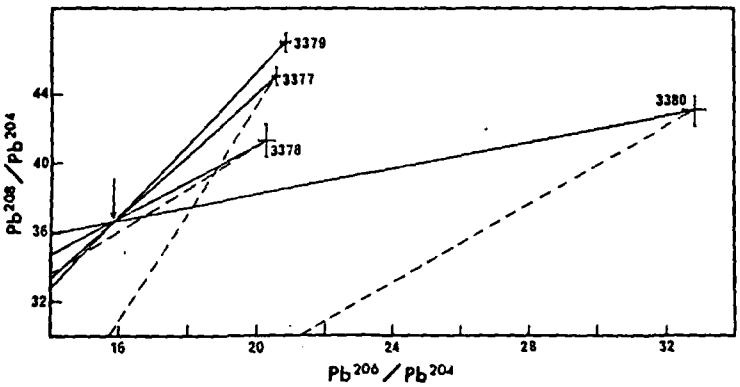

Fig. 5. Pb^{208}/Pb^{204} versus Pb^{206}/Pb^{204} plot of the four Kalkadoon granodiorite samples. Pb isotope development lines have been projected backwards from the measured (present day) values according to the Th/U ratios. The dashed lines represent isochrons for measured U concentrations, and exhibit no mutual intersection. The solid lines represent isochrons for U-loss corrected concentrations (with a Th correction applied to 3380), that intersect at a common point which is taken to be a common initial ratio

Table 2. Th *and* U *abundances*[a], *both measured and adjusted for loss; and* K(=Th^{232}/U^{238}) *values*

G.A. No.	Th	U	loss[a]	adjusted U	% loss	K
Kalkadoon Granite						
3371	29.9	5.91	5.02	10.93	~46	~1.91
3376	16.1	4.35	3.82	8.16	~47	~2.00
3377	17.5	1.66	1.53	3.91	42	6.31
3378	20.8	5.00	0.76	5.76	14	3.68
3379	66.5	9.35	—	—	—	7.41
3380	40.4	10.6	24.1	34.7	70	1.32
	(Th loss = 3.5, adjusted Th = 44.0, loss = 8.7%)					
379	16.0	3.05	—	—	—	~3.42
Sybella Granite						
3373	24.5	7.12	—	—	—	3.50
3374	35.8	7.35	—	—	—	5.03
3375	31.7	6.29	—	—	—	5.21
3381	26.4	7.74	—	—	—	3.52
3382	27.0	4.25	0.64	4.89	13	5.72
3384	23.1	7.38	—	—	—	3.23
586	22.3	6.16	1.16	7.31	~16	~3.15
Eastern Creek Volcanics						
3397	8.80	2.83	0.40	3.32	12	2.76
3399	5.90	1.40	—	—	—	4.35
3400	4.75	1.38	—	—	—	2.73
3401	4.72	0.82	0.46	1.28	36	3.81
3402	18.3	4.32	—	—	—	3.94

[a] in micrograms per gram.

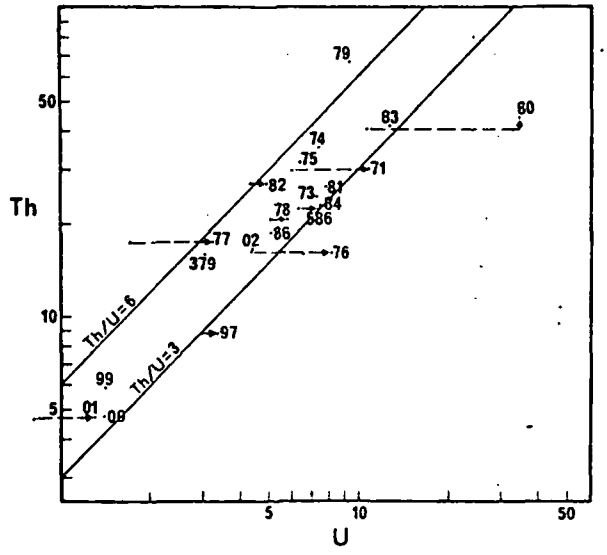

Fig. 6. Logarithmic plot of Th versus U concentrations in all samples. Most analyses lie between the Th/U reference lines of 6 and 3. The dotted lines indicate the shift of values from those measured to those recalculated for loss of U (Th). Sample numbers given as last two digits

3379. If the latter isochron is left at the position in Fig. 2, the K-values are altered and the isochrons as in Fig. 5 intersect over a much wider interval.

The effectiveness of this test depends largely on the extent of variation in K. The greater the divergence of isochrons, the more reliable are the intersections. In applying this same test to the Sybella Granite data, the results are less definitive than for the Kalkadoon granodiorite, largely because the acute intersections of isochrons produce a considerable scatter in the vicinity of the indicated initial ratios. If the U^{238}—Pb^{206} isochron of Fig. 3 is re-positioned to pass through 3384, on the supposition that this sample has suffered the least U-loss, the scatter of isochron intersections increases in the Pb^{208}/Pb^{204} versus Pb^{206}/Pb^{204} plot. This suggests that the U^{238}—Pb^{206} isochron of Fig. 3 is close to the "best position" for that suite of samples. The Eastern Creek volcanics samples have such a small variation in K as to preclude any useful test of the foregoing.

Table 2 is a listing of Th and U concentrations in micrograms per gram, with percent U-loss and revised U concentrations for those samples which are interpreted to have lost U. The K-values are also listed, and the abundance of Th and U in all samples is illustrated in Fig. 6. For the two Granites combined, the mean Th and U abundances (excepting the anomalously high values of 3380) are 27.8 and 7.05 parts per million, respectively. Individually, the Sybella Granite (mean K = 4.19) and the Kalkadoon Granite (mean K = 3.72) suites yield similar mean Th and U abundances. The mean K-value for the two Granites is 3.96. The Eastern Creek Volcanics samples yield means of; Th = 8.49 parts per million, U = 2.15 parts per million, K = 3.52. From ample evidence of U-loss provided here and by others (Black and Richards 1972; Rosholt *et al.* 1973), in rocks which exhibit no visible effects of open-system behaviour, it is apparent that geochemical surveys of primary U abundance in rocks may suffer to a considerable degree from underestimating the content of U.

Initial Ratios

Reasoned best estimates for initial Pb isotope ratios in the Mount Isa region are given in Table 3. These figures include the Sybella micro-

Table 3. *Initial* Pb *isotope ratios*

	Pb^{206}/Pb^{204}	Pb^{207}/Pb^{204}	Pb^{208}/Pb^{204}
Kalkadoon granodiorite	15.90	15.68	36.75
Kalkadoon adamellite[a]	(15.75)	(15.53)	(36.75)
Sybella granite	17.00	15.75	37.40
Sybella microgranite	17.67	15.83	37.04
Eastern Creek Volcanics	16.17	15.68	36.36
Mount Isa ore Pb	16.23	15.61	36.25

[a] tentative values, minimum estimates.

granite and pegmatite (FARQUHARSON and RICHARDS 1970), based for consistency on Pb isotope analyses which have been left uncorrected for fractionation. It is objectively impossible to assign error limits to these estimates, but uncertainties can be discussed with respect to fractionation, 204-error and U-loss. The data are presented in Fig. 7 with growth curves and the Mount Isa ore Pb for reference.

The two systematic errors associated with mass-spectrometric analysis of Pb are isotopic fractionation and error in the proportion of Pb^{204}, the common denominator of the three Pb isotope ratios. Since the initial ratios have been derived from several analyses, the effects of the random component of Pb^{204} — error should approximately cancel out. The effect of fractionation, however, may be more or less consistent, as has been demonstrated by the fact of recalculation of Pb isotope analyses according to "absolute" isotopic standards (CATANZARO *et al.* 1968). Thus, in Fig. 7, the initial ratios may be displaced along fractionation trends to varying degree, one relative to another, and possibly in a consistent manner relative to the Mount Isa ore Pb and the growth curve. The possibility of U-loss affects the estimation of inital ratios on the Nicolaysen diagrams. Transferred to the Pb—Pb diagram, the result of such error appears as an increase in Pb^{206} and Pb^{207}, the displacement being sub-tangential to the growth curve.

One aim of this study is to compare rock initial ratios with the Mount Isa ore Pb values as a test for possible genetic association between rock units and mineralization. With due regard for the uncertainties in the initial ratio values, the Eastern Creek Volcanics fall close to the Mount Isa ore Pb values. However, this unit stratigraphically underlies the Mount Isa shale, and orebodies, and thus could not have been involved in contemporaneous volcanism according to the popular submarine volcanic — exhalative model of mineralization. It could be argued that the Eastern Creek Volcanics are linked with the mineralization through an epigenetic lateral secretion mechanism involving transport of Pb and associated metals from the Volcanics to the present site of the orebodies. Such a hypothesis is not presently favoured. Alternatively, if a section of the Eastern Creek Volcanics was exposed to erosion at the time of sedimentation of the Mount Isa Shale, Pb leached from them could have been available for precipitation as syngenetic sulphide mineralization. However, it is unlikely that the Volcanics were exposed during such sedimentation since they lie more or less conformably below the Mount Isa Shale and Myally Beds.

The initial ratios of the other units are displaced to a sufficient distance from the Mount Isa value to preclude contemporaneity. The Sybella microgranite/pegmatite has previously been ruled out as a source of Pb in the orebodies (FARQUHARSON and RICHARDS 1970a). Similarly, the Sybella granite can be eliminated because it is too enriched in radiogenic Pb. The Kalkadoon granodiorite remains as a possible source, through a mechanism of surface exposure and weathering. At some time between emplacement of the granodiorite and subsequent intrusion of the Sybella granite, the former may have been uplifted and exposed as a tectonic high (see CARTER *et al.* 1961) to provide surficially leached Pb to the Mount Isa shale depositional basin. This suggestion

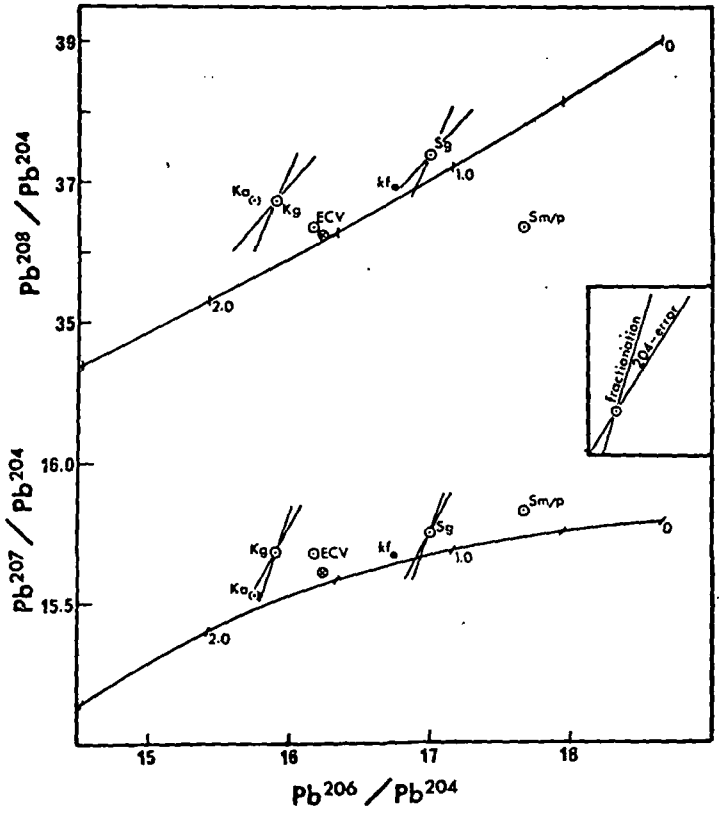

Fig. 7. Combined Pb–Pb plot which shows the estimated best values of initial ratios for the Kalkadoon granodiorite (Kg), Kalkadoon adamellite (Ka), Eastern Creek Volcanics (ECV), Sybella granite (Sg) and Sybella microgranite/pegmatite (Sm/p). The Mount Isa ore Pb (⊗) and 3375 microcline (kf) values, and the ore Pb growth curves ($\mu = 9$; $K = 3.95$) are plotted for reference. Isotope fractionation and Pb^{204}-error lines are indicated

avoids the question of a concentrating mechanism, the problem which generally renders normal continental erosion as a unsatisfactory source of metals for orebodies. An alternative suggestion would appeal to hydrothermal leaching of Pb from the granodiorite during volcanism, and transport of that Pb as a submarine exhalative product to the site of deposition. The association of tuff beds and sulphides supports such a model, but there is no visible evidence for hydrothermal leaching of the Kalkadoon granodiorite. By tenuous projection, it is possible that the Kalkadoon granodiorite represents local lower-level crustal material which may have been the source of both the volcanism and the mineralization. The initial ratios for the granodiorite lie close to a 1900 m.y. "primary" Pb isochron, which is concordant with the previously determined age of the unit and which suggests derivation from a source with "primary" Pb character.

The initial ratio of the Kalkadoon adamellite (samples 3371 and 3376) should lie somewhere along the Pb–Pb isochron in Fig. 2. If the whole-rock U^{238}–Pb^{206} isochron is assumed to go through 3372, the sheared adamellite, the initial Pb^{206}/Pb^{204} ratio is 15.75, and the corresponding Pb^{207}/Pb^{204} ratio (calculated according to the proportion of U-loss indicated by the U^{238}–Pb^{206} data) is 15.53. Although the values are tentative, the Kalkadoon adamellite could, by the previous argu-

ment of weathering and erosion, have supplied Pb for the Mount Isa orebodies. In the case of such surficial derivation it is probable that the Pb would be an isotopic mixture of the main and marginal phases of the Kalkadoon Granite, and may include contributions from other sources.

Inasmuch as the Sybella granite and microgranite/pegmatite initial ratios are isotopically different from the Mount Isa ore Pb, they are also considerably enriched in radiogenic Pb as compared with primary growth curve isotopic values at the respective times of emplacement. This radiogenic enrichment is apparent also in the initial Sr ratios which are, for the Sybella granite, 0.7114 (Farquharson and Wilson 1971) and for the microgranite/pegmatite, 0.736 (Farquharson and Richards 1970a). By contrast, the Kalkadoon granodiorite approximates to "primary" initial ratios for Pb and for Sr (initial Sr ratio, 0.7042; Farquharson and Wilson 1971).

Such isotopic enrichment is suggestive of crustal derivation for the two Sybella phases, a development which may have followed the course of a "Granite Series" as envisaged by Read (1955). The crustal block which generated the Sybella phases must have had a much higher average μ-value than the terrestrial average. For example, if the Pb isotopic composition of the crustal block were represented by the Kalkadoon granodiorite initial ratio at about 1900 m.y., generation of the Sybella granite would require a μ-value of about 20, and generation of the Sybella microgranite/pegmatite would require a μ-value of about 23. If the Sybella granite could be represented as the parent of the microgranite/pegmatite, the μ-value of that source would have been about 33. Note, however, that the low Pb^{208}/Pb^{204} initial ratio for the microgranite/pegmatite (Fig. 7) is relatively un-enriched, which suggests that neither the Kalkadoon not the Sybella Granite represents the source.

The question of derivation of the Granites is difficult to resolve and does not lend itself easily to simple models, isotopic or otherwise. Any fractionation involved in the generation of these different plutons was not a result of simple magmatic differentiation: the long time intervals between successive intrusives precludes that. Fractionation may be accounted for by partial melting of either a homogeneous crustal source, or a source which was re mobilized periodically with accompanying fundamental changes in chemical character, or a source which by its heterogeneity gave rise to anatectic products of different compositions at different times. Deep crustal metasomatism, or granitization (Joplin and Walker 1961) may have provided a vehicle for extensive redistribution of major and trace elements, including U, Th and Pb. It is now well established that U and Th migrate from a rock system during granulite-facies metamorphism (Heier 1965a; 1965b; Heier and Adams 1965, Gray and Oversby 1972). Depletion of these elements in lower crustal sections should result in enrichment elsewhere (Lambert and Heier 1967). The observed high U and Th contents of the Sybella granites, and the high μ-values of their inferred source, are compatible with such a mechanism, which could have involved a succession of stages.

The Mount Isa ore Pb occurs in a crustal block which evolved through a series of plutonic episodes leading progressively to greater enrichment in radiogenic Pb. The apparent enrichment in the Mount Isa Pb relative to the ore Pb growth curve is consistent with a model of crustal derivation related to magma generation in the region.

Summary and Conclusions

The foregoing study has revealed the following with regard to U—Th—Pb isotopic systems in igneous rocks from Mount Isa:

1. In a general sense the whole-rock data correspond with the geochronology outlined by previous Rb—Sr data.

2. Considerable open-system effects are apparent, and can be explained principally as the results of recent U-loss due to weathering. Accordingly, the Th-Pb "isochrons" are the most reliable.

3. On the basis of extrapolated initial ratios both the Sybella granite and the younger microgranite and pegmatite are genetically unrelated to the Mount Isa ore deposits. On the same basis the Eastern Creek Volcanics and the two isotopically distinguishable phases of the Kalkadoon Granite could be related to

orebodies, possibly
surface weathering
gically inferred seque
the isotopic scher
lues lying between th
stern Creek Volcan
nic (younger) Sybell

Whereas the Kalkad
reek Volcanics appro
b isotopic system, t
icrogranite/pegmatit
onsidered to be pr
ecycled crustal materi

The source of Pb (an
he Mount Isa orebod
The inescapable asso
eds argues very stron
us volcanic source
inor contribution fr
The source of the tuf
e examined. This cou
ossibility that Kalkad
he pile of sediments
ource of anatectic n
anism and mineraliza

Acknowledgements

This study was undert
Advanced Studies, Aust
to which we extend o
grateful for the support
and geological staff of
One of us (R. B. F.) also
of a National Research

References

Bennett, E. M.: Lea
deposits of Mount
wealth Mining and
233 (1965)

Black, L. P., Richards
in northeast Queensla
19, 321 (1972)

Carter, E. K., Brooks
The Precambrian mi
Queensland. Australi
Geol. Geophys., Bull

Catanzaro, E. J., Murp
Garner, E. L.: Abs
ratios of common, c
lead isotopic standa
Stand., A. 72A 3, 26

of either a homogeneous
source which was re-
ly with accompanying
in chemical character, or
heterogeneity gave rise to
different compositions a-
crustal metasomatism,
LIN and WALKER 1961)
a vehicle for extensive
or and trace elements.
Pb. It is now well estab-
migrate from a rock
te-facies metamorphism
HEIER and Adams 1965,
972). Depletion of these
al sections should result
e (LAMBERT and HEIER
igh U and Th contents
, and the high μ-values
e, are compatible with
ch could have involved

occurs in a crustal block
h a series of plutonic
essively to greater en-
ic Pb. The apparent
nt Isa Pb relative to the
consistent with a model
ated to magma genera-

sions

revealed the following
Pb isotopic systems in
unt Isa:

the whole-rock data
ochronology outlined

ystem effects are ap-
ined principally as the
due to weathering.
"isochrons" are the

apolated initial ratios
te and the younger
natite are genetically
Isa ore deposits. On
ern Creek Volcanics
listinguishable phases
e could be related to

orebodies, possibly through the mechanism
surface weathering and erosion. The geo-
gically inferred sequence of events is retained
the isotopic scheme, with the ore lead
lues lying between the less-radiogenic (older)
astern Creek Volcanics and the more-radio-
enic (younger) Sybella Granite.

Whereas the Kalkadoon Granite and Eastern
reek Volcanics approximate to the "primary"
b isotopic system, the Sybella granite and
icrogranite/pegmatite do *not*, and are thus
onsidered to be products of geologically
ecycled crustal material.

The source of Pb (and associated metals) in
he Mount Isa orebodies remains conjectural.
The inescapable association of ore and tuff
eds argues very strongly for a contemporane-
us volcanic source of metals with only
inor contribution from continental erosion.
The source of the tuff beds should therefore
e examined. This could even yet lead to the
ossibility that Kalkadoon-like material beneath
he pile of sediments and volcanics, was the
ource of anatectic magma generation, vol-
anism and mineralization.

Acknowledgements

This study was undertaken at the Institute of Advanced Studies, Australian National University, to which we extend our appreciation. We are grateful for the support given by the management and geological staff of Mount Isa Mines, Ltd. One of us (R. B. F.) also acknowledges the support of a National Research Council operating grant.

References

BENNETT, E. M.: Lead-zinc-silver and copper deposits of Mount Isa. In: Eighth Commonwealth Mining and Metallurgical Cong. **1**, 233 (1965)

BLACK, L. P., RICHARDS, J. R.: Rock lead isotopes in northeast Queensland. J. Geol. Soc. Australia **19**, 321 (1972)

CARTER, E. K., BROOKS, J. H., WALKER, K. R.: The Precambrian mineral belt of north-western Queensland. Australia Bur. Mineral Resources, Geol. Geophys., Bull. **51**, 344 (1961)

CATANZARO, E. J., MURPHY, T. J., SHIELDS, W. R., GARNER, E. L.: Absolute isotopic abundance ratios of common, equal-atom and radiogenic lead isotopic standards. J. Res. Natl. Bur. Stand., A. 72A **3**, 261 (1968)

COMPSTON, W., OVERSBY, V. M.: Lead isotopic analysis using a double-spike. J. Geophys. Res. **74**, 4338 (1969)

COOPER, J. A., REYNOLDS, P. H., RICHARDS, J. R.: Double-spike calibration of the Broken Hill Standard Lead. Earth Planet. Sci. Letters **6**, 467 (1969)

— RICHARDS, J. R.: Solid-source lead isotope measurements and isotopic fractionation. Earth Planet. Sci. Letters **1**, 58 (1966)

FARQUHARSON, R. B., RICHARDS, J. R.: Whole-rock U—Th—Pb and Rb—Sr ages of the Sybella microgranite and pegmatite, Mount Isa, Queensland. J. Geol. Soc. Australia **17**, 53 (1970a)

— — A re-analysis of the monazite from Mica Creek, Mount Isa, Queensland. J. Geol. Soc. Australia **16**, 767 (1970b)

— WILSON, C. J. L.: Rationalization of geochronology and structure at Mount Isa. Econ. Geol. **66**, 574 (1971)

FISHER, N. W.: Review of evidence and genesis of Mount Isa orebodies. Rept. 21st International Geol. Cong. **16**, 99 (1960)

GALE, N. H.: Episodic U—Pb models and the interpretation of variations in the isotopic composition of Pb in rocks. Rev. Geophys. Space Phys. **11**, 37 (1973)

GRAY, C. M., OVERSBY, V. M.: The behaviour of lead isotopes during granulite facies metamorphism. Geochim. Cosmochim. Acta **36**, 939 (1972)

HEIER, K. S.: Radioactive elements in the continental crust. Nature **208**, 479 (1965a)

HEIER, K. S.: Metamorphism and the chemical differentiation of the crust. Geol. Foren. Stockholm Forh. **87**, 249 (1965b)

— ADAMS, J. A. S.: Concentration of radioactive elements in deep crustal material. Geochim. Cosmochim. Acta **29**, 53 (1965)

HEWETT, R. L., SOLOMON, P. J.: The role of mobilization in silver-lead-zinc sulphide assemblages with particular reference to Mount Isa, Australia. presented at the 22nd International Geol. Cong., Section 2, New Delhi (1964)

JOPLIN, G. A., WALKER, K. R.: The Precambrian granites of north-western Queensland. Proc. Roy. Soc. Queensland **72**, 21 (1961)

KANASEWICH, E. R., FARQUHAR, R. M.: Lead isotope ratios from the Cobalt-Noranda area, Canada. Can. J. Earth Sci. **2**, 361 (1965)

KNIGHT, C. L.: Regional geology of Mount Isa. In: Geology of Australian Ore Deposits, 1st Ed. (Fifth Emp. Min. Metall. Cong.) 352 (1953)

LAMBERT, I. B., HEIER, K. S.: The vertical distribution of uranium, thorium and potassium in the continental crust. Geochim. Cosmochim. Acta **31**, 377 (1967)

McDougall, I., Dunn, P. R., Compston, W., Webb, A. W., Richards, J. R., Bofinger, V. M.: Isotopic age determinations on Precambrian rocks of the Carpentaria region, Northern Territory, Australia. J. Geol. Soc. Australia 12, 67 (1965)

McIntyre, G. A., Brooks, C., Compston, W., Turek, A.: The statistical assessment of Rb—Sr isochrons. J. Geophys. Res. 71, 5459 (1966)

Murray, W. J.: Notes on Mount Isa geology. Proc. Australasian Inst. Mining Met. 197, 105 (1961)

Nicolaysen, L. O.: Graphic interpretation of discordant age measurements of metamorphic rocks. Ann. N. Y. Acad. Sci. 91, 198 (1961)

Ostic, R. G., Russell, R. D., Stanton, R. L.: Additional measurements of the isotopic composition of lead from stratiform deposits. Can. J. Earth Sci. 4, 245 (1967)

Pliler, R., Adams, J. A. S.: The distribution of thorium and uranium in a Pennsylvanian weathering profile. Geochim. Cosmochim. Acta 26, 1137 (1962)

Read, H. H.: Granite series in mobile belts. Geol. Soc. Am. Spec. Paper 62, 409 (1955)

Richards, J. R.: Isotopic composition of Australian leads — III; Northwestern Queensland and the Northern Territory — a reconnaissance. Geochim. Cosmochim. Acta 27, 217 (1963)

— Some Rb—Sr measurements on granites near Mount Isa. Proc. Australasian Inst. Mining Met. 218, 19 (1966)

— Major lead orebodies—mantle origin? Econ. Geol. 66, 425 (1971)

Rosholt, J. N., Bartel, A. J.: Uranium, thorium and lead systematics in Granite Mountains, Wyoming. Earth Planet. Sci. Letters 7, 141 (1969)

— Peterman, Z. E., Bartel, A. J.: U—Th—Pb and Rb—Sr ages in granite reference sample from southwestern Saskatchewan. Can. J. Earth Sci. 7, 184 (1970)

Rosholt, J. N., Zartman, R. E., Nkomo, I. T.: Lead isotope systematics and uranium depletion in the Granite Mountains, Wyoming. Bull. Geol. Soc. Am. 84, 989 (1973)

Russell, R. E.: Rationalization of geochronology and structure at Mount Isa (discussion). Econ. Geol. 67, 1276 (1972)

Stanton, R. L., Russell, R. D.: Anomalous leads and the emplacement of lead sulphide ores. Econ. Geol. 54, 588 (1959)

Stieff, L. R., Stern, T. W., Oshiro, S. and Senftle, F. E.: Tables for the calculation of lead isotope ages. U. S. Geol. Surv. Profess. Papers 334, 40 (1959)

Tatsumoto, M.: Isotopic composition of lead in volcanic rocks from Hawaii, Iwo Jima and Japan. J. Geophys. Res. 71, 1721 (1966)

Tilton, G. R., Patterson, C. C., Brown, H. S., Inghram, M. G., Hayden, R. J., Hess, D. C., Larson, E. S.: Isotopic composition and distribution of lead. uranium and thorium in a Precambrian granite. Bull. Geol. Soc. Am. 66, 1131 (1955)

Ulrych, T. J., Reynolds, P. H.: Whole-rock and mineral leads from the Llano Uplift, Texas. J. Geophys. Res. 71, 3089 (1966)

Wilson, C. J. L.: Rationalization of geochronology and structure at Mount Isa — a reply. Econ. Geol. 68, 1343 (1973)

— Farquharson, R. B.: Rationalization of geochronology and structure at Mount Isa — a reply. Econ. Geol. 67, 1279 (1972)

York, D.: Least-squares fitting of a straight line with correlated errors. Earth Planet. Sci. Letters 5, 320 (1969)

Received May 28, 1974

Robin Bruce Farquharson
Department of Geology, The University of Calgary, Calgary, Alberta, Canada

Mineral. Deposita (Berl.) 10, 27–41 (1975)

Uranium Mineralization in the South Alligator River Valley

D. E. Ayres and P. J. Eadington

CSIRO Division of Mineralogy, Sydney, Australia

The South Alligator uranium deposits are located in the Northern Territory, Australia, south-west from the recent discoveries of Nabarlek, Ranger, Koongarra and Jabiluka. All five deposits occur in intensely folded Early Proterozoic rocks around the perimeter of the Kombolgie Formation, a flat-lying Middle Proterozoic sandstone unit. It is proposed that during reconstitution (weathering or diagenesis) of acid volcanic rocks, groundwaters leached uranium and percolated down into the groundwater system of the permeable sandstone and conglomerate unit at the base of the sequence. Uranium as uranyl ion was stable in relatively high Eh groundwater conditions and was carried in solution until active reducing conditions were met with which resulted in reduction of uranyl ion to insoluble UO_2. Reduction occurred where faulting had brought underlying carbonaceous shales up against the sandstone aquifer, or where groundwater could percolate down permeable fault zones into the carbonaceous shales. These structural, chemical traps were sites of uranium accumulation.

I. Introduction

This investigation considers the geochemical factors which control uranium mineralization in the South Alligator River area, an area typical of the North Australian deposits. It was selected for study as a joint project with United Uranium N. L. Samples were collected from the mines and surrounding areas by the authors in 1970 and were supplemented by material collected for a previous study made by the Division of Mineralogy, Commonwealth Scientific and Industrial Research Organization (CSIRO).

The principal Proterozoic Australian uranium deposits are situated at Rum Jungle, 80 km south of Darwin; in the South Alligator and East Alligator Rivers area in the Northern Territory 320 km east of Darwin; and at Westmoreland a further 700 km to the east on the Northern Territory-Queensland border (Fig. 1). The deposits in the South Alligator Valley were discovered in the early 1950's and, until production ceased in 1964, had produced 147077 tonnes of ore averaging 5.73 kg U_3O_8/tonne. The somewhat larger deposits closer to the East Alligator River — Nabarlek, Ranger, Jabiluka and Koongarra — were found between 1969 and 1972 and could be brought into production in 1975.

The Alligator Rivers deposits occur in deformed, Precambrian geosynclinal rocks, at or near an unconformity with a flat-lying massive sandstone, the Kombolgie Formation, which has at its base a volcanic-conglomerate association dated by K-Ar at 1800 m.y. The Westmoreland group of deposits occurs in 1800 m.y. old volcanics and conglomerates that are correlated with the South Alligator volcanic-elastic sequence (South 1972).

The mineralization in both areas is essentially uraninite (variety pitchblende) occurring as vein-type lodes in faults or shears and associated with either carbonaceous shales (or their metamorphosed equivalents) or basis dykes. Concordant age determinations of 850 m.y. for the pitchblende from seven of the deposits

have been reported (HILLS and RICHARDS 1972; COOPER 1973); however the spread of data points indicates a complex history of element losses.

II. Regional Geology

The Darwin Alligator Rivers region (longitude 131 °E to 134° E, Fig. 1) has a basement complex of Archean metamorphics overlain by deformed Early Proterozoic and undeformed Middle Proterozoic sediments. For approximately 1300 m.y., the area has been a stable platform with subsequent sedimentation restricted to thin veneers of shallow water sediments, now largely eroded.

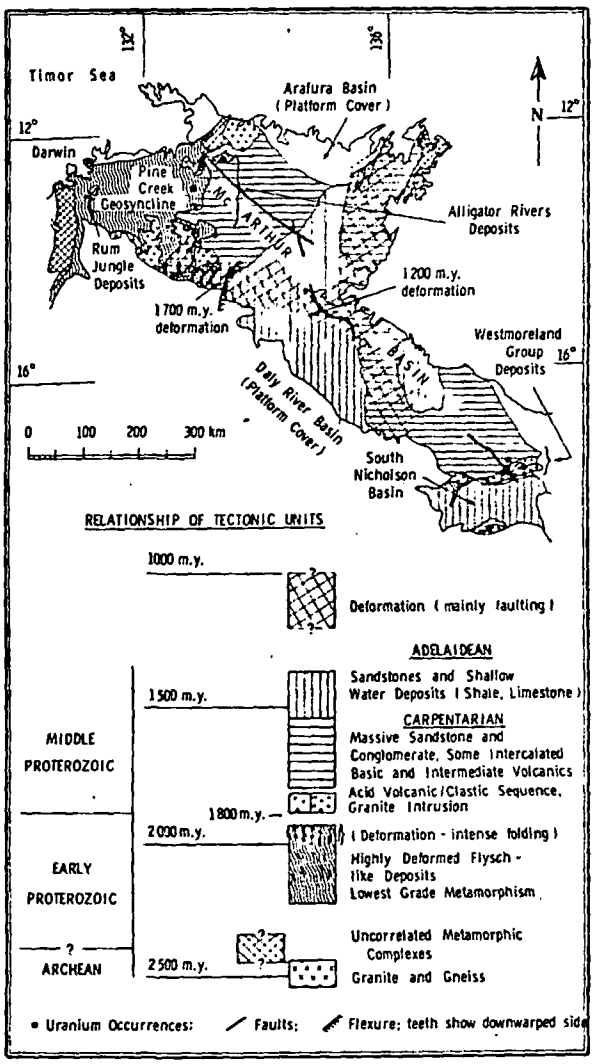

Fig. 1. Regional tectonic environment of some Northern Australian uranium deposits (Geology after Geol. Soc. of Aust. 1971, Tectonic Map of Australia and New Guinea.)

The Pine Creek Geosyncline contains a flysch-like sequence of lutites and arenites which were tightly folded during a deformation at approximately 2000 m.y., but remained unmetamorphosed, or metamorphosed to a maximum of lower greenschist grade. Archean rocks outcrop at the margins of the Geosyncline and also occur as inliers in several places, suggesting that the region was part of an Archean shield area. This would explain the shallow nature of the geosyncline and succeeding basins, and the lack of high-grade regional metamorphism in ancient sedimentary sequences.

A prominent feature in the eastern part of the region is a sequence of flat-lying Middle Proterozoic (Carpentarian) sediments and volcanics which unconformably overlie the geosynclinal sediments and form the basal rocks of the McArthur Basin to the east (Fig. 1). Deposition of the sequence commenced with volcanics which occurred simultaneously with the intrusion of granites into the geosynclinal rocks. The volcanics were overlain by a 2750 metre sequence of terrestrial (conglomerate-sandstone) and shallow water (shale-limestone) rocks which, apart from faulting, have remained undeformed and unmetamorphosed since deposition ended, a period of approximately 1300 m.y.

Between the South Alligator and East Alligator Rivers there are several major strike slip faults, striking northwest. Some, at least, were initiated in Carpentarian time, since they appear to have controlled the distribution of certain rock units (WALPOLE *et al.* 1968). There is also evidence for much later movement along some faults. The time-sequence of faulting in the region has not yet been properly established.

III. Geology of the South Alligator River Area

The area of study has been mapped in detail by company geologists (SHEPHERD 1962; TAYLOR 1970) and also by the Bureau of Mineral Resources (BMR). (WALPOLE *et al.* 1968). The summary below, depends largely on their

studies. A geological map of the South Alligator Valley and an interpretive cross-section illustrating the relationship of rock units are shown in Figure 2.

The Early Proterozoic rocks are tightly folded about NW—SE axes and have dips of 70—90°. The Carpentarian rocks deposited above the unconformity are flat-lying and form a plateau bounded by high cliffs, with the Edith River Volcanics exposed at the base and the Kombolgie Formation exposed in the cliffs and on the plateau surface. There is a major fault zone extending NE—SW down the valley, parallel to the strike of the Early Proterozoic rocks. The only granitic rock in the immediate area is a microgranite and both it and the Edith River Volcanics have concordant ages of 1750 m.y. (COMPSTON and ARRIENS 1968).

The uranium deposits all occur near the Middle Proterozoic unconformity, in carbonaceous

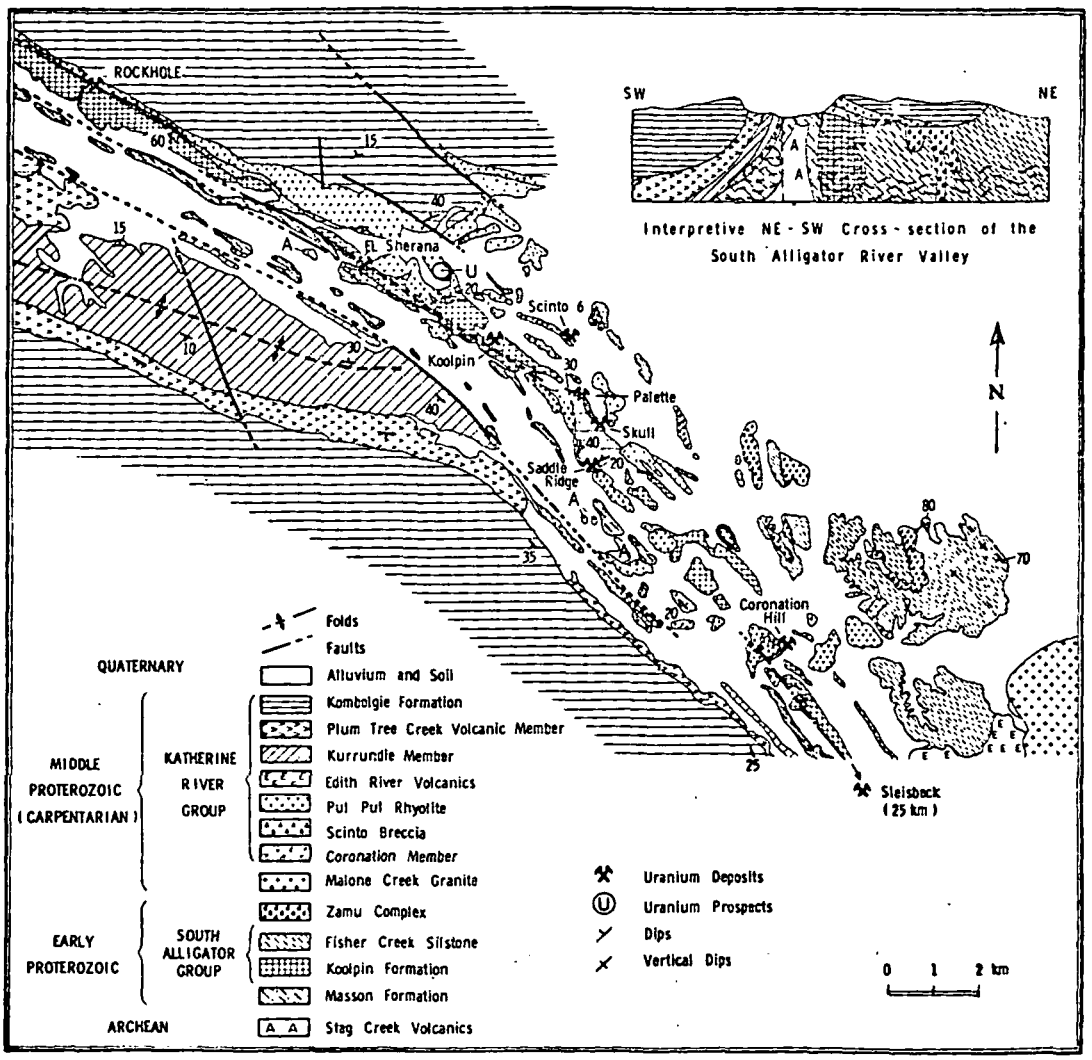

FIG. 2. GEOLOGY OF THE SOUTH ALLIGATOR RIVER VALLEY
(After BMR) 1" = 1 mile or 1:63,360 map (1962)

shale and siltstone of the Koolpin Formation, in sandstone of the lowest member of the Edith River Volcanics, and in faults that displace the volcanics. There is another uranium deposit at Sleisbeck, 32 km along strike to the SE, also in carbonaceous shale of the Koolpin Formation.

IV. Lithology and Geochemistry of the Host Rocks

In the following description of rock units, much data has been taken from the geological reports already cited. Because of their close association with uranium mineralization, the overlying acid volcanic rocks and the carbonaceous shales of the Koolpin Formation were the subject of geochemical and petrographic studies by the authors.

1. *Early Proterozoic*

(a) Masson Formation — Stratigraphically underlying the Koolpin Formation is the Masson Formation of the Goodparla Group. It consists of units, commonly 500—666 m thick, of interbedded arenite (medium-grained quartz greywacke) and lutite (red and buff-banded siltstone). At depth, the unweathered siltstone may be carbonaceous and pyritic (Walpole *et al.* 1968, p. 32). The uranium contents of samples of the siltstone and quartz greywacke are 7 ppm and 1.5 ppm respectively.

(b) Koolpin Formation — This Formation in the South Alligator Group comprises interbedded carbonaceous shale and cherty ferruginous siltstone, with restricted lenses of dolomite. The carbonaceous shales are, in places, pyritic and contain lenses and nodules of chert. The essential minerals are quartz and sericite, with kaolinite, siderite, chlorite and hematite being locally important. The carbonaceous material was examined by differential thermal analysis and was found to be similar in composition to semi-anthracite.

Average analyses of carbonaceous shales from Palette, El Sherana, Coronation Hill and Rockhole mines are compared with an 'average' black shale from the United States in Table 1. (It is recognized that the Australian rocks are affected by mineralization.) The major elements of the South Alligator shales have similar values to the 'average' black shale, but the trace elements B and Co are higher and Ca and Na are lower. The uranium content of carbonaceous shales from Palette, Rockhole and El Sherana mines are generally in the range <30 ppm with occasional values up to 300 ppm.

As a result of recent, and perhaps also Early Proterozoic, weathering, carbonaceous shales outcrop poorly and are bleached to depths of about 16 m. Mine sections show bleached lenses within carbonaceous shale extending to depths of 100 m, which are claimed to be the result of hydrothermal alteration. However, no alteration mineral assemblages have been described and the bleached zones could equally well have been the result of surface waters penetrating along faults and shear zones.

(c) Fisher Creek Siltstone — This formation overlies and interfingers with the Koolpin Formation. It consists of a poorly bedded, monotonous sequence of brown and mauve siltstone with minor greywacke siltstone. The essential minerals are quartz, muscovite, feldspar and chlorite.

2. *Middle Proterozoic*

These rocks belong to the Katherine River Group and unconformably overlie the Lower Proterozoic sequence. They consist of basal Edith River Volcanics overlain by the Kombolgie Formation. In the area of the ore deposits, the Edith River Volcanics are represented by the Coronation Member overlain by the Pul Pul Rhyolite Member.

(a) Edith River Volcanics — The Coronation Member in the Katherine River Group is a valley fill deposit overlying the Early Proterozoic unconformity. It is predominantly sandstone with some interbedded conglomerate, tuffaceous sediments and rhyolite. The sandstone consists of quartz grains with a matrix of kaolinite and dickite. Analyses of unmineralized sandstone and rhyolite from this Member are listed in Table 3.

The Pul Pul Rhyolite Member consists of rhyolite, ignimbrite and tuff. (The terminology of South Alligator volcanic rocks is inexact, since the so-called rhyolites are probably a complex mixture of ignimbrite, rhyolite and

tuff. The term rhyolite is used here to cover all rock types.)

All these rocks have been reconstituted and the most common mineral assemblage consists of quartz phenocrysts (often with overgrowths) in a fine-grained groundmass of quartz, kaolinite and hematite. Locally, there may be feldspar phenocrysts (largely sericitized) and chlorite and sericite may be present in the groundmass.

Clearly, this is not a primary mineral assemblage and since the volcanics appear to resist modern chemical weathering, it is thought to result from deuteric alteration at the time of eruption, or subsequent diagenesis.

The Edith River Volcanics and the Pul Pul Rhyolite in particular are known to have above background radioactivity (STEWART 1965). STEWART suggests that the radioactivity originates in minute grains or intergranular films of uranium minerals and attributes radiometric anomalies (e.g. Charvats Prospect) to local accumulation of secondary uranium minerals.

(b) Kombolgie Formation — This consists of 1730 m of sediments (quartz greywacke, conglomerate) and minor volcanics (tuff, undiffer-

Table 1. *Comparison of analyses of carbonaceous shales*

	Average Black Shale[1]	South Alligator Black Shales				
		Rockhole	El Sherana	Palette	Coronation Hill	All Shales
Average Analyses (%)						
Al_2O_3	13.3	19	18	14	21	18
SiO_2	—	69	68	77	70	69
Fe	2.0	3.3	2.8	0.5	1.3	2.8
Mg	0.7	1.4	0.8	3.3	2.3	1.5
P	—	0.2	0.3	0.2	0.2	0.2
Ti	0.2	0.4	0.3	0.7	0.6	0.4
C	3.5	3.0	5.2	0.7	1.1	3.3
Minor and Trace Elements (ppm)						
B	50	340	257	330	500	330
Ba	300	314*	320*	400	400	330
Ca	1500	455*	480*	367	330	444
Co	10	38*	57*	37	27	42
Cr	100	118	83	417	117	132
Cu	70	267	86	27	9	177
Ga	20	31	29	30	28	30
Mn	150	302	35	32	37	186
Mo	10	4*	10*	1*	1*	5
Na	7000	305	200	250	667	302
Ni	50	62	63	47	133	67
Pb	20	66*	36*	30	10*	51
Sc	10	13*	15*	32	33	17
V	150	614	216	400	183	454
W	—	100*	255*	150	100	146
Y	30	47*	84*	25	27	54
Zr	70	120*	116	87	117	116
U	—	131	84	50	20	103

[1] Ref. VINE and TOURTELOT, 1970.

* These median values are probably slightly high since substitutions were made for results below the limit of detection. (Mo(3), Pb(15), Sc(8), W(150), Y(10), Zr(100)).

Major and minor elements by semi-quantitative optical emission spectroscopy. Uranium by X-ray fluorescence spectroscopy.

Table 2. *Geological features of South Alligator uranium deposits*

	El Sherana	Palette	Rockhole
Mineralogy	*pitchblende, secondary U minerals;* minor galena-clausthalite, pyrite, marcasite, Co-Ni arsenides, Cu sulphides	*pitchblende, U secondary minerals;* minor galena-clausthalite, coloradoite, pyrite, marcasite, gold	*pitchblende;* minor clausthalite, eskebornite pyrite, marcasite, chalcopyrite, rare U secondary minerals
Electron microprobe analysis of pitchblende	U Pb Fe Si U/Pb 80.4 7.0 0.4 0.2 11.6 80.9 7.4 0.8 0.3 11.0	U Pb Fe Si U/Pb 77.5 10.7 0.6 0.2 7.3 74.1 11.3 0.3 0.4 6.6	
Gangue	red and grey chert, quartz veinlets	siliceous gangue, apatite, introduced in to host sandstone	siderite
Host rock	ferruginous siltstone and carbonaceous shale, secondary deposit of open cut in sandstone and rhyolite	sandstone	carbonaceous shale and chert, at higher levels near the unconformity, sandstone host
Texture	lenticular pitchblende masses in a fault zone enveloped by secondary mineralization, abundant spherical nodules of pitchblende	rich ore shoots along a fault, spherical nodules of pitchblende imperfectly developed	narrow veins of pitchblende similar to Palette
Pitchblende	present	present	present
Carbonaceous shale	present	present	present
Gold	present	present	present
Fault	present	present	present
Shape	tabular ore body tapering with depth		ore shoots form a ribbon dipping to west along a fault zone
Vertical extent	120 ft (36.6 m)	100 ft (30.5 m)	200 ft (61 m)
Size (tonnes ore)	61200	5100	13260
Relation to igneous rocks	rhyolite overlying deposit	rhyolite overlying deposit	rhyolite overlying deposit and in fault contact with host rocks

entiated volcanics and a basalt member), conformable, and in places disconformable, over the Edith River Volcanics.

V. Mineral Deposits

The location of the known uranium deposits in the South Alligator Valley is shown in Figure 2, and a comparison of pertinent geological features of the deposits is presented in Table 2. The deposits are of two types, those containing uraninite (variety pitchblende) with or without uranium ochres, and those consisting entirely of uranium ochres. The uranium ochres, often called "secondary" uranium minerals, are the brightly-coloured minerals such as the torbenite and metatorbernite groups which contain uranium in an oxidized (six valent) state, and may form either by oxidation of uraninite or by direct precipitation in an oxidizing environment. This paper

Table 2 (continued)

	Rockhole	Coronation Hill	Saddle Ridge	Scinto 6	Skull	Koolpin
y ena- ite, d	*pitchblende;* minor claus-thalite, eskebornite pyrite, marcasite, chal-copyrite, rare U sec-ondary minerals	*pitchblende, U secondary minerals* minor pyrite, Cu sulphides	all 'secondary' uranium minerals trace pyrite	'secondary' uranium minerals only	*pitchblende, secondary U minerals;* minor gold, Cu mineralization	*pitchblende,* secondary ura-nium minerals
U/Pb .3 .6						
ite,	siderite	minor quartz veinlets	no introduced gangue, some chalcedony	no introduced gangue	no introduced gangue	no introduced gangue
	carbonaceous shale and chert, at higher levels near the unconformity, sandstone host	tuffaceous rocks intimately asso-ciated with car-bonaceous shale and siltstones	Early Proterozoic silt-stone and Middle Pro-terozoic tuffaceous sandstone and volcanics	rhyolite	sandstone	carbonaceous shale and ferru-ginous siltstone
a s tly	narrow veins of pitch-blende similar to Pal-ette	sooty variety of pitchblende, some pitchblende veinlets	secondary U minerals filling joints and fractures	uranium ochres filling joints and fractures	pitchblende veinlets, no-dules, sooty pitchblende	sooty pitch-blende and sec-ondary U min-erals in thin stringers occu-pying fractures
	present present present present	present present present present	not present not present not present present	not present not present not present present	present present present present	present present not present present
	ore shoots form a rib-bon dipping to west along a fault zone	a number of ore shoots at higher lev-els, at lower levels ore body is pipe like				
	200 ft (61 m)	180 ft (55 m)	80 ft (24.4 m)	120 ft (36.6 m)	—	50 ft (15.2 m)
	13260	26520	30600	1734	534	2244
	rhyolite overlying de-posit and in fault con-tact with host rocks	rhyolite host for part of deposit inti-mately associated with other host rocks	tuffaceous rocks, host	rhyolite host	rhyolite overly-ing deposit	Middle Protero-zoic rocks re-moved by ero-sion

te (variety pitchblende)
ım ochres, and those
uranium ochres. The
ılled "secondary" ura-
rightly-coloured min-
te and metatorbernite
anium in an oxidized
may form either by
by direct precipita-
ronment. This paper

deals in detail only with the uraninite deposits. The pitchblende deposits were all located on faults and there was a spatial correlation between the presence of pitchblende, gold and carbonaceous shales (see Table 2). All deposits were located at or near the Middle Proterozoic unconformity, with a vertical extent ranging from 15 m up to a maximum of 90 m. This holds true for many other uranium deposits in the region

The ore was predominantly massive and dispersed uraninite with a colloform habit, i.e. the pitchblende variety, and occurred in masses of up to about 50 kg. Associated minerals were pyrite (<2%) and sparse Co-Ni arsenides, galena, clausthalite (PbSe) and native gold. The gangue was chiefly country rock (shale, sandstone, chert) with some quartz and, at the Rockhole mine, siderite (THREADGOLD 1960).

Table 2. *Analysis of main rock types in the South Alligator Valley*

	Major Elements (%)												
	SiO_2	Al_2O_3	Σ Fe as Fe_2O_3	MgO	CaO	Na_2O	K_2O	TiO_2	P_2O_5	MnO	CO_2	H_2O^-	H_2O^+
Malone Creek Granite	74.4	12.28	1.62	0.20	<0.14	0.07	8.08	0.03	<0.02	<0.01	0.22	0.28	1.03
Edith River Volcanics (Undifferentiated)	72.5	12.92	3.27	0.66	<0.14	0.03	3.55	0.15	0.02	<0.01	0.46	0.49	2.49
	69.5	9.33	7.19	2.16	<0.14	0.05	2.35	0.60	0.09	0.06	0.39	0.61	2.97
Pul Pul Rhyolite	71.0	17.93	1.80	<0.17	<0.14	<0.007	0.11	0.22	0.09	<0.01	0.14	0.29	6.57
Coronation Member (Rhyolite)	71.7	13.11	1.59	0.53	0.69	0.48	5.53	0.08	<0.02	0.06	0.60	0.47	1.56
Coronation Member (Sandstone)	84.1	5.54	1.14	<0.17	<0.14	<0.007	1.51	0.13	0.09	<0.01	0.17	0.20	1.22
Fisher Creek Siltstone	59.5	19.46	6.73	2.04	<0.14	0.05	6.17	0.70	0.11	0.09	0.22	0.69	3.79

	Minor Elements (ppm)														
	B	Ba	Co	Cr	Cu	Ga	Mo	Ni	Pb	Sc	Th	U	V	Y	Zr
Malone Creek Granite	60	n300	n20	150	6	25	4	n10	20	n10	48	35	<10	40	200
Edith River Volcanics (Undifferentiated)	40	n300	n20	80	20	20	n3	n10	20	n10	32	25	<10	20	300
	20	n300	20	200	8	15	n3	30	n20	10	16	n10	60	10	250
Pul Pul Rhyolite	20	n300	n20	80	6	20	n3	10	20	n10	42	10	15	30	200
Coronation Member (Rhyolite)	40	n300	n20	100	6	15	n3	n10	40	n10	56	20	n10	60	200
Coronation Member (Sandstone)	100	N.D.	<20	300	10	8	3	20	<20	n10	N.D.	10	40	15	100
Fisher Creek Siltstone	10	2000	30	100	4	30	<3	40	<20	N.D.	N.D.	<10	100	15	100

Major elements, and U, by X-ray fluorescence. Minor elements by optical emission spectroscopy. Th by spectrophotometric analysis. N.D. = not detected. nx means element line could not be detected; sensitivity for that element x ppm.

1. *Rockhole Al*

The mine ha
averaging 11
number of s
up to 15 m
the 600 m str
a vertical ra
with depth

Because of the
tween the ore
shales, a study
istry of the sh
by statistical a
collected from
and by determ
tions in the
namely the R
chosen because
not completely
than the other

Fig. 3.

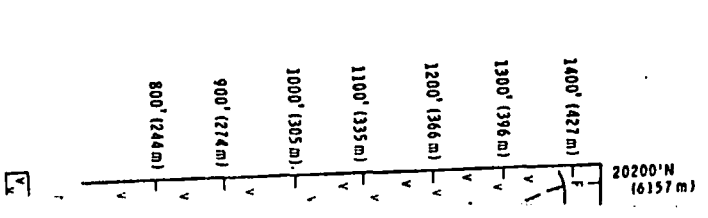

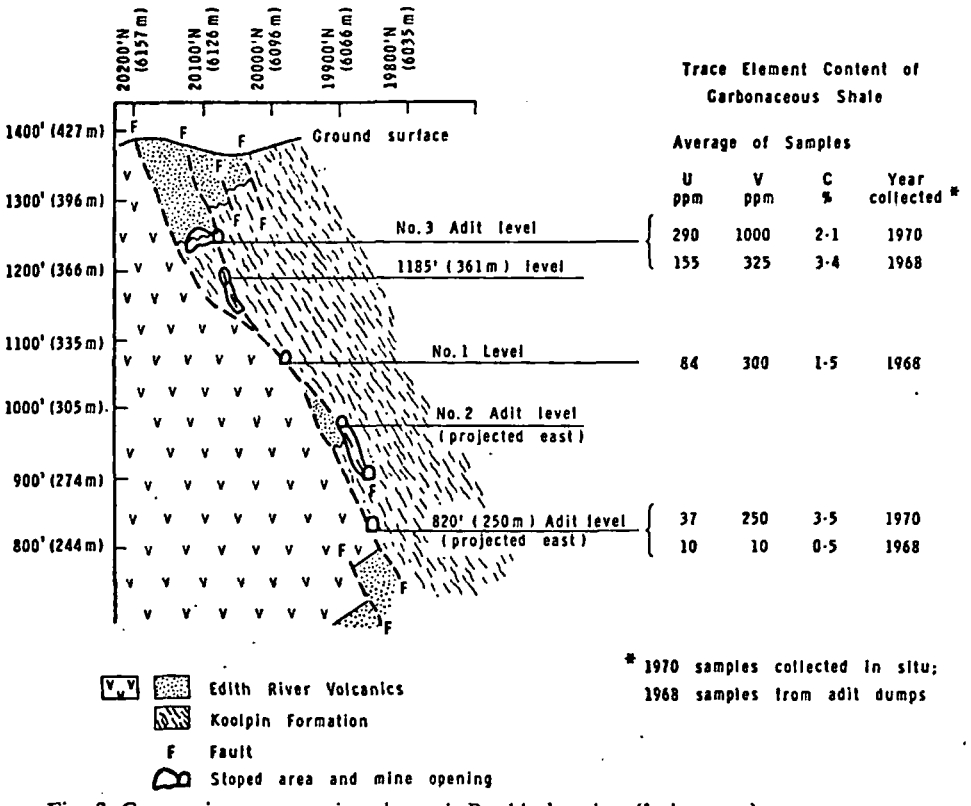

Fig. 3. Composite cross-section through Rockhole mine (facing east)

Because of the close spatial relationship between the ore deposits and carbonaceous shales, a study of the trace element geochemistry of the shales was made on two scales: by statistical analysis, on a suite of 59 samples collected from deposits up to 16 km apart; and by determination of trace element variations in the wallrocks of a single deposit, namely the Rockhole mine. This mine was chosen because it was more accessible (although not completely) and had a more regular shape than the other mined deposits.

1. *Rockhole Mine*

The mine has produced 13260 tonnes of ore averaging 11.1 kg U_3O_8/tonne taken from a number of small stopes, about 3 m wide and up to 15 m high, which were located along the 600 m strike length of a fault zone and over a vertical range of 91 m. Ore grades decreased with depth and at the lower level (820 ft (250 m)) were only 0.45 kg U_3O_8/tonne, considerably lower than the average for the mine. The host rocks are the basal sandstone member of the Edith River Volcanics and carbonaceous shales (with thin interbedded chert bands) of the Koolpin Formation faulted against a ferruginous rhyolite member of the Edith River Volcanics.

The most significant trace element data for the Rockhole mine are summarized in Figures 3 and 4. In Figure 3 the U, V and C concentrations shown are the average of several samples taken along the line of load for each of three levels, 820 ft (250 m), 1080 ft (329 m) and 1240 ft (378 m), with data for samples from adit dumps and those collected *in situ* presented separately. The systematic decrease in the U and V content of carbonaceous shales with depth, contrasts with the varying distribution of carbon, which at each level has a broad distribution of values. The elements Cu, Ni,

(Anyoute) Coronation Member (Sandstone)	100	N.D.	<20	300	10	8	3	<20	n10	N.D.	10	40	100	15	100								
Fisher Creek Siltstone	10	2000	30	100	4	30	<3	40	<20	N.D.	<10	100	15	100									

Major elements, and U, by X-ray fluorescence. Minor elements by optical emission spectroscopy. Th by spectrophotometric analysis.
N.D. = not detected. nx means element line could not be detected; sensitivity for that element x ppm.

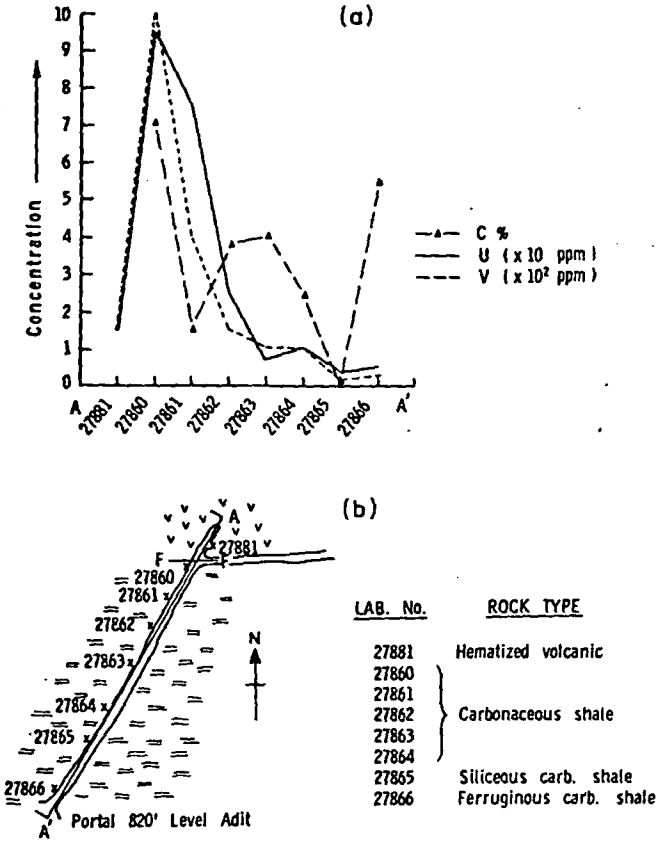

Fig. 4. Geochemical profile along part of Rockhole 1 adit (820′ level)

Co and Ga have the same distribution as for U and V.

A number of samples were taken from the line of the lode out into the carbonaceous shale wallrocks. The samples were taken along an access adit at the 250 m level, from the fault, extending in a southerly direction for 100 m. Figure 4 shows a plan of part of the 250 m level, with the fault contact of carbonaceous shale against volcanics and line of lode, the access adit, and location of samples taken along the section AA′. Above this, are shown trace element data for the samples, which have the following features. The erratic carbon values noted previously are well illustrated here, with a range of 0.1% to 7.0%, compared with U and V, which are independent of C, and increase systematically in the carbonaceous shales towards the fault, dropping to low values in the footwall volcanic rocks. B, Na and Ni also show this pattern.

The C content of the carbonaceous shales, then, depends on their stratigraphic position and thus on the original depositional composition of the rock. U and V distributions are independent of C, and therefore rocktype, and instead they have two controls that indicate an epigenetic origin — faulting, and reaction with wallrock. The fault control is evident and the reaction with wallrock is seen in the higher element concentrations in carbonaceous shale to the south of the fault (Fig. 4) and lower concentrations in the volcanics to the north of the fault.

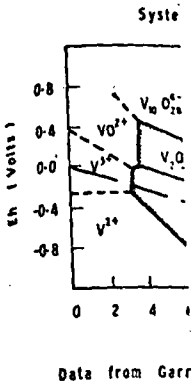

Fig. 5. Eh–pH

2. *El Sherana*

Additional evi
naceous shale
El Sherana mi
two siltstone
both showed
side of the con
in Figure 4. T
observation th
were mostly
contacts, are s
that carbonace
alization and s
ore fluid and
shales are note
(TAYLOR 1972)
most likely, a
consideration
uranium and th

Most notable is
tion which has
Plateau deposi
between Figur
et al. 1959). Fig
for U and V
1965). These
and V have a
water (Eh + 0.
(slightly lower
elements are
ported; indee
they will be

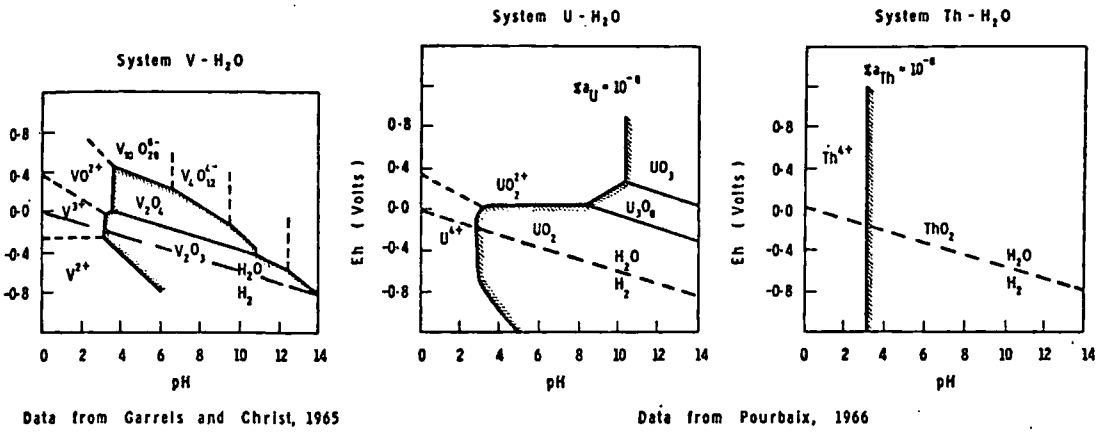

Fig. 5. Eh–pH equilibrium diagrams at 25 °C (Cross-hatched areas represent insoluble species)

2. *El Sherana Mine*

Additional evidence for the uranium-carbonaceous shale relationship was obtained at the El Sherana mine, where samples collected at two siltstone-carbonaceous shale contacts both showed higher uranium on the shale side of the contact. One of these is illustrated in Figure 4. These data, combined with the observation that ore shoots at El Sherana were mostly at siltstone-carbonaceous shale contacts, are strong evidence of the control that carbonaceous shale has had over mineralization and suggests a reaction between the ore fluid and the shales. Since carbonaceous shales are noted for their reducing properties (TAYLOR 1972), a redox control of uranium is most likely, and this opinion is supported by consideration of the elements associated with uranium and their redox stability fields.

Most notable is the uranium-vanadium association which has also been observed for Colorado Plateau deposits. (There is a striking similarity between Figure 4, and Figure 51 in GARRELS *et al.* 1959). Figure 5 includes Eh-pH diagrams for U and V at 25 °C (GARRELS and CHRIST 1965). These show that at a pH about 7, U and V have a similar Eh response. In surface water (Eh + 0.5 V at ph 7) and groundwaters (slightly lower Eh) the stable phases for both elements are soluble and they will be transported; indeed, under these Eh-pH conditions they will be leached from rocks having any available U and V and taken into solution. If, however, the Eh drops to values of about 0.0 V (at pH 7), and this is the case for near equilibrium conditions in the presence of carbonaceous material, the stable phases for U and V are insoluble and they will precipitate.

The geochemistry of the other elements associated with U is more complex, but they too could have been transported by groundwater and precipitated by interaction with carbonaceous shales (POURBAIX 1966; GARRELS and CHRIST 1965).

3. *The Deposits in General*

In the statistical analysis of 59 samples collected from four ore deposits, linear correlation coefficients were determined for the 23 elements analysed. Of these, only seven showed significant positive associations (at the 95% confidence limit level) with uranium (Table 4).

Table 4. *Significant element correlations with uranium*

	Confidence level 99%	95%
A. All carbonaceous shales	Cu V	Ga
B. Rockhole shales	Cu	V Cr Zr
El Sherana shales	V	Zr
Palette shales	—	Ba SiO_2

The significant element associations for uranium were considered in two groups — A, in which all shales were analysed together, and B, in which the shales from the Rockhole mine, El Sherana, and Palette were considered separately.

Considering all the carbonaceous shales, it is clear that U is strongly associated with Cu, V and Ga. From the data of Vine and Tourtelot (1970) it would appear that Cu, V and U can be related to either the organic fraction or the minor-element fraction of the shales. The association of U and Ga is with the detrital fraction. From the statistical data, it is also clear that U is not related in any way to variation in the total carbon of the shales (total carbon = organic carbon + mineral carbon) since a negative correlation at the 90% level is shown. Thus, although U is present in most of these carbonaceous shales (average 96 ppm), those with high total C do not necessarily contain high U values.

This result is more in accord with the hypothesis that the carbonaceous shales have provided a suitable reducing environment for uranium to precipitate and that it associates with multivalent Cu and V, than with the hypothesis that carbonaceous matter has concentrated the uranium during deposition. In the latter case, U could be expected to associate with organic matter, and the high U values would correlate with high carbon.

When the shales are grouped according to location (Table 4, group B), a strong correlation between U and V is observed only for Rockhole and El Sherana mines. (Zr and Cr apparently indicate a lesser association with the detrital fractions.) With the Palette samples, however, the association is with Ba and SiO_2, which would seem to indicate that U is associated with these elements in secondary minerals.

The data presented so far, can be accounted for by a mechanism involving transport of uranium as uranyl complexes in groundwater (or artesian water) in the sandstone conglomerate aquifer above the unconformity. Where the underlying shales (which would otherwise have been isolated by a weathered zone produced during Middle Proterozoic erosion) have been brought into contact with the groundwater by faulting, suitable conditions would have existed for the subsequent reduction and precipitation of uranium. Such a mechanism would explain:

1. the pitchblende/carbonaceous shale association,
2. the decreasing ore grades and trace element distributions in wallrocks with depth,
3. the location of the orebodies at the unconformity and limited vertical extent below that,
4. the fault control of orebodies,
5. the trace element associations of uranium, and is in agreement with the known behaviour of uranium under varying Eh conditions.

The source of the uranium in this groundwater is suggested to be the acid volcanics near the base of the Carpentarian sequence. Uranium is known to be a mobile element in surface and near-surface conditions and since the Edith River Volcanics have been reconstituted, uranium could have been released during alteration of primary mineral assemblages. Most acid igneous rocks in the Darwin-Alligator Rivers areas have higher-than-average radioactivity, and abnormally high radioactivity is common for the Edith River Volcanics (Stewart 1965). Our analyses indicate up to 25—30 ppm U for the volcanics and since Rosholt and Noble (1969) and Rosholt *et al.* (1971) have shown that crystallized volcanic rocks have probably lost 60% of their original uranium, the original values for the Edith River Volcanics were probably higher. Additional evidence for uranium loss is obtained from the Eh-pH diagrams for U and Th. Under most natural Eh-pH conditions Th has only one stable compound (ThO_2), which is essentially insoluble. This contrasts with the mobile element uranium, which may have one of several forms (Fig. 5). Under oxidizing conditions, the comparatively soluble uranyl ion is the stable compound. Uranium and thorium, therefore, are fractionated during surface and near-surface processes and the Th/U ratio may be used as an indicator of the extent of uranium leaching from these volcanic rocks.

Table 5 compares U, Th data on the acid Edith River Volcanics with the average for similar rocks throughout the world. The element concentrations are higher than for average

Table 5. *Comp*

Rock Type	
Reported Rhy Edith River V	

* Imbo *et al.*

rhyolites but
The average
above the ran
It could be
River Volcan
in the region
of U relative
ratio.

If it is assur
leached from
culations sho
have provide
extracted fro
assumed that
a conservativ
recorded nea
WART 1965) —
of volcanics
a small fracti
Alligator Vall

VI. Discussio

Hypotheses p
origin of the u
two possible
of uranium in
pin Formatio
supergene pr
1955; Pricha
uranium from
HERD 1962; T
Considerations
these hypothe

1. Although
bonaceous sh
higher than i
geochemical
elements in t
ment appear

Table 5. *Comparison with world averages, of U and Th in Edith River Volcanics*

Rock Type	Th (ppm)		U (ppm)		Th/U	
	Range of Variation	Arith. Mean	Range of Variation	Arith. Mean	Range of Variation	Arith. Mean
Reported Rhyolites*	6.0–56.0	27.8	2.0–35.0	8.4	1.5–2.5	2.1
Edith River Volcanics	12.0–56.0	33.1	8.0–35.0	13.4	1.3–5.5	2.8

* IMBO *et al.* (1968).

rhyolites but fall within the reported range. The average Th/U ratio of 2.8 is, however, above the range of 1.5–2.5 for other rhyolites. It could be expected, then, that the Edith River Volcanics originally had a Th/U ratio in the region of 2.1, but that subsequent loss of U relative to Th has resulted in the higher ratio.

If it is assumed that 10 ppm U have been leached from the Edith River Volcanics, calculations show that 3 km³ of rock would have provided all the uranium which was extracted from the deposits. If it is further assumed that the volcanics are 66 m thick — a conservative estimate in view of the 300 m recorded near Malone Creek Granite (STEWART 1965) — this would correspond to an area of volcanics of 5 km × 9 km, which is only a small fraction of the area of the South Alligator Valley (Fig. 2).

VI. Discussion

Hypotheses previously put forward for the origin of the uranium deposits have considered two possible modes: 1) syngenetic deposition of uranium in carbonaceous shales of the Koolpin Formation and its later concentration by supergene processes (CONDON and WALPOLE 1955; PRICHARD 1965) and 2) deposition of uranium from ascending mineralizers (SHEPHERD 1962; THREADGOLD 1960).

Considerations which are inconsistent with these hypotheses are as follows.

1. Although syngenetic uranium in the carbonaceous shales is at a concentration level higher than in the average shale, study of the geochemical association of uranium and other elements in the shales makes supergene enrichment appear unlikely. In addition, age relations suggest that the ores were formed in post-Middle Proterozoic time when there was a sediment cover of approximately 330 m. Eh conditions in the carbonaceous shale would therefore have been highly reducing, thus rendering the uranium immobile, even if it were only adsorbed on clays or organic matter.

2. Introduction of uranium by ascending mineralizing solutions is also unlikely since, as the deposition of U was redox controlled, any precipitation would be expected to have commenced at depth, thus resulting in higher ore grades at depth — the reverse of what is observed. The solutions at depth would also be expected to be of very low Eh. Additionally, such ascending mineralizers would not necessarily show the established close spatial relationship of ore with the Middle Proterozoic unconformity.

Preliminary data (Table 6) from sulphur isotope measurements of minerals associated with the pitchblende ores suggest that a high-temperature hydrothermal origin was not feasible. The δS^{34} values have a wide spread, typical of a low-temperature sedimentary source for the sulphur and not resembling the narrow range to be expected from sulphur of magmatic origin or from sulphur equilibrated at high temperatures during metamorphism.

It must be noted, however, that these results are for only a limited sampling from the ore deposits and need to be verified by additional measurements.

VII. Conclusions

It is concluded that the South Alligator pitchblende deposits were precipitated from groundwater, the ultimate source of uranium being

Table 6. δS^{34} *determinations for ore sulphides*

Sample No.	Locality	Mineral	δS^{34}
27843	Rockhole	Pyrite in fractures in sediment	+12.3
27844	Rockhole	Pyrite in fractures in sediment	+11.5
27880	Rockhole	Pyrite in fractures in sediment	+11.7
27922	El Sherana	Massive galena in ore	— 3.4
27923	El Sherana	Coarse galena in ore	+10.4
27939	El Sherana	Pyrite in carbonaceous shale	— 1.2
27953	El Sherana	Pyrite in veins in pitchblende	— 5.6

the Edith River Volcanics, particularly the Pul Pul Rhyolite Member and igneous components of the Coronation Member. The mineralogy of the igneous material of these rock units indicates that the rocks have undergone either weathering and oxidation or diagenetic recrystallization, either of which would aid the leaching of uranium by groundwater. The uranium-bearing groundwater percolated down to an aquifer, the sandstone-conglomerate unit at the base of the volcanics, which rested unconformably on essentially impervious shales and siltstones. Uranium was stable in the groundwater as a complex of the uranyl ion, provided there was no active reduction, in which case reduction of uranium to the insoluble UO_2 (pitchblende) would occur. It is suggested that precipitation of pitchblende (or a finely dispersed precursor) occurred where faulting brought the uranium into contact with the reducing action of carbonaceous shales. This conclusion is supported by the close association of pitchblende with faulting of carbonaceous shale against the overlying rocks.

On a regional scale, the availability of 'leachable' uranium would have been controlled by the extent of Carpentarian volcanics, and the migration of uranium-bearing groundwaters would have been influenced by the structure of the aquifer. Thus groundwaters would have been channelled away from structural highs in the Early Proterozoic unconformity surface and from anticlines in the Middle Proterozoic rocks. It is possible that basic igneous rocks, as well as carbonaceous shale, may have been reducers of uranium.

The striking similarity between the geological setting of the Koongarra deposit (Pederson 1973) and that of the South Alligator deposits suggests that the ore formation processes may have been similar also. However, there is an obvious need for additional studies to characterize other uranium deposits in the region and to test whether this hypothesis can be extended, or modified, to explain their origin.

Acknowledgements

The authors are indebted to United Uranium N. L. for assistance in the field. Dr. G. H. Taylor made many helpful suggestions during the course of the study and, with Dr. J. McAndrew, critically reviewed the manuscript.

The laboratory work was carried out at the CSIRO Division of Mineralogy and the authors wish to acknowledge the assistance of staff of the Geochemistry Section for the many chemical analyses, in particular, Mr. S. Goadby for XRF and Mr. N. Morgan for optical emission spectroscopy. Mr. D. Rigby arranged the computer programming for statistical treatment of the chemical data.

References

Compston, W., Arriens, P. A.: The Precambrian geochronology of Australia. Can. J. Earth. Sci. 5, 561 (1968)

Condon, M. A., Walpole, B. P.: Sedimentary environment as a control of uranium mineralization in the Katherine-Darwin region, Northern Territory. Bur. Miner. Resources Aust. Rep. 24 (1955)

Cooper, J. A.: On the age of uranium mineralization at Nabarlek, N. T., Australia. J. Geol. Soc. Australia 19, 483 (1973)

Garrels, R. M., Christ, C. L.: Solutions, Minerals and Equilibria. New York: Harper and Row 1965

— Larsen, E. S. 3:
R. G.: Detaile
relations in tw
Garrels, R. M
chemistry and
Plateau uranium
Paper 320 (1959

Hills, J. H., Richa
mineralization i
3, 382 (1972)

Imbo, G., Gaspari
A.: Contributio
arches by deterr
eruptive rocks.

Pedersen, C.: The
In Abstracts fo
in Australia", C
cialist Group in
(1973)

Pourbaix, M.: Atla
in Aqueous Solu

Prichard, C. E.: I
Alligator River,
ogy of Austral
8th Comm. Min

Rosholt, J. N., N
from crystallize
Planet Sci. Lett

— Prijana, Nobli
and thorium in
rocks. Econ. G

Shepherd, J. S.: U
Ph. D. Thesis, U

– Larsen, E. S. 3rd., Pommer, A. M., Coleman, R. G.: Detailed chemical and mineralogical relations in two vanadium-uranium ores. In: Garrels, R. M. and Larsen, E. S. 3rd; Geochemistry and mineralogy of the Colorado Plateau uranium ores. U.S. Geol. Survey Prof. Paper 320 (1959)

Hills, J. H., Richards, J. R.: The age of uranium mineralization in Northern Australia. Search 3, 382 (1972)

Imbo, G., Gasparini, P., Luongo, G., Rapolla, A.: Contributions to the volcanological researches by determination of the radioactivity of eruptive rocks. Bull. Volcanol. 32, 317 (1968)

Pedersen, C.: The Koongarra Uranium Deposit. In Abstracts for the Symposium "Uranium in Australia", Geol. Soc. of Aust. Inc., Specialist Group in the Genesis of Ore Deposits (1973)

Pourbaix, M.: Atlas of Electrochemical Equilibria in Aqueous Solutions. Oxford: Pergamon 1966

Prichard, C. E.: Uranium deposits of the South Alligator River, Northern Territory. In: Geology of Australian Ore Deposits (2nd edn.) 8th Comm. Min. Metall Congress 1, 219 (1965)

Rosholt, J. N., Noble, D. C.: Loss of uranium from crystallized silicic volcanic rocks. Earth Planet Sci. Letters 6, 268 (1969)

– Prijana, Noble, D. C.: Mobility of uranium and thorium in glassy and crystallized volcanic rocks. Econ. Geol. 66, 1061 (1971)

Shepherd, J. S.: Uranium in Northern Australia. Ph. D. Thesis, University of Queensland (1962)

South, S. A.: Uranium in Australia. Atomic Energy in Australia (1972)

Stewart, J. R.: Middle Proterozoic volcanic rocks in the Katherine-Darwin area, Northern Territory. Bur. Miner. Resources Aust., Report 90 (1965)

Taylor, G. H.: Carbonaceous matter – a guide to the genesis and history of ores. Soc. Mining Geol. Japan, Special Issue 3, 283 (1972)

Taylor, J.: Origin and controls of uranium in the South Alligator Valley. Atomic Energy in Australia 12, 18 (1970)

Threadgold, I. M.: The mineral composition of some uranium ores from the South Alligator River Area, Northern Territory. Mineragraphic Investigations Technical Paper No. 2, CSIRO Melbourne (1960)

Vine, J. D., Tourtelot, E. B.: Geochemistry of black shale deposits – a summary report. Econ. Geol. 65, 253 (1970)

Walpole, B. P., Crohn, P. W., Dunn, P. R., Randal, M. A.: Geology of the Katherine-Darwin Region, Northern Territory. Bur. Miner. Resources Aust. Bull. 82 (1968)

Received July 17, 1974

D. E. Ayres and P. J. Eadington

CSIRO Division of Mineralogy, Minerals Research Laboratories, P.O. Box 136, North Ryde, NSW, Australia 2113

Economic Geology
Vol. 74, 1979, pp. 260–284

On the Geochemistry and Origin of the D Tree, Wonarah, and Sherrin Creek Phosphorite Deposits of the Georgina Basin, Northern Australia

PETER F. HOWARD AND M. J. HOUGH

Abstract

The early Middle Cambrian phosphorites of the Georgina Basin were deposited in shallow nearshore marine environments varying from lagoonal, estuarine, littoral, to intertidal. Some deposits show penecontemporaneous erosion by stream channels in addition to subaerial weathering during periods of regression. There are three distinct types of phosphorite: mudstone phosphorite, replacement phosphorite, and pelletal phosphorite, the latter two were formed by diagenetic phosphatization of carbonate skeletal sands, bioclastic and micritic limestones, and dolomites. By comparison, the mudstone phosphorite, which predominates in the three deposits studied, shows little textural evidence of such an origin and has been accepted as an orthochemical sediment. However, this paper proposes a diagenetic origin identical to the other types.

Some fifteen known deposits occur over a distance of about 1,000 km along the periphery and insular portions of the basin. The geochemistry of two of these deposits, D Tree and Sherrin Creek, which lie 75 km apart on the eastern edge of the basin, has been studied and compared with that of the Wonarah deposit, which lies within the basin 200 km to the west. Fifty-eight analyses reveal four element associations: apatite group (Ca, P, F), clay group (Al, K, Ti, Cr, Zr), heavy minerals group (Fe, Mn, Zn, Ni, Cu), and a leached group. Although the elements Na, S, CO_2, Y, La, Ce, Sr, U, and Th correlate with apatite in the little-leached Sherrin Creek deposit, they exist as a separate leached group, or correlate with clays, in the more leached D Tree and Wonarah samples. Ba, V, Cu, and Pb do not behave to a consistent trend. The strongest correlations in the leached deposits are at a lower level of significance than at D Tree.

Intense Cenozoic weathering extends beyond the maximum known depth of phosphorite. It, together with certain though unquantifiable Cambrian subaerial weathering effects, has been responsible for leaching, increasing in the order Sherrin Creek, D Tree, and Wonarah. Uranium, Th, La, Ce, Y, Ba, Sr, Na_2O, SO_3, and CO_2 are leached from the system to the extent of 45 to 80 weight percent. Comparison of the composition of leached and unleached phosphorites suggests there were discernible differences in the geochemistry of waters in the different embayments at the time the phosphorites were formed.

Introduction

THE early Middle Cambrian phosphorite deposits of of the Georgina Basin in northern Australia, discovered in the period 1966–1968, comprise fifteen known deposits occurring over a distance of approximately 1,000 km along the periphery and insular portions of the basin (Fig. 1). They contain proven, indicated, and inferred reserves approaching 4 billion tons. Due to economic factors, none of the deposits are currently in production, Duchess having ceased operations in August 1978. The exploration techniques, history of the exploration activity, and discovery of these deposits is best covered by Thomson and Russell (1971) and Howard (1971).

The phosphorites are located in the Beatle Creek Formation and various lateral equivalents such as the Wonarah Beds and the Burton Beds. Since then, de Keyser (1973) and Cook (1976a) have proposed a framework of magnafacies defining lithosomes to correlate the numerous lithostratigraphic and biostratigraphic names into mappable rock units.

Figure 1 is a paleogeographic map showing the distribution of the phosphorite deposits with respect to the lithosomes which comprise the early Middle Cambrian sedimentary sequence. It can be seen that they everywhere overlie either Precambrian basement rocks, early Cambrian basic volcanics, or locally, on the fringes of the basin, the basal sandstone-conglomerate lithosome.

The geology and origin of some of the phosphorite deposits have been well described since they were found by de Keyser (1968, 1969, 1973), de Keyser and Cook (1972), Cook (1972), Russell (1967), Russell and Trueman (1971), Fleming (1974, 1977),

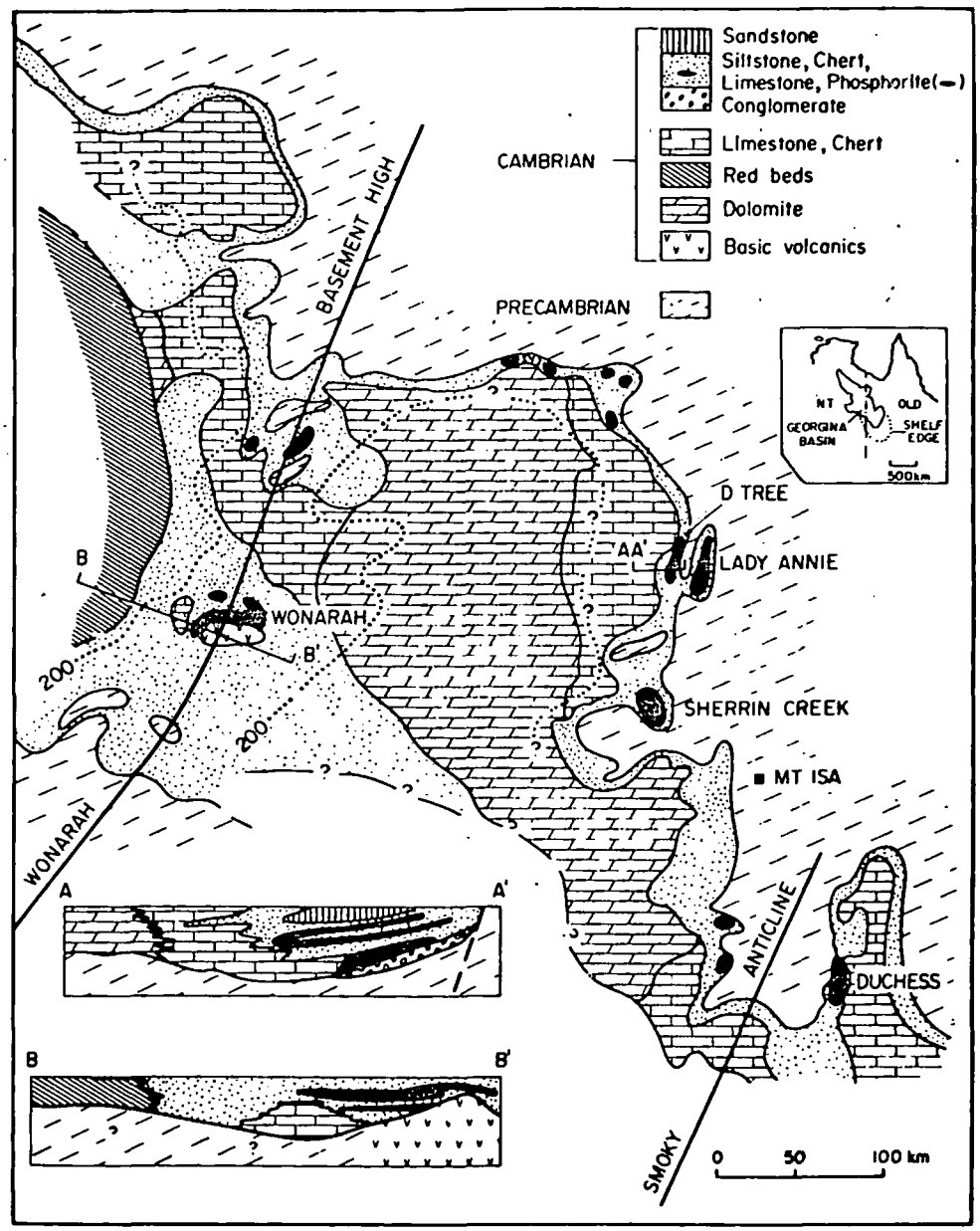

FIG. 1. Generalized paleogeographic map of the northeastern portion of the Georgina Basin showing the distribution of the early Middle Cambrian lithosomes and phosphorite deposits, (after Howard, 1972; and Cook, 1976a). The dotted lines indicate the approximate position and the reduced level (AMSL) of the top of the phosphatic unit at the point of its wedge out toward the center of the basin (after Howard and Perrino, 1976).

Rogers and Keevers (1976), Howard (1972), Howard and Cooney (1976), and Howard and Perrino (1976).

In the papers mentioned there has been much discussion of the petrological types of phosphorites and little agreement as to their origin. In his study of the geochemistry of the phosphorites of the Georgina Basin, Cook (1972) reported differences between the geochemistry of the pelletal and nonpelletal types and also the effects of laterization at one locality. However, as his analyses (17 major elements and 48 minor element analyses) embraced some six or more deposits, his results indicated broad but nonquantifiable differences in the types.

In this study the geochemistry of three deposits has been investigated comparatively, using data from Sherrin Creek and D Tree, 75 km apart on the eastern edge of the basin, and from Wonarah, equidistant from the first two and 200 km to the west (Fig. 1). The purposes of the study were three-fold: to

reexamine the geochemical differences among the petrological types; to detect differences in geochemistry of the deposits, knowing that they may have formed in unconnected subbasins and/or had different sources of nutrient waters; and to discuss the findings in terms of the several models which have been proposed for the genesis of the phosphorite types in the Georgina Basin as a whole.

Phosphorite Types

The Sherrin Creek, D Tree, and Wonarah deposits have generally similar dimensions ranging from 20 to 25 km long and 4 to 7 km wide. Each deposit parallels the Middle Cambrian shoreline and interfingers with an offshore limestone facies. The thickness of the phosphatic chert-siltstone-limestone-phosphorite lithosome varies from 27 m at Sherrin Creek to approximately 43 m at both D Tree and Wonarah, and the thickness of phosphorite in the orebodies ranges from 1 m to a maximum of 15 to 19 m at different localities. At Sherrin Creek the phosphorite occurs as a single bed whereas at Wonarah and D Tree the maximum thickness quoted above is the aggregate thickness of three beds. The beds exhibit sharp lateral and vertical facies changes from beds composed of chert and phosphorite to beds of phosphatic and barren siltstone (Howard, 1972; Howard and Cooney, 1976; Howard and Perrino, 1976).

There are three types of phosphorites; in order of abundance they are mudstone phosphorite, replacement phosphorite, and pelletal phosphorite.

Mudstone phosphorite: This phosphorite is generally a buff to tan soft rock contsisting of microcrystalline carbonate fluorapatite, detrital quartz, chert, clay, poorly crystalline mica, goethite, and phosphatized fossil debris. These detrital components may be evenly distributed through the sediment or distributed into thin silty laminae or lenses imparting an indistinct thin bedding. Large lenses of siltstone, phosphatized and/or silicified coarse coquina, and platy or nodular chert, containing phosphatized fossil fragments, are up to 30 cm thick. The mudstone phosphorite also contains thin beds of pelletal phosphorite.

Of importance is the presence of numerous thin brown, red, or black beds rich in base metals within the middle phosphorite unit. Such beds are shown by drilling to have a maximum grade and thickness of 45 percent Fe_2O_3, 6 percent MnO, and 1 percent combined base metals over one meter. The commonest mineral is goethite. Other minerals recognized in surface exposure are hematite, pyrolusite, malachite, and azurite. Separates from heavy liquid separation of drill hole samples are very fine grained and yield poor X-ray diffraction patterns. Preliminary study has identified goethite, natrojarosite, lithiophorite (Al, Li) MnO_2 $(OH)_2$, and a spinel phase, possibly franklinite, (Zn, Mn) Fe_2O_4, and/or gahnite, (Zn, Fe) Al_2O_4. The beds consist of the above-listed minerals together with detrital quartz and chert grains, kaolinite, and apatite, as a minor or major component, identifiable as mudstone or pelletal phosphorite. The metal dispersion patterns presented in Figure 2 c-g and discussed later indicate that the major proportion of the components in the beds are terrigenous and were derived from the mineralized Precambrian hinterland to the east.

Replacement phosphorite: There are two types of replacement phosphorites: first, buff to tan thin discontinuous beds of phosphatized coarse coquinas referred to above and, second, white to porcellanous massive beds of phosphatized calcarenite and micritic carbonate up to a meter thick.

Phosphatized coquina is common in the phosphorite beds at Wonarah and in the upper two beds at D Tree but is not recognized at Sherrin Creek. The fossil fragments may be wholly replaced by collophane, although silica replacement is locally prominent. At D Tree, when collophane and silica replacement are evident in the one rock, collophane everywhere appears to be the earlier. Where one portion of a bed is wholly replaced by buff to tan collophane, and the other portion by clear silica, the contact between the two is sharp and has not been observed to cut across bedding. The buff to tan color of the phosphatized coquina is similar to that of the enclosing mudstone phosphorite. De Keyser (1969) interpreted the color as organic staining, though some of it can be identified as a dusting of goethite.

The white and porcellanous phosphatized calcarenite and micritic carbonate, which forms the lowermost phosphorite bed at D Tree, was previously named "hardrock" by Howard and Cooney (1976), but the name "replacement phosphorite" used by Rogers and Keevers (1976) at Lady Annie is preferred as a more fitting descriptive name. The grade of the rock is about 30 to 40 percent P_2O_5 dependent on the percentage of quartz, chert, and clay in the original carbonate sediment. In the macroscopically featureless porcellanous variety, the original carbonate composition of the sediment is recognized by the presence of pseudomorphically replaced carbonate rhombs.[2] A second variety that has 1-cm-thick layers and fine laminae of detrital quartz and clay also shows microtextures and structures identi-

[1] Variously named nonpelletal phosphorite, collophane mudstone microsphorite, and phospholutite.

[2] Phoscrete, as defined by de Keyser and Cook (1972) forms as a thin white film on the weathered surface of high-grade replacement phosphorites. The usage of the term is reviewed under the heading of Discussion.

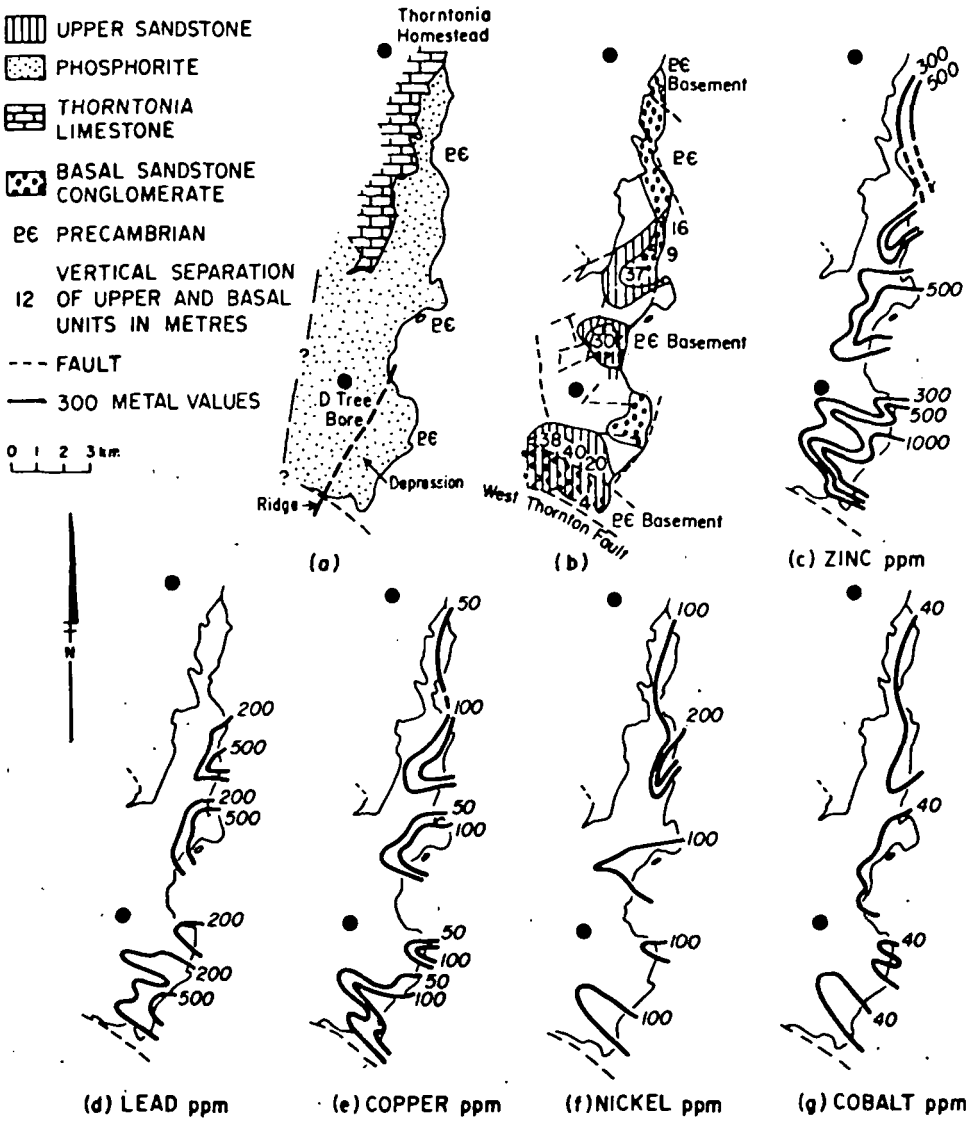

FIG. 2. Map showing (a) the surface and subsurface distribution of phosphorites and the outcrop of intertonguing Thorntonia Limestone; (b) the surface and subsurface distribution of the basal sandstone-conglomerate unit and upper sandstone unit of the Beetle Creek Formation, and (c) to (g) the distribution of the average zinc, lead, copper, nickel, and cobalt contents of the intervening phosphatic unit based on five element analyses of approximately 3,500 samples of 0.76 m interval intersections from approximately 70 drill holes. (a) also shows the location of a slight depression in the Precambrian basement east of a ridge or line of small hillocks.

cal with some of the carbonate rocks of the Thorntonia Limestone which interfinger with the phosphorite beds. These structures include wavy banding, graded bedding, cross-bedding, and scour and fill structures. Interbands of vuggy gray quartzitic chert exhibit similar features.

Pelletal phosphorite: This phosphorite is minor and is recorded only at D Tree and Wonarah. Where it occurs as laminae as little as 0.2 mm thick, the collophane pellets have diameters of 0.05 mm or less. In thick beds, up to 30 cm, the pellets range up to 1 mm in diameter (Howard and Cooney, 1976). The pellets may consist wholly of phosphatized fossil fragments, though, in general, approximately 50 percent of them are microcrystalline and featureless. The pelletal phosphorites are commonly uncemented by collophane mud and are therefore soft and friable. The type occurs as interbands within mudstone phosphorite and, as in the case of the middle phosphorite bed, it may contain brown, red, or black beds or laminae rich in base metals.

Geologic Setting

Because phosphorites do not crop out at Sherrin Creek or Wonarah, reference in this section is made principally to the D Tree area. The northern and

central portions of the D Tree deposit are interpreted to have been a narrow tapering lagoonal trough 1 to 3 km wide which at its southern end opened onto a shallow open-marine shelf (Figs. 1 and 2a). The southern portion is interpreted as an easterly trending embayment which shelved from open-marine to estuarine environments in the direction of the Lady Annie deposit (Howard and Cooney, 1976). Figure 2b illustrates the distribution of conglomerate and sandstone beds which underlie and overlie the phosphorite deposit and, together with section A-A′ in Figure 1, show their vertical separation. The nature of the facies (sorted quartz sands, through conglomerates, and ferruginous breccias) and their distribution in relation to the paleotopography of their depositional surface (Howard and Cooney, 1976) indicate environments varying from littoral to fluvial fan to submarine scree slides similar to those described at Lady Annie (Rogers and Keevers, 1976). The provenances of these rocks were tectonically active fault scarps in the Precambrian hinterland which were periodically active through the deposition of the whole of the chert-siltstone-limestone-phosphorite lithosome. Such tectonism had a marked effect on the depositional environment because it affected the nature and amount of detritus deposited but also for the physical effects tremors had on unconsolidated or partly lithified sediments. The period of tectonism coincided with eustatic changes in sea level.

Eustatic changes in sea level resulted in three transgressive-regressive cycles, upon which minor fluctuations of sea level are superimposed. These three cycles are (1) dolomite and limestone [3]—chert member [3] and phosphorite with base metals, (2) carbonate sands (replaced by chert)—phosphorite with base metals, and (3) phosphorite and carbonate sands (replaced by chert)—sandstone. Interbedded micritic and bioclastic carbonates of the Thorntonia Limestone which overlie the basal sandstones and conglomerates represent the first transgression. The most easterly extending portion of this limestone was replaced by carbonate fluorapatite during deposition or early diagenesis. Significant tectonic activity following replacement caused these partly lithified to lithified replacement phosphorites to slump due to gravity sliding prior to the deposition of younger rocks. At Sump Creek, one kilometer east of D Tree bore (Howard and Cooney, 1976), replacement phosphorite and interbedded gray quartzitic chert crop out in 10-m-high cliffs as vertical isoclinal folds where the slide was arrested by a basement hillock: flat-lying siltstone-chert overlies the structure. Elsewhere, chert breccias or phosphorite-chert breccia formed, the latter showing examples of comminution of phosphorite intraclasts down to rounded sand-sized grains by autogenous grinding during sliding. Present studies by P. N. Southgate [4] illustrate the presence of evaporite casts within chert breccias near the base of the Beetle Creek Formation elsewhere, suggesting that some breccias may have formed as a result of dissolution of evaporites.

The detrital ferruginous base metal beds, previously described, occur at the top of the basal sandstone-conglomerate lithosome and within the middle mudstone phosphorite bed. They have sharply defined lower boundaries but commonly have transitional tops, becoming increasingly diffuse basinward from the Cambrian shoreline. Such material, together wtih detrital quartz and clays, was contributed to the system in accessory proportions throughout the period of deposition of the phosphorite and phosphatic siltstone sections. The concentrated zones, however, represent periods of regression when residual ferruginous debris from the Precambrian erosion surface was flushed across tidal flats and into the lagoon and estuary. Subaerial exposure of the phosphorites was common on the basement high separating the lagoonal and the estuarine areas in the vicinity of the D Tree bore (Fig. 2). The most significant instance of exposure and stream erosion (Howard and Cooney, 1976) extends down the westerly axis of the estuarine zone, along which the ferruginous detritus was flushed further down the paleoslope and beyond the limits of drilling. The plots for the individual base metals (Fig. 2c–g) show identical dispersion patterns that are similar to the patterns of outwash of the underlying and overlying sandstones, conglomerates, and breccias, suggesting similarity in provenance. The metal values in Figure 2c-g are the respective means for the entire chert-siltstone-limestone-phosphorite lithosome. The distribution of metals associated with the individual ferruginous beds is similar though the concentrations in these horizons are substantially higher, attaining a maximum combined zinc-lead-copper grade of 1 percent over a 1 m interval.

Although the three transgressive-regressive-cycles are recognized at Wonarah, the basal sandstone-conglomerate is not evident in drill cuttings nor are the base metal-rich ferruginous outwash beds prominent, either because of the lack of mineralization in the basic volcanic hinterland or the distance of mineralization from the depositional site. At Sherrin Creek, sandstone-conglomerate beds are present above and below the phosphorite. However, only one phosphorite bed is present, and this likewise is lacking in base metal-rich ferruginous zones. It is

[3] Thorntonia Limestone.

[4] James Cook University, Townsville, Queensland.

possible that the phosphorite bed at Sherrin Creek was formed high on a basement structure during the transgression which deposited the upper phosphorite bed at D Tree.

Geochemistry

Sampling

Samples ranging from slightly phosphatic siltstone and dolomite to high-grade phosphorite were collected from the three widely separated deposits at Sherrin Creek, D Tree, and Wonarah (Fig. 1). All samples from the subsurface Sherrin Creek and Wonarah deposits are International Minerals and Chemical Development Corporation splits of air-return cuttings from Mayhew 1000 drill rigs. Because the D Tree deposit crops out largely as rubble, all samples from there are also drill hole splits, except 3A, 3C, FG53, and 21, which are from creek exposures.

The IMC sampling interval was 2.5 feet (0.76 m) and the technique of sampling was as follows. Cuttings from the interval were continuously returned and collected in a cyclone, the bulk sample from which was passed through a series of splitters to give a 2-kilogram sample for beneficiation studies, a 50-gram sample for preliminary 5-element analysis, and a 50-gram library sample. The reliability of the splitting was proven by multiple splitting and chemical analysis. Because the holes were not cased, contamination of a given sample interval by spalling from shallowed intervals was tested by drilling core holes alongside previously drilled "open" holes and comparing the chemistry of samples from corresponding intervals. Contamination could be illustrated where the volume of cuttings for 0.76-m intervals differed measurably, and, as this was not common, the open air-return cuttings holes were used generally. All samples in this study are from either the original 50-gram analytical pulp sample or the 50-gram library sample.

It is recognized that, although the 0.76-m interval is satisfactory for calculating ore grades, it involves some mixing of phosphorite types, in particular mudstone phosphorite with thin beds (1–30 cm) of replacement phosphorite after coquina. A further disadvantage of the drilling technique was that mudstone and pelletal phosphorite types are partly reduced to fine powder, and, though this largely destroys the gross fabric of the rock, chips still allow megascopic and microscopic observations to be made.

In all three deposits Cenozoic weathering extends below the maximum depth (61 m) of drilling. A few wildcat holes were drilled down to 108 m, but in no case was unoxidized sediment encountered. The phosphorites are varicolored and show least sign of weathering at Sherrin Creek, but at D Tree and Wonarah the phosphorites are variably weathered, in places extremely so, as illustrated by cavernous ground acting as ground-water solution channels.

Analytical methods

A total of 58 samples were analyzed for 30 major and trace elements. All except 47 fluorine determinations were measured in the Earth Sciences Laboratories at Macquarie University. Cutting and pulps were dried at 110°C and then ground in a Tema tungsten carbide mill. Apatite concentrates (Table 1, 7–12) were separated from Sherrin Creek samples (1–6) by ultrasonic disaggregation and centrifuging in heavy liquids (tetrabromoethane, di-iodomethane). Heavy minerals were similarly concentrated from samples high in Fe_2O_3, MnO, and base metals.

Major elements were determined in duplicate from lithium borate glass discs by Siemens X-ray fluoresence spectrometer, using USGS standards and the matrix correction procedure of Norrish and Hutton (1969). NBS120a was used as a phosphorus standard. Quartz and NBS120a were run as internal standards. Our data for NBS120a include: SiO_2, 4.68 ± 0.08 percent; SO_3, 0.88 ± 0.028 percent. Sodium was measured by flame photometry, ferrous iron by metavanadate titration, and H_2O^- by drying at 110°C for two hours. H_2O^+ and CO_2 were evolved by Leco induction furnace, H_2O^+ being absorbed on anhydrone and CO_2 on soda asbestos. An MnO_2 train removed any interfering HF, H_2S, and SO_2. The Phosphate Co-operative Company of Australia Ltd. determined fluorine by steam distillation and spectrophotometry, except for eleven samples which were done by X-ray fluorescence on pressed-powder pellets at Macquarie University.

Trace elements were measured by X-ray fluorescence on pressed-powder pellets, using USGS standards (Norrish and Chappell, 1967; Chappell et al., 1969). Quartz and NBS120a served as internal standards. Mass absorption coefficients were calculated from major element data. Our data for NBS120a include (in ppm): Ti, 697 ± 16; V, 72 ± 4; Cr, 76 ± 8; Mn, 178 ± 5; Ni, 18 ± 5; Cu, 38 ± 8; Zn, 97 ± 3; Ga, 2; Sr, 526 ± 1; Y, 113 ± 1; Zr, 82 ± 8; Ba, 34 ± 7; La, 73 ± 4; Ce, 76 ± 7; Pb, 20 ± 2; Th, 11 ± 1; and U, 94 ± 1 (two to nine replicate measurements).

The Australian Mineral Development Laboratories (Adelaide), on behalf of the International Minerals and Chemical Development Corporation, analyzed approximately 10,000 samples of drill cuttings for Cu, Pb, Zn, Ni, and Co by atomic absorption spectrometry, and these were used in the preparation of Figure 2.

TABLE 1. Major Element Analyses of Phosphorites, Phosphatic Siltstones, and Dolomites
Sample identification shown in Table 2.

	Sherrin Creek																		
Percent	1	2	3	4	5	6	7	8	9	10	11	12	13	14	15	16	17	18	19
P_2O_5	2.84	20.37	23.94	24.07	23.41	23.21	37.34	37.64	35.41	36.01	36.06	35.85	17.57	21.07	16.25	9.67	3.73	2.88	6.38
CaO	4.21	28.05	33.06	32.99	32.49	32.35	51.32	51.82	49.11	49.84	50.05	49.90	24.86	29.85	23.14	15.46	27.97	27.42	20.66
SiO_2	86.01	43.37	32.85	32.50	32.86	32.82	4.03	3.12	4.35	3.51	3.59	3.67	44.30	39.48	50.62	60.74	14.08	12.94	37.62
Al_2O_3	3.22	2.43	1.85	1.78	2.00	2.11	1.29	0.88	1.16	1.06	1.01	1.05	6.14	4.45	4.36	3.24	1.25	1.81	4.34
Fe_2O_3	0.75	1.00	3.14	3.13	3.18	2.86	0.40	0.81	3.80	3.23	3.16	3.07	0.96	0.66	0.99	3.31	1.57	1.36	1.33
FeO	0.00	0.40	0.00	0.00	0.00	0.00	0.00	0.22	0.00	0.00	0.00	0.00	0.11	0.17	0.00	0.00	0.00	0.00	0.00
MgO	0.21	0.27	0.25	0.25	0.36	0.43	0.23	0.26	0.26	0.28	0.32	0.32	0.29	0.29	0.25	0.66	16.96	17.00	8.73
Na_2O	0.02	0.15	0.22	0.16	0.19	0.21	0.34	0.35	0.28	0.34	0.33	0.27	0.12	0.16	0.14	0.12	0.05	0.05	0.10
K_2O	0.35	0.29	0.25	0.25	0.28	0.29	0.11	0.14	0.20	0.19	0.20	0.19	0.65	0.42	0.59	0.46	0.17	0.17	0.33
TiO_2	0.53	0.31	0.18	0.18	0.23	0.21	0.48	0.05	0.07	0.06	0.06	0.07	0.31	0.23	0.23	0.22	0.08	0.10	0.30
MnO	0.00	0.04	0.28	0.27	0.34	0.34	0.02	0.03	0.36	0.33	0.34	0.40	0.02	0.03	0.09	0.26	0.25	0.27	0.30
H_2O^+	ND	1.32	1.32	1.48	1.20	1.38	0.46	0.54	0.71	0.60	0.72	0.58	3.17	2.34	2.55	2.13	1.56	1.11	2.51
H_2O^-	0.00	0.00	0.00	0.00	0.00	0.00	0.00	0.00	0.00	0.00	0.00	0.00	0.00	0.00	0.00	0.00	0.00	0.00	0.00
CO_2	0.84	1.05	1.05	0.89	1.55	1.94	0.73	1.01	1.20	1.60	1.00	1.05	0.79	0.60	0.55	3.01	33.30	35.40	18.10
SO_2	0.10	0.55	0.66	0.68	0.63	0.65	0.97	1.04	0.99	0.99	1.03	1.01	0.41	0.53	0.43	0.25	0.18	0.14	0.21
F	ND	2.04	2.42	2.43	2.39	2.40	3.90	3.75	3.59	3.66	3.57	3.62	1.73	2.01	1.60	1.01	0.45	0.32	0.69
$-O \equiv F$	—	0.86	1.02	1.02	1.01	1.01	1.64	1.57	1.51	1.54	1.50	1.52	0.73	0.85	0.67	0.43	0.19	0.13	0.29
Total		100.78	100.45	100.04	100.10	100.19	99.98	100.09	99.98	100.11	99.94	99.53	100.70	101.44	101.22	100.11	101.41	100.84	101.26

	D Tree (Y99) north							Wonarah								D Tree (replacement)			
Percent	20	21	22	23	24	25	26	27*	28	29*	30	31	32	33	34	35	36	37	38*
P_2O_5	15.46	12.34	3.83	8.58	4.54	7.28	8.82	22.53	24.30	25.24	17.29	20.26	27.17	30.24	30.87	37.64	38.06	39.48	39.53
CaO	20.93	17.45	5.11	11.62	6.13	9.96	11.91	29.97	33.21	34.74	24.02	27.31	37.34	41.64	40.88	54.48	52.36	54.79	55.10
SiO_2	46.31	54.92	83.14	69.30	83.53	75.53	67.51	36.98	32.39	31.87	42.63	36.95	24.78	18.64	20.35	3.04	4.26	2.29	1.83
Al_2O_3	9.99	8.59	3.40	5.48	2.60	3.07	6.08	5.00	5.05	3.42	6.24	4.64	4.82	3.40	1.79	0.90	0.55	0.34	0.39
Fe_2O_3	0.86	0.93	1.12	0.98	0.60	1.23	1.15	0.59	0.97	0.72	2.89	5.34	0.90	1.37	1.17	0.46	0.36	0.15	0.36
FeO	0.00	0.00	0.00	0.00	0.08	0.00	0.00	0.00	0.00	0.00	0.00	0.00	0.00	0.00	0.00	0.00	0.00	0.00	0.00
MgO	0.21	0.22	0.12	0.12	0.22	0.11	0.16	0.21	0.18	0.26	0.32	0.20	0.32	0.31	0.18	0.26	0.18	0.23	0.27
Na_2O	ND	ND	ND	ND	ND	ND	ND	0.06	0.08	0.08	0.11	0.12	0.08	0.06	0.05	0.04	0.15	0.07	0.11
K_2O	0.76	0.93	0.72	0.62	0.26	0.44	0.74	0.36	0.40	0.52	0.72	0.48	0.50	0.34	0.13	0.11	0.07	0.02	0.08
TiO_2	0.45	0.41	0.17	0.27	0.10	0.15	0.35	0.18	0.23	0.18	0.42	0.30	0.23	0.16	0.09	—	0.02	0.01	0.02
MnO	0.00	0.01	0.09	0.15	0.10	0.23	0.14	0.02	0.19	0.04	0.08	0.15	0.01	0.02	1.20	—	0.05	0.03	0.06
H_2O^+	1.05	1.97	1.06	0.96	0.63	0.78	1.14	2.18	1.12	ND	2.51	2.39	1.74	1.22	1.13	ND	0.57	0.00	0.15
H_2O^-	0.65	0.00	0.34	0.00	0.00	0.43	0.81	0.62	0.41	0.35	1.01	0.00	0.28	0.36	0.00	0.00	0.00	0.00	—
CO_2	0.67	0.92	0.32	0.61	0.30	0.43	0.53	0.55	0.74	0.95	0.64	0.90	0.73	0.84	0.59	0.40	1.61	1.41	0.81
SO_3	0.17	0.28	0.15	0.16	0.06	0.15	0.24	0.27	0.20	0.17	0.26	0.25	0.22	0.22	0.15	0.12	0.16	0.19	0.26
F	1.51	1.19	0.36	0.87	0.44	0.73	0.82	2.02	2.47	2.54	1.72	1.94	2.60	2.93	2.93	3.42	3.72	4.15	3.72
$-O \equiv F$	0.64	0.50	0.15	0.37	0.19	0.31	0.35	0.85	1.04	1.07	0.72	0.82	1.09	1.23	1.23	1.44	1.57	1.75	1.57
Total	98.38	99.66	99.78	99.35	99.41	100.31	100.06	100.69	100.90	102.15	100.14	100.41	100.63	100.52	100.28	99.43	100.55	101.42	101.10

TABLE 1.—(*Continued*)

	D Tree central south																		
Percent	39	40	41	42*	43*	44*	45	46*	47	48	49*	50	51	52*	53	54	55*	56	57*	58
P_2O_5	7.77	27.45	26.48	15.90	16.32	18.60	26.85	14.87	24.39	23.62	23.09	14.43	15.89	25.63	20.03	20.59	26.80	27.89	21.94	23.07
CaO	10.36	38.93	37.49	21.61	22.41	25.14	37.47	19.99	32.94	31.98	31.45	19.24	21.70	34.87	27.08	27.72	36.66	37.78	30.11	31.35
SiO_2	49.93	26.37	28.44	48.99	50.84	30.93	27.10	46.70	30.86	35.98	23.52	35.41	38.63	23.83	43.25	34.52	21.65	21.35	35.18	33.84
Al_2O_3	5.25	2.26	2.30	6.04	3.36	6.76	3.14	3.48	2.10	3.06	3.15	1.90	5.46	3.75	3.30	6.35	5.27	4.91	4.14	4.90
Fe_2O_3	20.05	1.08	1.14	1.28	2.58	11.67	0.83	9.87	4.58	0.64	13.10	22.99	9.94	5.22	2.33	4.48	2.63	2.64	3.06	1.23
FeO	0.00	0.06	0.11	0.01	0.00	0.00	0.00	0.00	0.00	0.12	0.00	0.00	0.00	0.00	0.00	0.00	0.00	0.00	0.00	0.00
MgO	0.25	0.17	0.24	0.23	0.19	0.27	0.25	0.14	0.19	0.17	0.21	0.16	0.31	0.28	0.14	0.20	0.24	0.25	0.22	0.23
Na_2O	0.15	0.24	0.23	0.17	0.22	0.11	0.18	0.07	0.19	0.08	0.08	0.09	0.16	0.04	0.03	0.01	0.20	0.16	0.09	0.05
K_2O	1.95	0.72	0.75	0.91	0.50	1.08	0.62	0.31	0.46	0.45	0.56	0.22	1.22	1.04	0.30	0.61	0.38	0.46	0.66	0.84
TiO_2	0.28	0.13	0.14	0.32	0.18	0.34	0.21	0.16	0.11	0.17	0.16	0.09	0.25	0.24	0.15	0.27	0.20	0.24	0.23	0.27
MnO	2.87	0.01	0.02	0.03	0.05	0.13	0.04	0.16	0.32	0.03	0.13	0.37	1.17	0.85	0.18	0.54	0.06	0.33	0.46	0.12
H_2O^+	3.87	0.87	0.89	2.28	1.50	3.10	0.75	ND	1.56	1.67	1.91	3.44	3.22	2.02	1.69	2.79	2.36	2.21	1.94	1.86
H_2O^-	0.67	0.00	0.00	0.43	0.46	0.69	0.30	ND	0.31	0.34	0.00	0.00	0.00	0.48	0.00	0.00	1.02	0.00	0.00	0.33
CO_2	ND	0.91	1.08	0.62	0.56	0.93	1.11	ND	0.63	0.78	0.87	0.51	0.74	0.50	0.65	1.14	0.73	0.68	1.10	0.69
SO_3	0.17	0.51	0.50	0.31	0.35	0.31	0.51	0.12	0.23	0.18	0.18	0.10	0.19	0.15	0.11	0.10	0.25	0.18	0.19	0.13
F	0.78	2.93	2.78	1.61	1.70	1.63	2.73	1.55	2.42	2.45	2.40	1.42	1.59	2.63	1.80	1.87	2.47	2.81	2.28	2.38
$-O = F$	0.33	1.23	1.17	0.68	0.72	0.69	1.15	0.65	1.02	1.03	1.02	0.62	0.67	1.11	0.76	0.79	1.04	1.18	0.96	1.00
Total	98.02	101.41	101.42	100.06	100.50	101.00	100.94		100.27	100.69	99.79	99.75	99.80	100.42	100.28	100.40	99.88	100.71	100.64	100.29

ND = not determined.
* Fluorine by X-ray fluorescence.

Interpretive techniques

Our data are listed in Tables 1 and 2, grouped according to geographic distribution, namely Sherrin Creek, northern D Tree (Y99), central and southern D Tree, and Wonarah.

Kendall's rank correlation coefficient (Conover, 1971, chapter 5.5) was calculated for each element pair in each geographic group (Tables 1 and 2). This distribution-free measure of correlation was used because the data for some elements are markedly skewed, and for others there are too few data to ascertain the statistical distribution. An X-Y scatter diagram was plotted for each correlation significant at the 95 percent level to test its validity. If an outlying data point seriously biased the correlation coefficient, it was subjectively discarded and the coefficient recomputed.

Element association

The positive interelement correlations of highest significance in each geographic group are listed in Table 3 and schematically summarized in Figure 3. Mg and Ga data are not precise and are excluded from consideration, as is Si, whose distribution is controlled by quartz. The intercorrelations define four distinct associations, recognized as apatite, clays, heavy minerals, and a leached group, even though the individual intercorrelations differ from one geographic locality to another. Each element association reflects a grouping of elements: structurally substituted in major minerals (e.g., apatite); adsorbed onto a mineral surface; or existing in discrete minerals derived from a major mineral by weathering. Many of the trace elements actually exist in more than one association but their correlation is masked by a more significant correlation.

Those reduced major axis regression plots which are the most significant in terms of structural substitution in the case of carbonate fluorapatite are reproduced in Figure 4. Positive correlations between trace elements and CaO and P_2O_5 are interpreted as structural substitutions in apatite; and negative correlations are interpreted as lack of substitution and an association with other minerals. To check against the possibility that positive correlations were due to extraneous minerals locked within the apatite grains, high-grade samples from Sherrin Creek were studied on a scanning electron microscope and probed for Ca, P, F, and Na. No heavy mineral contaminants were observed and the Na analysis was close to the normalized values of that element in Table 4.

Figures 3 and 4 show a progressive decrease in the trace element substitution in the apatite structure coinciding with the appearance of a separate element association, the leach group, and increasing com-

TABLE 2. Minor Element Analyses of Phosphorites, Phosphatic Siltstones, and Dolomites

Analysis	Sample no.		P_2O_5 (%)	Ti [10]	V [2]	Cr [2]	Mn [10]	Ni [2]	Cu [5]	Zn [2]	Ga [2]	Sr [2]	Y [2]	Zr [2]	Ba [5]	La [2]	Ce [5]	Pb [2]	Th [2]	U [2]
Sherrin Creek																				
1	Y331	30B	2.8	3,164	65	261	71	10	20	48	6	54	93	243	136	39	86	40	13	5
2		31B	20.4	1,680	71	124	379	9	31	177	<2	123	262	168	125	68	79	62	14	19
3		32B	23.9	1,176	97	107	2,541	38	44	378	3	138	262	104	494	70	67	56	12	20
4		33B	24.1	1,168	96	96	2,559	33	37	384	2	141	264	95	532	75	77	56	17	16
5		34B	23.4	1,349	103	99	3,151	40	31	371	2	139	264	123	572	70	76	64	17	19
6		35B	23.2	1,321	101	88	3,065	31	29	341	2	141	280	103	485	81	94	67	17	21
7	Y331	30C	37.3	4,624	50	50	140	3	33	58	2	216	624	160	55	148	214	77	27	32
8		31C	37.6	524	54	20	402	12	40	178	3	195	442	58	89	115	95	62	23	31
9		32C	35.4	686	118	19	3,505	35	26	457	<2	190	371	55	706	100	84	49	21	22
10		33C	36.0	580	112	25	3,234	42	36	421	4	192	373	54	654	94	87	50	24	20
11		34C	36.1	565	109	27	4,243	45	41	432	2	193	379	52	769	99	90	51	24	23
12		35C	35.3	481	119	30	4,962	44	31	426	<2	198	408	53	828	102	101	56	22	27
13	Y333	22B	17.6	2,385	81	105	202	4	10	41	7	312	340	137	310	96	133	64	20	36
14		23B	21.1	1,741	54	107	276	9	24	45	6	181	270	96	182	84	107	68	14	33
15		24B	16.3	1,694	61	126	781	11	20	74	7	141	222	95	305	78	93	92	18	40
16		25B	9.7	1,538	152	146	2,424	51	35	463	3	100	148	92	531	50	72	72	12	42
17		26B	3.7	512	55	<5	2,476	20	<5	219	2	62	48	32	174	14	29	40	10	20
18		27B	2.8	671	58	51	2,683	21	7	200	2	59	40	44	151	15	17	36	11	22
19		28B	6.3	2,206	78	72	2,858	26	11	230	6	83	92	111	206	38	80	61	16	35
D Tree (Y99) north																				
20	Y99	18,157	15.5	3,057	114	77	85	13	57	71	12	227	482	143	380	142	169	59	28	61
21		18,158	12.3	3,374	129	76	116	19	89	99	12	127	355	133	244	99	142	45	18	38
22		18,170	3.8	1,459	113	34	931	53	121	167	5	78	66	56	301	37	47	84	8	19
23		18,171	8.5	2,550	138	50	952	60	122	176	7	89	103	108	433	48	72	91	10	28
24		18,172	4.5	868	52	24	925	37	94	117	3	64	36	39	205	22	33	46	3	19
25		18,173	7.2	1,329	91	25	2,020	79	215	224	4	42	46	52	276	25	31	44	7	30
26		18,176	8.3	2,919	99	43	822	59	189	192	7	187	67	146	269	33	67	76	11	28
Wonarah																				
27	W20	19,659	22.5	1,545	52	53	127	39	58	67	4	218	163	94	178	45	68	145	6	53
28	W60	21,879	24.3	2,204	107	39	763	49	119	230	<2	145	46	92	127	24	59	1,049	9	23
29	W65	21,970	25.2	1,318	55	59	146	14	45	158	4	83	95	63	151	41	40	117	6	21
30	A50	22,295	17.3	3,136	45	44	731	75	62	235	7	89	214	138	186	48	70	35	6	7
31		22,296	20.3	1,483	34	41	743	89	117	302	9	115	336	111	126	41	51	68	5	12
32	W119	23,957	27.2	1,712	73	42	99	21	57	216	3	96	133	80	113	31	52	282	7	24
33		23,958	30.2	1,318	68	39	134	31	64	346	4	136	91	65	110	32	34	323	4	29
34		23,980	30.9	899	181	31	9,804	28	158	303	28	46	42	116	95	28	35	6,356	13	<2
D Tree (replacement)																				
35	FG53		37.6	400	50	20	700	10	10	ND	ND	70	ND	ND	80	ND	ND	400	ND	ND
36	Y116	17,252	38.1	117	2	3	119	40	81	1,047	8	74	8	26	18	5	<5	1,662	2	45
37	3C		39.5	32	7	18	134	16	52	80	<2	81	6	13	5	26	15	134	8	36
38	3A		39.5	23	2	<2	439	45	76	88	<2	50	8	16	64	12	5	570	2	18
D Tree central south																				
39	Y114	17,056	7.8	2,004	86	53	18,129	321	9	2,914	9	79	60	62	240	38	48	165	5	41
40	Y142	17,672	27.4	1,321	93	68	112	70	57	441	5	174	339	65	282	76	86	62	8	86
41		17,673	26.5	1,067	64	84	134	41	33	445	3	170	364	69	261	94	91	60	6	78
42	Y114	17,811	15.9	2,663	165	120	213	47	75	179	9	129	165	92	362	56	79	75	9	21
43	Y199	19,339	16.3	1,549	52	29	332	102	65	481	8	230	217	86	194	43	57	77	14	19
44	Y203	19,448	18.6	2,924	161	60	996	77	80	819	12	212	225	136	533	81	114	355	16	55
45	Y273	20,981	26.8	1,551	83	111	361	80	48	240	4	138	461	71	313	120	110	66	10	28
46	Y116	17,230	14.9	1,189	54	19	941	69	72	536	8	95	92	54	385	30	58	108	6	8
47		17,240	24.4	899	27	30	1,976	55	65	1,092	5	76	52	35	187	29	19	109	4	11
48	Y120	18,436	23.6	1,365	68	32	198	33	62	211	4	69	129	62	158	47	57	63	5	14
49		18,437	23.1	1,305	174	32	870	93	112	2,054	8	65	95	51	129	60	54	472	8	17
50		18,440	14.4	691	121	9	2,710	165	110	2,324	5	52	34	31	160	33	13	327	4	13
51	Y198	19,324	15.4	2,252	182	45	7,756	243	264	1,809	8	45	100	82	514	50	75	177	9	34
52	Y199	19,335	25.6	1,928	37	13	5,139	109	60	1,405	2	61	20	89	337	18	28	748	9	11
53	Y203	19,460	20.0	1,181	39	18	1,273	52	54	226	4	65	49	47	189	24	28	270	4	74
54		19,473	20.6	2,011	90	77	2,346	66	82	646	7	150	58	72	514	31	56	226	6	25
55	Y214	19,961	26.8	2,198	62	34	541	54	67	316	9	141	193	60	497	62	88	73	7	13
56		19,965	27.9	1,965	58	23	1,983	71	63	523	6	68	37	57	263	20	56	60	6	19
57	Y231	21,246	21.9	1,614	101	82	2,523	55	96	404	6	60	80	72	386	35	51	151	2	28
58	21		23.1	1,722	56	29	920	13	67	63	6	43	44	69	224	38	22	63	14	26

ND = not determined.

All elements in ppm, except P_2O_5(%).

The number in square brackets is the detection limit of each trace element (in ppm).

Y331, W20, etc., denote drill hole numbers; 19,659 and 30B are sample numbers of splits from bulk samples; 30C is a concentrate from 30B; 3A, 3C, and FG53 are samples from Sump and Galah Creeks; and 21 is from Cowlick Creek.

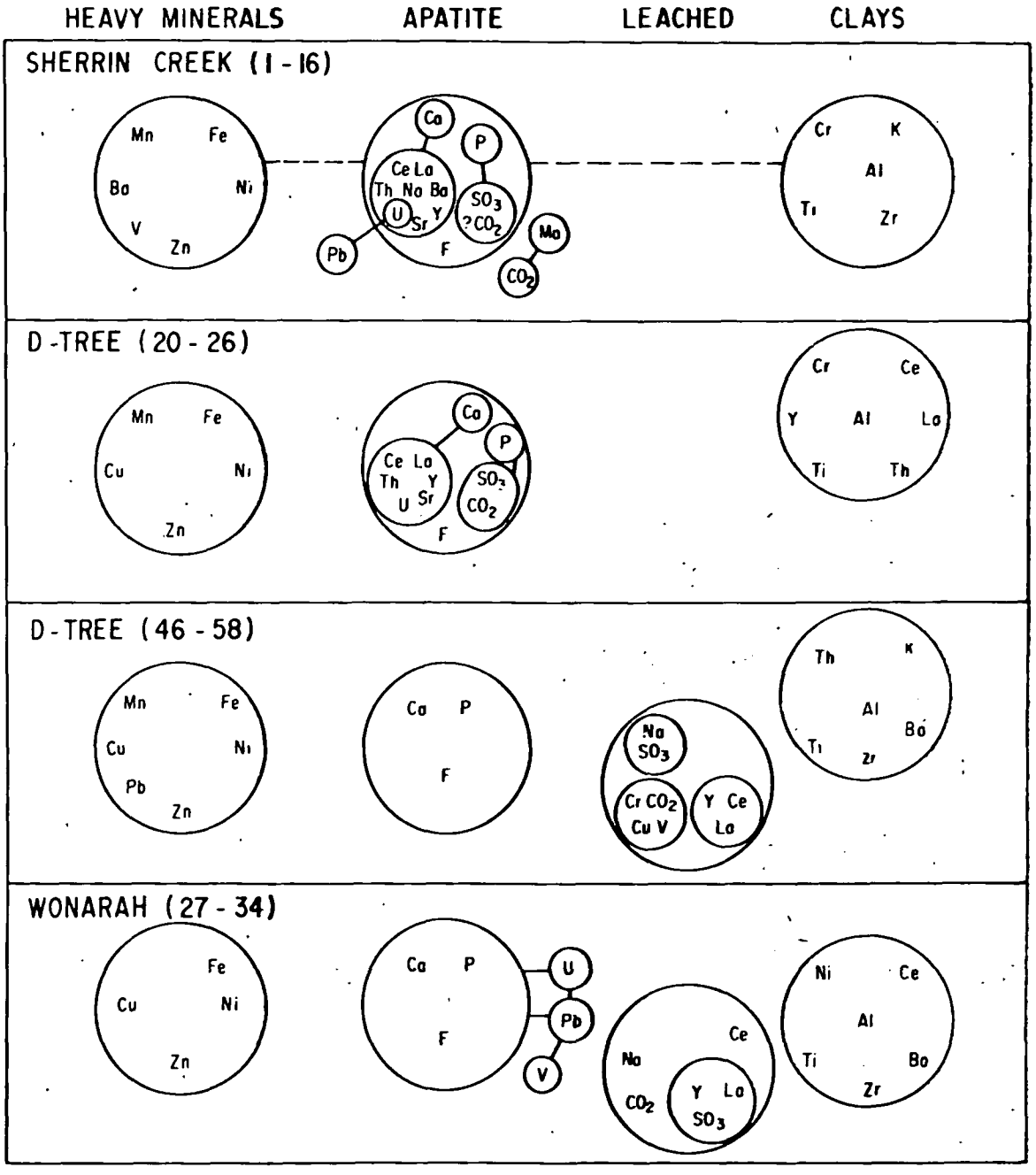

FIG. 3. Schematic diagram interpreting the element associations, apatite, clay, heavy mineral, and the leach group in terms of interelement rank correlations of greater than 95 percent significance (Table 3), and X-Y line plots. Positive correlations are indicated by elements within circles and by small circles joined by solid lines. Dashed lines indicate negative correlations.

plexity of the element intercorrelations in the clay group. With these changes, the correlation coefficients decrease to a lower order of significance (Table 3). These progressive geochemical changes illustrate the varying degree of weathering at the different localities. Using the Sherrin Creek deposit as the least weathered reference, the degree of leaching, as described below, increases in the order: drill hole Y99 at the northern end of the D Tree deposit (20–26), samples in the south-central portion of the D Tree deposit (39–45) and (46–58), and lastly the Wonarah deposit (27–34).

In the Sherrin Creek samples (excluding a few erratic results) the trace elements S, Na, La, Y, Ce,

TABLE 3. Kendall's Rank Correlation Coefficients of Highest Significance in the Sherrin Creek, D Tree, and Wonarah Phosphatic Rocks

Sample numbers refer to Tables 1 and 2.

	Sherrin Creek		D Tree		D Tree		Wonarah	
Samples (Tables 1, 2)	1–16		20–26		46–58		27–34	
No. of samples	16[A]		7		12[B]		7[C]	
Apatite	P-F	0.90 (1)	(Ca, P)-F	0.90 (1)	(Ca, P)-F	0.73 (1)	(Ca, P)-F	1.0 (1)
	(Ca, P)-Na	0.87 (1)	F-CO_2	0.81 (2)			(Ca, P, F)-Pb	0.62 (3)
	(Ca, P)-S	0.86 (1)	Ca-Th	0.81 (2)				
	Y-La	0.85 (1)	CO_2-S	0.78 (2)				
	Sr-La	0.85 (1)	(Ca, P, F)-U	0.75 (3)				
	(Ca, P, F)-Y	0.73 (1)	Ca-Y	0.71 (3)				
	Y-Th	0.73 (1)	Ca-La	0.62 (3)				
	Sr-Ce	0.61 (1)	Ca-Ce	0.62 (3)				
	Pb-U	0.51 (2)	Ca-Sr	0.62 (3)				
	Mg-CO_2	0.48 (2)						
	*Ca-U	0.62 (2)						
Leached group					Na-S	0.84 (1)	V-Pb	0.71 (3)
					La-Y	0.70 (1)	Y-La	0.59 (3)
					Cr-V	0.63 (2)	La-S	0.55 (3)
					V-Cu	0.60 (2)		
					V-CO_2	0.55 (2)		
					Y-Ce	0.55 (2)		
Clays	Al-K	0.84 (1)	(Al, Ti)-Th	1.0 (1)	Ti-Zr	0.72 (1)	Al-Ce	0.90 (2)
	Ti-Zr	0.71 (1)	Y-Cr	1.0 (1)	Al-Ba	0.69 (1)	Ti-Zr	0.65 (3)
	Al-Ti	0.66 (1)	(Al, Ti)-Cr	0.90 (2)	Al-Ti	0.63 (2)	Ce-Zr	0.62 (3)
	Al-Cr	0.64 (1)	Cr-La	0.90 (2)	Ti-K	0.59 (2)	Ni-Zr	0.71 (3)
			Cr-Ce	0.90 (2)	Th-Ti	0.45 (3)	Ce-Ba	0.62 (3)
Heavy minerals	Ni-Zn	0.78 (1)	Cu-Zn	1.0 (1)	Fe-Zn	0.85 (1)	Fe-Zn	0.81 (2)
	Fe-V	0.76 (1)	(Cu, Zn)-Ni	0.90 (2)	Ni-Zn	0.75 (1)	Ni-Cu	0.62 (3)
	Ba-V	0.73 (1)	Mn-Ni	0.90 (2)	Ni-Mn	0.53 (2)	Ni-Zn	0.62 (3)
	Ba-Mn	0.71 (1)			Pb-Zn	0.47 (3)		
			(Cu, Zn)-Fe	0.71 (3)				
	Fe-Zn	0.70 (1)			Fe-Cu	0.41 (3)		

Induced correlations excluded from the table. (1) = significant at >99.9%; (2) at 99–99.9% level; (3) at 95–99% level.
[A] Excluding 16 (high CO_2). [B] Excluding 50 (high Fe). [C] Excluding 34 (high Mn).
* Twelve samples (drill hole Y331) only.

U, and Ba correlate strongly with CaO and P_2O_5 (apatite) (Fig. 4). By contrast, at Wonarah, S, Na, La, Y, Ce, and Ba correlate negatively with CaO and P_2O_5 and constitute an antipathetic association here interpreted as a leach group. (U correlates positively with apatite; see later.) The components CO_2, Sr, and Th which do not correlate so strongly with apatite at Sherrin Creek [5] display weak or completely random correlations at Wonarah. In either case (antipathetic or random correlations with apatite) it is clear that these trace elements have been strongly leached from apatite at Wonarah, by comparison with Sherrin Creek.

The three subgroups in the D Tree deposit, namely unleached Y99 (20–26), partly leached (39–45), and leached (46–58), also illustrate progressive depletion of trace elements from the apatite structure (Fig. 4) and provide the links between the Sherrin Creek and Wonarah "end members." Element correlations with apatite in Y99 are nearly as good as for Sherrin Creek. In the D Tree (partly leached) subgroup (39–45), only SO_3 and Y show excellent positive correlations with apatite. The leached D Tree subgroup (46–58) shows a completely random distribution of trace elements in respect to CaO and P_2O_5, and these are shown as a field in Figure 4. In all cases this field lies below the regression line of the partly leached subgroup and corresponds to the large leach group shown in Figure 3.

There are too few analyses of replacement phosphorite (35–38) to be sure of its compositional range. To supplement our data, six partial analyses of samples from deposits from elsewhere in the Georgina Basin were reproduced from Cook (1972).[6] All of the replacement phosphorites are characteristically high grade and deficient in most trace elements (Fig. 4 and Tables 2 and 4).

Apatite association

Uranium and lead: Uranium correlates with apatite in most of the unleached [7] Sherrin Creek and D

[5] Many samples contain minor calcite and dolomite.

[6] Analyses 4, 6, 8, and 10 of his table 2 and analyses 15, 17, 18, 20, 22, and 24 of his table 3.

[7] This usage is in the sense of intensity of weathering and not to be equated with the leached group which is the association of elements that was derived from intense weathering or leaching of the phosphorites.

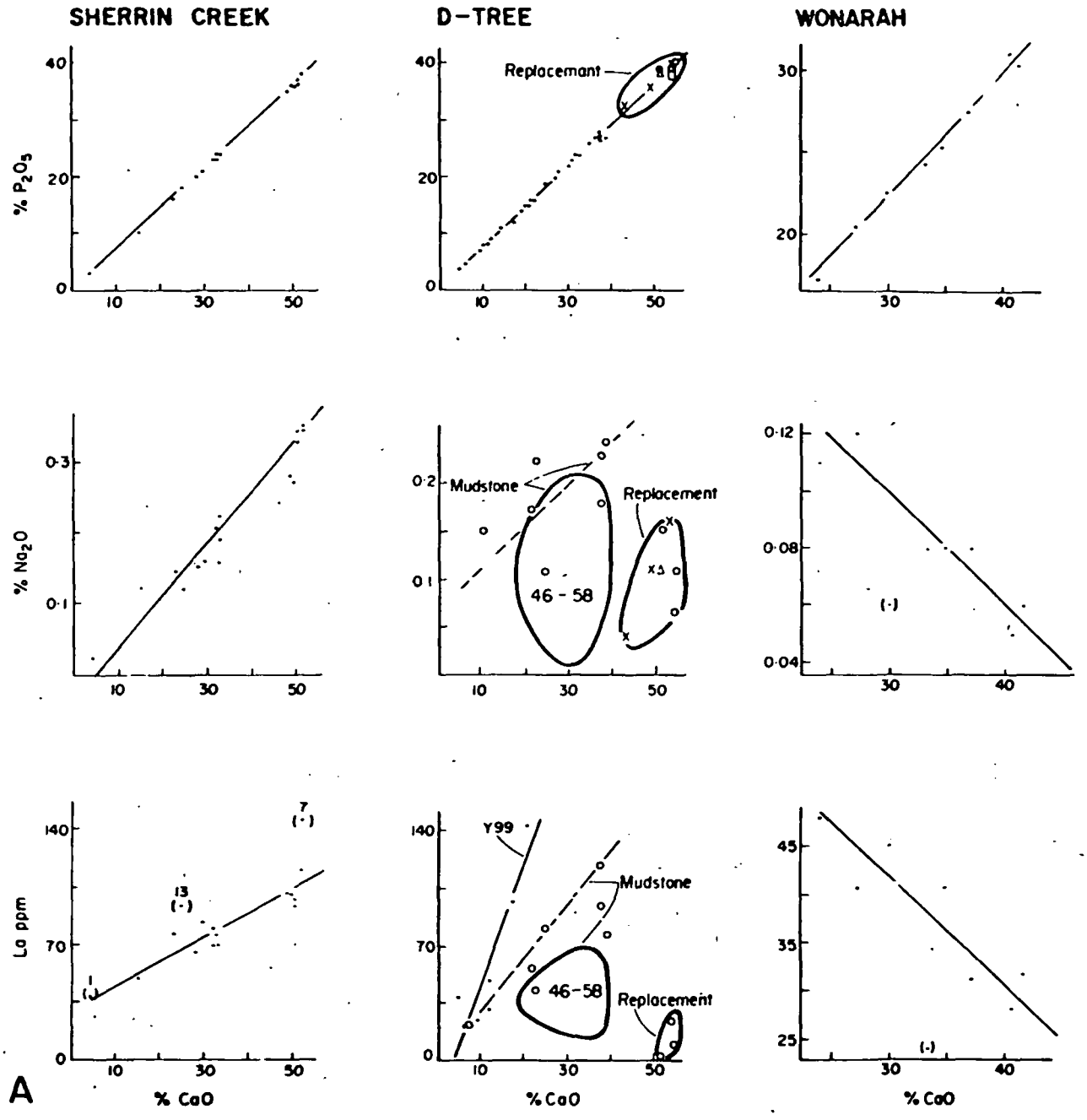

FIG. 4. X-Y plots of selected components from Tables 1 and 2, with reduced major axis regression lines (Till, 1974, p. 99). A and B show CaO versus P_2O_5, Na_2O, La, U, Th, and Ba and C, P_2O_5 versus F, SO_3, and CO_2. For Sherrin Creek, analyses (•) for La, Y, Th, and Ba are from the top of sections and affected(?) by weathering. Y333 values are erratic and not plotted for U, Th, and Ba. Random distribution of CO_2 versus P_2O_5 is partly due to presence of calcite and/or dolomite. For D Tree minor elements are indicated by (•) for Y99, (○) for D Tree central-south, (□) IMC sample FG53, (x) phoscrete (Cook, 1972), (△) replacement phosphorite D Tree (Cook, 1972). Analyses 46 to 58 are shown as a field and not plotted individually. For Wonarah, the dashed line for U is the regression line of Sherrin Creek data for comparison.

Tree phosphorites, but because U^{+4}/U^{+6} were not determined, it is not known whether U^{+4} substitutes for Ca^{+2}, or UO_4^{-2} for PO_4^{-3}. Both are possible (McConnell, 1973, p. 52); the former is sketched in Figure 3. By contrast, the leached phosphate deposits show variable behavior. Uranium in the D Tree leached phosphorites appears to be only partly leached (Fig. 4B) and shows no correlation with other elements, but at Wonarah it correlates with apatite (Figs. 3, 4B). In view of the fact that all other

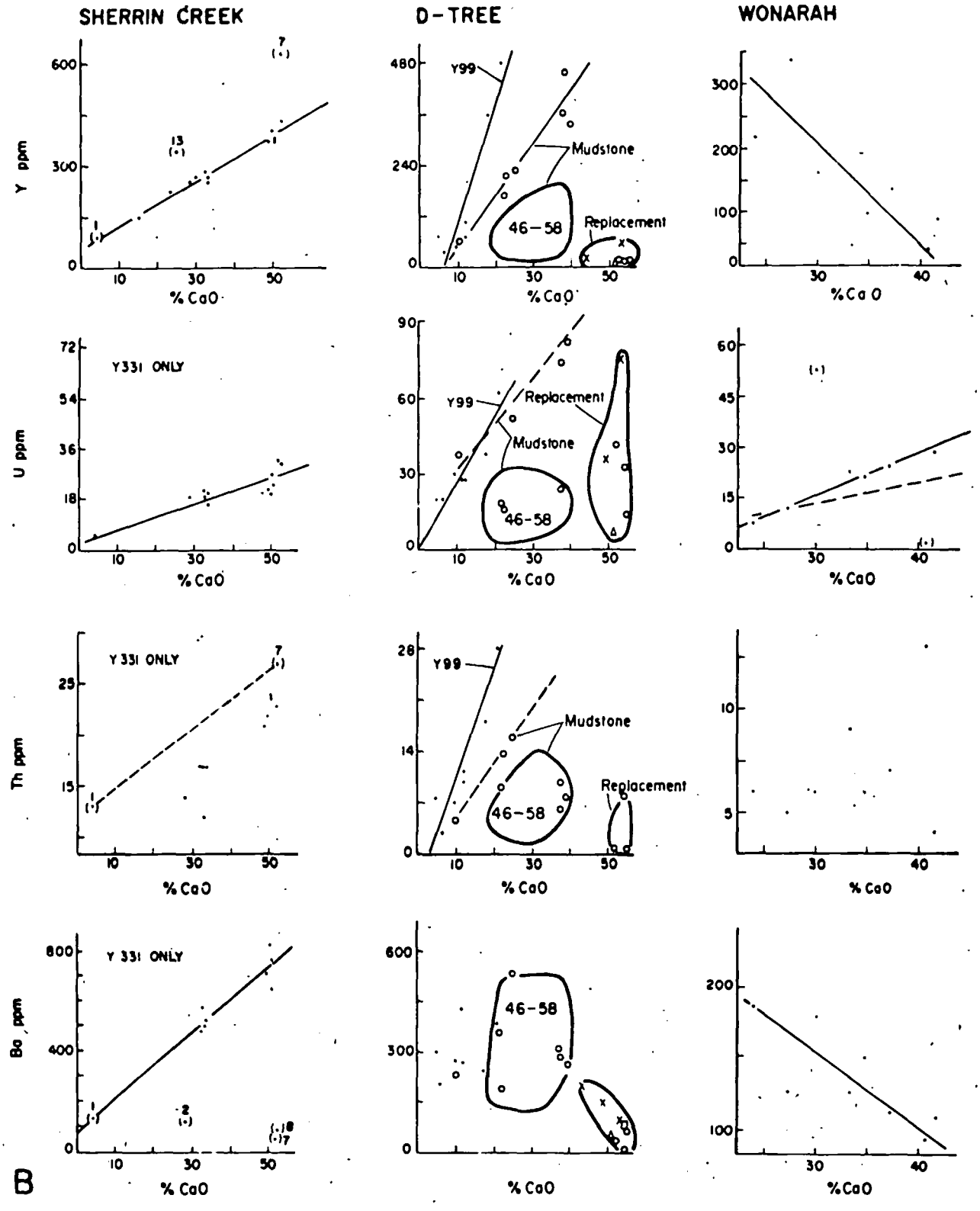

FIG. 4. (*Continued*).

components substituting for Ca have been leached or partly leached from the structure (Fig. 4) the preferred interpretation of the Ca-P-U correlation at Wonarah is that uranium has also been leached and fixed in situ as a secondary mineral, perhaps autunite, $Ca(UO_2)_2\ (PO_4)_2 \cdot$ 10–12 H_2O. Lead correlates

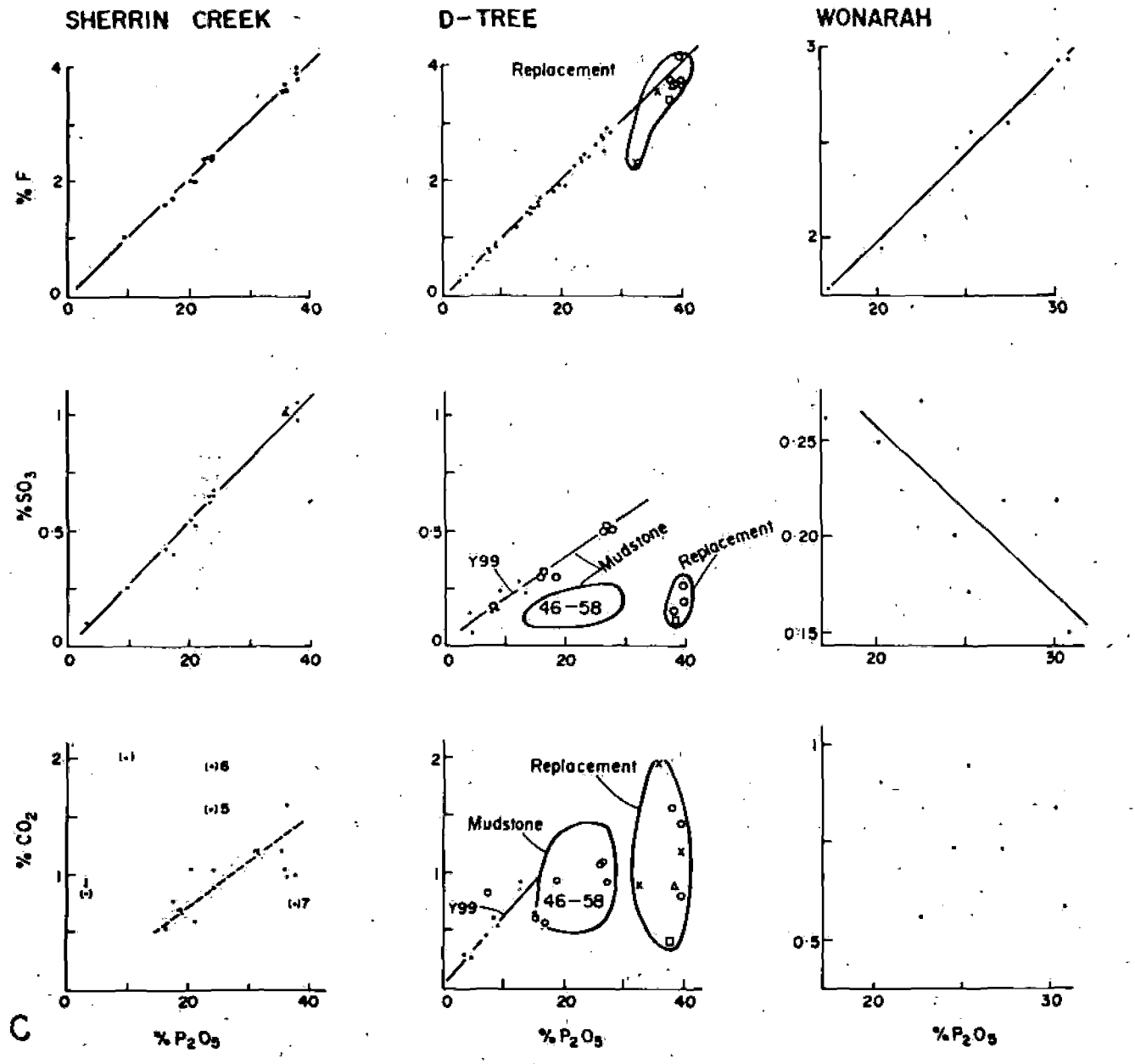

FIG. 4. (*Continued*).

with uranium substituting in the apatite structure at Sherrin Creek and with uranium within the leach group at Wonarah.

There is a trend in the absolute abundance of uranium with progressive leaching within the D Tree deposits but not between deposits (Table 4). Considering the overall range and mean concentration (1–86 ppm and 28 ppm) in all samples, the values are at the lower end of the worldwide range, 50 to 300 ppm, compiled by McKelvey (1956) and the range, 8 to 1,300 ppm, of Tooms et al. (1969).

Thorium: In unleached Sherrin Creek and D Tree phosphorites, Th correlates with apatite where it substitutes for Ca. By contrast, Th in leached D Tree phosphorite correlates with clays, but at Wonarah no affinity for other elements can be recognized.

The range of thorium content of phosphorites from all areas is 2 to 28 ppm and their mean is 11 ppm (Table 4), and, though these values are high compared to the world range of 1 to 5 ppm quoted by Wedepohl (1969), they are within the range of 5 to 100 ppm quoted by Tooms et al. (1969). The range of the Th/U in Georgina Basin phosphorites is 0.12 to 0.7 with a mean of 0.39, and this is much higher than a worldwide average ratio of <0.1 (Wedepohl, 1969).

TABLE 4. *Range, Arithmetic Mean, and Normalized Concentrations of Elements Substituting in the Apatite Structure, Together with Leached Equivalents and Other Values in the Georgina Basin*

	Sherrin Creek	D Tree			Wonarah	D Tree	All analyses	Cook (1972)			Russell/ Trueman (1971)
	(unleached)	Y99 (unleached)	(partly leached)	(leached)	(leached)	(replace-ment)		Mudstone	"Phoscrete" (replace-ment)	Pelletal	Pelletal
Analyses (Tables 1, 2)	1–16	20–16	39–45	46–58	27–34	35–38					
No. of samples	16	7	7	13	8	3–4	54–55	24	6	13	4
P_2O_5, range %	2.8–37.8	3.8–15.5	7.8–27.5	14.4–27.9	17.3–30.9	37.6–39.5	2.8–39.5	7.8–39.1	28.0–39.2	33.7–37.4	36.5–38.8
Mean/S.D.	25.0 (10.6)	8.6 (4.2)	19.9 (7.4)	21.7 (4.5)	24.7 (4.7)	38.7 (1.0)	22.4 (9.7)	18.6 (8.9)	35.3 (4.3)	35.6 (1.2)	—
Uranium (ppm)								(4)*	(3)	(3)	—
Range	5–42	19–61	19–86	8–74	1–53	18–45	1–86	15–65	10–80	45–130	—
Arith. mean/S.D.	25 (10)	32 (14)	47 (27)	23 (17)	21 (16)	33 (14)	28 (18)	48 (28)	43 (35)	78 (45)	—
—normalized[1]	40	149	94	42	34	34	50	103	49	88	
Thorium (ppm)								—	—	—	—
Range	12–27	3–28	5–16	2–14	4–13	2–8	2–28	—	—	—	—
Arith. mean/S.D.	18 (5)	12 (8)	10 (4)	6 (3)	7 (3)	4 (4)	11 (7)	—	—	—	—
—normalized	29	56	20	11	11	4	20				
Th/U	0.72	0.38	0.21	0.26	0.33	0.12	0.39				
Lanthanum (ppm)								(2)	(3)	(3)	—
Range	39–148	22–142	38–120	18–62	24–48	5–26	5–148	15–40	2–4	200–300	—
Arith. mean/S.D.	86 (26)	58 (45)	73 (29)	37 (14)	36 (9)	14 (11)	57 (34)	28 (18)	3 (1)	240 (60)	500
—normalized	138	270	147	68	58	14	102	60	3	258	
Cerium (ppm)								(2)	(3)	(3)	—
Range	72–214	31–169	48–114	13–88	34–70	3–15	3–214	40–80	6?	120–160	—
Arith. mean/S.D.	97 (35)	80 (54)	84 (25)	47 (23)	51 (14)	8 (6)	69 (40)	60 (20)	—	140 (20)	—
—normalized	155	372	169	87	83	8	123	129	—	157	
Yttrium (ppm)											
Range	93–624	36–482	60–461	20–193	42–336	6–8	6–624	10–300	10–200	200–1,500	—
Arith. mean/S.D.	313 (124)	165 (178)	262 (135)	76 (47)	140 (98)	7 (1)	187 (150)	48 (67)	53 (75)	655 (335)	600
—normalized	501	767	527	140	227	7	334	103	60	736	
Y/La	3.6	2.8	3.6	2.1	3.9	0.5	3.3	1.7	18	2.8	

TABLE 4.—(*Continued*)

	Sherrin Creek	D Tree			Wonarah	D Tree	All analyses	Cook (1972)			Russell/ Trueman (1971)
	(unleached)	Y99 (unleached)	(partly leached)	(leached)	(leached)	(replace-ment)		Mudstone	"Phoscrete" (replace-ment)	Pelletal	Pelletal
Barium (ppm)											
Range	55–828	205–433	194–533	129–514	95–186	5–80	5–828	100–800	50–200	50–500	—
Arith. mean/S.D.	423 (255)	301 (79)	312 (111)	303 (144)	136 (33)	42 (36)	296 (196)	300 (200)	25 (52)	210 (40)	—
—normalized	677	1,400	627	559	220	43	529	645	142	236	
Strontium (ppm)											
Range	54–312	42–227	79–230	43–150	46–218	50–81	42–312	10–200	40–150	100–800	—
Arith. mean/S.D.	166 (58)	116 (68)	162 (51)	76 (34)	116 (52)	69 (13)	123 (62)	73 (48)	98 (35)	375 (205)	275
—normalized	266	540	326	140	188	71	220	157	111	421	
Sodium (Na_2O%)											
Range	0.02–0.35	—	0.11–0.24	0.01–0.20	0.05–0.12	0.04–0.15	0.01–0.35	0.01–0.16	0.01–0.17	0.11–0.63	0.28–0.47
Arith. mean/S.D.	0.21 (0.10)	—	0.19 (0.05)	0.10 (0.06)	0.08 (0.02)	0.09 (0.05)	0.13 (0.08)	0.06 (0.04)	0.08 (0.06)	0.24 (0.17)	0.36 (0.08)
—normalized	0.34	—	0.38	0.18	0.13	0.09	0.23	0.13	0.09	0.27	
Sulfur (SO_3%)											
Range	0.10–1.0	0.06–0.28	0.17–0.51	0.10–0.25	0.15–0.27	0.12–0.26	0.10–1.0	—	—	—	0.6–1.2
Arith. mean/S.D.	0.68 (0.30)	0.17 (0.07)	0.38 (0.13)	0.16 (0.05)	0.22 (0.04)	0.18 (0.06)	0.35 (0.28)	—	—	—	0.9 (0.3)
—normalized	1.1	0.79	0.76	0.29	0.36	0.19	0.63	—	—	—	
CO_2%								(6)	(4)	(3)	—
Range	0.55–3.0	0.30–0.92	0.56–1.1	0.50–1.1	0.55–0.95	0.40–1.6	0.30–1.6	0.6–1.4	0.9–2.0	1.3–2.0	0.7–1.6
Arith. mean/S.D.	1.2 (0.7)	0.54 (0.22)	0.86 (0.21)	0.77 (0.21)	0.74 (0.15)	1.1 (0.6)	0.89 (0.44)	0.8 (0.3)	1.2 (0.5)	1.7 (0.4)	1.1 (0.4)
—normalized	1.9	2.5	1.7	1.4	1.2	1.1	1.6	1.7	1.4	1.9	

N.B. Dashes indicate no data available.
* Data available only for 4 of the 24 samples.
[1] Arithmetic mean, recalculated to 40% P_2O_5.

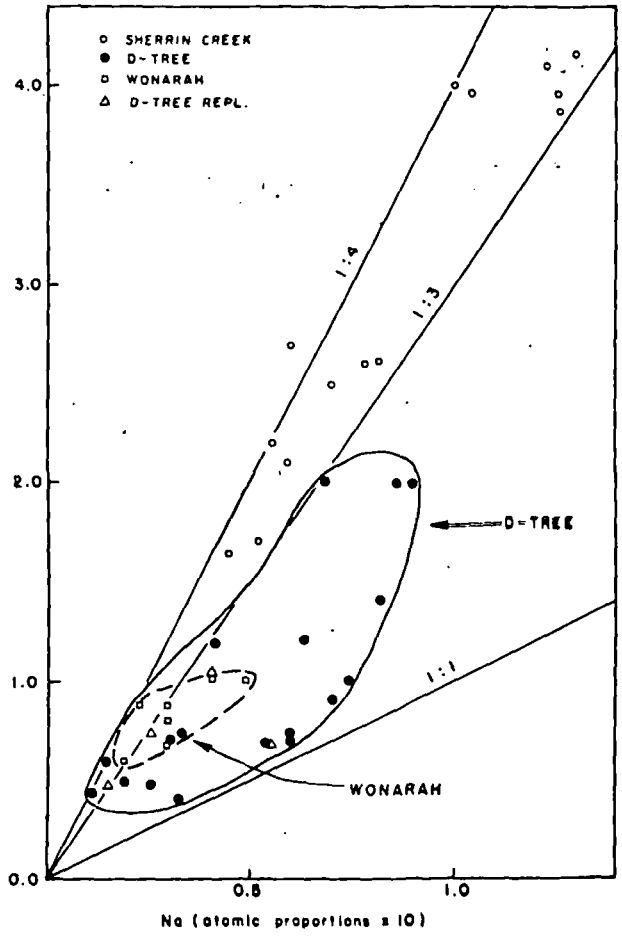

FIG. 5. Plot of atomic Na : S.

Yttrium, lanthanum, and cerium: In the unleached Sherrin Creek and D Tree phosphorites, Y, La, and Ce correlate with apatite, where they substitute for Ca. However, approximately 80 percent of each element is leached from the system at D Tree (Table 4), and the remainder, on the basis of random or negative correlations with apatite, is fixed in the leach group as an unidentified rare earth-bearing secondary mineral (Fig. 3). Despite this extensive remobilization, Y/La, representing the ratio of heavy to light rare earth elements, remains constant in the range of 2 to 4, and no differential fractionation is evident.

Barium: The range of barium content of phosphorites from all areas is 5 to 828 ppm and the mean 296 ppm. It is contained in the apatite structure at Sherrin Creek in addition to its association with the heavy minerals, presumably as lithiophorite. In the Y99 and partly leached D Tree (39–45) samples, barium is partly leached from the apatite structure and displays a random correlation with all elements. However, in the leached D Tree and Wonarah samples it strongly correlates with clay fraction elements (Fig. 3). Fenner and Hagner (1967) have shown a correlation in shales between barium concentration and the amount of illite present, due to cation exchange. This association probably accounts for the fact that barium is leached from the system only to the extent of 60 percent as compared to substantially higher percentages for all other elements substituting for Ca in the apatite srtucture.

Normalized mean concentrations of barium in the unleached mudstone phosphorites of this study, 667 and 1,400 ppm (Table 4), are greater than the 645 ppm quoted by Cook (1972) from elsewhere in the Georgina Basin and compare with the 1,000 ppm worldwide average of Tooms et al. (1969).

Strontium: In the unleached Sherrin Creek and D Tree phosphorites, Sr correlates with apatite. McArthur (1978) suggests that Sr is relatively mobile in relation to the apatite structure, and this is supported by the normalized mean values at D Tree (Table 4), which show that approximately 75 percent of Sr is leached from the system. Values of Cook (1972) for mudstone phosphorites from elsewhere in the basin are similarly low. This degree of mobility is also common to U, Th, La, Ce, and Y (Table 6).

Sodium, sulfur, and CO_2: At Sherrin Creek and D Tree (Y99), sodium,[8] sulfur, and CO_2 substitute in the apatite structure, but elsewhere all three components illustrate either a random or a negative correlation with apatite (Fig. 4A and C). The leached components appear as an undetermined Na-SO_3 phase (Fig. 3).

The degree of leaching of components from the system is indicated in the data of Tables 4 and 6, where it can be seen that more than 60 percent of SO_3 is removed from the system. However, from the smaller weight percent loss in the case of CO_2 and the fact that it has a random correlation with apatite (rather than the negative relationship of Na_2O and SO_3), it is evident that CO_2 is far more strongly bound to the apatite structure than is either Na_2O or SO_3.

The removal of these components from the apatite structure requires the recrystallization of the mineral, something which has not been noted petrographically. In this study no systematic examination of samples was made with a scanning electron microscope, and the matter requires further investigation.

Leaching has had a marked effect on the atomic ratio Na : S (Fig. 5). At Sherrin Creek the ratio lies in the range of 1 : 4 to 1 : 3, but, with differential leaching of the components elsewhere, the ratio varies between 1 : 4 and 1 : 1 at D Tree and between 1 : 4 and 1 : 2 at Wonarah. Coupling Sr, Y, Ba, La, Ce, Th, and U with sodium, the ratios become 1 : 2 to

[8] Sodium was not determined at D Tree (Y99).

TABLE 5. Unit-Cell-Edge Lengths of the *a*-Axis of Apatite in the Georgina Basin Phosphorites

This study	No. of samples	*a* axis, Å (mean/S.C.)	Mean standard error, Å
Sherrin Creek (unleached)	9	9.3519 (0.0057)	0.0028
D Tree (partly leached)	6	9.3528 (0.0019)	0.0028
D Tree (leached)	9	9.3520 (0.0080)	0.0023
Wonarah (leached)	7	9.3531 (0.0068)	0.0019
D Tree (replacement)	2	9.3556 (0.0030)	0.0021
Cook (1972)			
Pelletal	29	9.3540	
Nonpelletal	27	9.3571	

Measured by X-ray diffractometer (Cu Kα radiation, graphite monochromator, Si internal standard, 0.25° 2θ per min.), from 7 line profiles within the angular range 20° to 54° 2θ. Lengths refined by least-squares computer program (Appleman, USGS) supplied by P. J. Cook.

1 : 1, but these are still high in terms of achieving the charge balance. The marked deficiency of Na in all samples of Georgina Basin phosphorites suggests that it has been very mobile even in the Sherrin Creek deposit.

The sumary of the lengths of the *a* axes in the unit cells of apatite (a_0) in 33 phosphorites (Table 5) shows no significant difference between the mean length in leached and unleached phosphorites of this study or between those of pelletal and mudstone phosphorites from elsewhere in the Georgina Basin (Cook, 1972). When a_0 is plotted against CO_2 (Fig. 6), the data of this study show both lower CO_2 and a_0 values. The Sherrin Creek samples demonstrate a well-defined trend, although its field is enlarged by samples 5 and 6 (Figs. 4C, 6) which contain traces of dolomite.[9] The distribution of the Wonarah values shows a similar trend to Sherrin Creek, but in the case of D Tree the relationship is random. The interpretation of the data is uncertain, because CO_2 is retained in the phosphorite samples as dolomite. If it could be extracted, the D Tree and Wonarah samples would possibly illustrate a more scattered distribution than shown and depart still further from the $CO_2 : a_0$ worldwide trend illustrated by Smith and Lehr (1966) and Carlstrom (*in* McConnell, 1973). The random relationship is interpreted as an effect of leaching.

[9] Citrate extraction of phosphorites was not undertaken because it does not completely dissolve dolomite (Smith and Lehr, 1966, p. 345) and its leaching effect on trace elements is unknown.

Heavy mineral association

The genesis and provenance of the metals contained in the siltstone-chert-limestone-phosphorite lithosome was discussed previously, as was their mineralogy.

Rank correlation coefficients reveal a consistent grouping of Fe-Mn-Ni-Zn in the phosphorites (Fig. 3). In the unleached Sherrin Creek samples V and Ba correlate here also, and it is possible that V is present as vanadiferous magnetite and the Ba as the

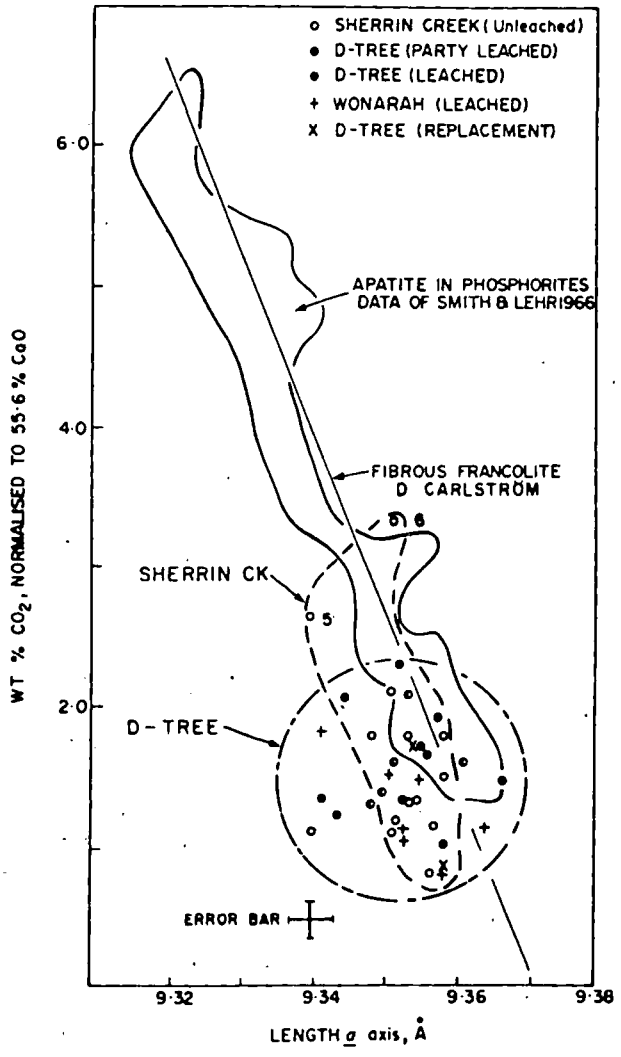

FIG. 6. Plot of *a* axis length for the unit cell versus CO_2 content of the apatite for the Sherrin Creek, D Tree, and Wonarah phosphorites (within citrate extraction of carbonates). The dashed-line field encloses the Sherrin Creek data which include the bulk and concentrate pairs. The circular field indicates a random distribution for the D Tree and Wonarah leached and partly leached phosphorites. Also plotted is the field for apatite in a worldwide sample of phosphorites (data of Smith and Lehr, 1966) and the trend for a series of "fibrous francolites" (D. Carlstrom, quoted by McConnell, 1973, p. 44).

manganese phase, lithiophorite, which can contain 0.5 to 8 percent BaO (Norrish, 1975).

Clay association

A preliminary study of the clay fraction of 100 phosphorites, using the laboratory and determinative techniques of Brown (1961) and Thorez (1975), show that kaolinite, illite, smectite, and minor chlorite are present.

Sherrin Creek phosphorites contain appreciably higher percentages of smectite and chlorite than does D Tree or Wonarah and show only minor variation in the proportions of the minerals quantified as kaolinite > smectite > illite ≫ chlorite. At D Tree and Wonarah, smectite is subordinate or minor compared to illite, and chlorite is not usually identifiable. At these two deposits the proportions vary widely but are generally in the order kaolinite > illite ≫ smectite. Unlike Sherrin Creek, where little variation occurs in the clay distribution in vertical section, samples from drill holes in the other deposits show considerable variation from kaolinite = illite to 100 percent kaolinite.

The changes in the proportion of clay minerals suggest that smectite and chlorite have been weathered to kaolinite. However, the study could not determine whether the changing proportions of kaolinite to illite arise from original differences during sedimentation, from Cenozoic weathering, or from Cambrian weathering during regressive periods.

Figure 3 shows that the elements Al-K-Ti-Zr consistently group as clays, and that, with leaching of the phosphorites, Ba, Th, Ce, Ni, and Sr substitute for elements in the clay structures or are adsorbed onto clay surfaces.

Discussion

The technique used in this study to establish element substitution in the apatite structure was the recognition of positive correlations between trace elements and CaO or P_2O_5. To obtain an acceptable linear relationship, samples were chosen which had the widest possible range of P_2O_5 values, namely 2.8 to 39.5 percent. However, within the overall range, the availability of samples was such that values for some specific geographic areas fall at the bottom of the range, e.g., 3.8 to 15.5 at Y99; and others near the top, e.g., 17.3 to 30.9 at Wonarah. For this reason neither the range of values of minor elements nor their arithmetic means are significant for the purposes of making meaningful comparisons of concentration levels between petrological types, different deposits, or leached groups. For this reason, arithmetic means have been normalized to 40 percent P_2O_5, that is, a value approaching the composition of a carbonate fluorapatite with no detrital contamination.

Geochemical variations in the phosphorites

An unexpected outcome of this study was the recognition of the progressive leaching of the phosphorite deposits by the likely combination of Cambrian and Cenozoic weathering. The progressive changes in the geochemistry of the apatite, clay, and leach group evident in Figures 3 and 4 is quantified in Table 4. The normalized values are represented in Table 6 together with ratios which indicate the degree of leaching and removal of elements on a weight percent basis. The only certain measure of leaching is the data presented in the within-deposit values of D Tree, where the composition of unweathered mudstone phosphorites is assumed to have had little primary variation. The ratios of normalized values for the substituting elements indicate that 44 to 82 weight percent has been leached from the sediment. However, of the ten elements, six (U, Th, La, Ce, Y, and Sr) have been leached to the extent of 72 to 82 percent, two (SO_3 and Ba), 58 and 64

TABLE 6. Comparisons of Normalized Element Concentrations in Leached Rocks Compared to Element Concentrations within the Apatite Structure in Unweathered Phosphorites

	Sherrin Creek	A	B	C	D	E				
		D Tree			Wonarah	Mudstones				
		Y99					Ratio			
	(unleached)	(unleached)	(partly leached)	(leached)	(leached)	(Cook, 1972)	B/A	C/A	D/A	E/A
U ppm	40	149	94	42	34	103	0.63	0.28	0.23	0.69
Th "	29	56	20	11	11	—	0.36	0.20	0.20	—
La "	138	270	147	68	58	60	0.54	0.25	0.21	0.22
Ce "	155	372	169	87	83	129	0.45	0.23	0.22	0.35
Y "	501	767	527	140	227	103	0.69	0.18	0.30	0.13
Ba "	677	1,400	627	599	220	645	0.45	0.42	0.16	0.46
Sr "	266	540	326	140	188	157	0.60	0.26	0.35	0.29
Na_2O percent	0.34	—	0.38	0.18	0.13	0.13	—	—	—	—
SO_3 "	1.1	0.79	0.76	0.29	0.36	—	0.96	0.36	0.46	—
CO_2 "	1.9	2.5	1.7	1.4	1.2	1.7	0.68	0.56	0.48	0.68

TABLE 7. Comparisons of Normalized Structurally Substituted Concentrations in Unweathered Mudstone to Replacement Phosphorites at Sherrin Creek and D Tree

	1 Sherrin Creek	2 D Tree (Y99)	3 D Tree (replacement)	4 Pelletal (Cook, 1972)	5 D Tree (Y99)/ Sherrin Creek	6 D Tree (Y99)/ Pelletal
U ppm	40	149	34	80	3.7	1.9
Th "	29	56	4	—	1.9	—
La "	138	270	14	258	2.0	1.1
Ce "	155	372	8	157	2.4	2.4
Y "	501	767	0.5	736	1.5	1.0
Ba "	677	1,400	43	236	2.1	5.9
Sr "	266	540	71	421	2.0	1.3
Na_2O percent	0.34	—	0.09	0.27	—	—
SO_3 "	1.1	0.79	0.19	—	0.7	—
CO_2 "	1.9	2.5	1.1	1.9	1.3	1.3

The pelletal phosphorite samples of Cook (1972) can be assumed to be leached to a varying but unknown degree.

percent, respectively, and the least leached is CO_2, 46 percent. All of the elements show a random correlation with apatite, and positive interelement correlation within the leach group of the clay association (Fig. 3), suggesting that only a minor proportion of the residual concentration is contained in the apatite structure.

In contrast to the D Tree data, seven of the elements at Wonarah have negative correlations with apatite, and all have positive interelement correlations with the leach group or the clay association, suggesting that perhaps CO_2 is the only significant component remaining in the apatite structure. As no unleached Wonarah samples are known, there is no standard by which leaching can be positively measured. Figure 4B shows that there is a similarity of uranium concentration at Sherrin Creek (dashed line) and Wonarah, although this is not significant in the light of the leaching which has occurred. For instance, Table 6 shows that there is a striking resemblance between the Wonarah concentrations and those of the D Tree leached suite; U, Th, La, and Ce are marginally lower, and only Y, Sr, and SO_3 are greater than at D Tree. If the original composition of the Wonarah and D Tree suites were substantially different, it is now only evident in the higher concentration levels of Y, Ba, Sr, and SO_3 at Wonarah.

In considering the little-weathered phosphorites, the composition of their contained carbonate fluorapatite, as indicated by normalized structural concentrations, may be a measure of the chemical composition of the water at the time of their formation. In the case of the unweathered mudstone phosphorites of Sherrin Creek and D Tree (Y99), Table 7 (columns 1, 2, and 5) shows that their compositions are markedly different. The concentration levels of eight of the ten elements are greater at D Tree by factors of 1.3 (CO_2) to 3.7 (U), and only SO_3 is less, by a factor of 0.70. The higher Na_2O and SO_3 concentrations at Sherrin Creek suggest that the Sherrin Creek embayment may have been more restricted and consequently had higher seawater salinities. Alternatively, the lagoonal and estuarine environments at D Tree could be a reason for lower salinity conditions in a shallower system fed by streams. In either case the remaining eight trace elements substituting in the apatite structure are greater at D Tree (Y99) by a factor of approximately 2, and these compositional differences are interpreted as differences in the composition of the water at the time of deposition.

The analyses of 24 surface samples of mudstone phosphorites ("non-pelletal") of Cook (1972) are tabulated in Table 4 and compared to the Sherrin Creek and D Tree samples in Table 6. His samples came from five widely separated deposits along the eastern edge of the basin and, on the evidence presented above, considerable variation in the primary concentrations of structural-substituting elements could be expected. However, the concentrations of all the elements, except uranium, are lower than those of Sherrin Creek, and five out of the eight elements which Cook (1972) analyzed have values similar to or lower than the most intensely altered phosphorites at D Tree and Wonarah (Table 6). It is likely, therefore, that Cook's suite is intensely leached, although the age of the weathering is uncertain. Although the chemistry of his suite shows a likeness to the leached mudstone phosphorites of D Tree and Wonarah, it is strikingly dissimilar to the chemistry of lateritized pelletal phosphorite from Quita Creek, which he clearly demonstrated to be a Cenozoic residual concentration showing systematic increases in SiO_2, Fe_2O_3, MnO, H_2O^+, and base metals.

A meaningful comparison of the geochemistry of the mudstone, replacement, and pelletal phosphorites requires that the specimen material be unweathered. Table 7 lists unweathered Sherrin Creek and D Tree

mudstone, unweathered D Tree replacement phosphorites, and, in addition, normalized concentrations for thirteen of Cook's (1972) pelletal phosphorites whose state of weathering is uncertain. Comparison of these analyses with those of unleached mudstone phosphorites of this study is difficult because of the geochemical variations which exist between the two reference areas, Sherrin Creek and D Tree (Y99). The pelletal phosphorites have similar Ce and CO_2 values to Sherrin Creek, and similar La, Y, and Sr values to D Tree. However, only Ba shows a consistent overall relationship, namely, that it is less in the pelletal phosphorite with respect to both of the unleached mudstone phosphorites.

Cook (1972) referred to a Ce deficiency in the pelletal phosphorites and suggested that this indicated a normal marine environment during deposition. However, although it is deficient compared to D Tree (Table 7), it is similar to the content at Sherrin Creek and clearly a general case cannot be supported. In fact the La/Ce ratio 1.64 for the pelletal phosphorites, as compared to ratios of 0.89 and 0.73 for Sherrin Creek and D Tree, suggests that the low Ce values may be the result of leaching. During weathering Ce^{+3} is readily oxidized to Ce^{+4}, whereas La remains as La^{+3}. As Ce^{+4} is more readily leached than La^{+3}, weathering produces high La/Ce ratios. In this respect the pelletal phosphorite analyses show similarity to the D Tree replacement phosphorites which have a similar La/Ce ratio of 1.75.

The composition of the white dense *replacement phosphorite* is very different from the other phosphorite types. It is clear from the data in Tables 1, 2, 4, and 7 that it is highly deficient in all minor and trace elements even when compared to the highly leached mudstone phosphorites at Wonarah. There is no detectable structural substitution.

Summarizing the geochemical data for all phosphorite types, it can be said that (1) the normalized values of elements substituting in the apatite structure indicate that there were discrete differences in the chemistry of waters in different embayments, (2) the compositions of the pelletal phosphorites from elsewhere in the basin are randomly different from the mudstone phosphorites at Sherrin Creek and D Tree (Y99) and this may reflect a different geochemical environment, and (3) the white replacement phosphorite is distinctly different geochemically and formed from waters depleted in minor and trace elements common to the other types.

Origin

Weathering, crusts, and replacement phosphorite: The exposure of replacement phosphorite at D Tree has been referred to as phoscrete by Cook and by de Keyser (pers. commun.), and it is so recorded in the analytical data of Cook (1972). Some elucidation of the different terminology is necessary. Figure 4 shows the field of four replacement phosphorites of this study together with the partial analyses of Cook's phoscretes, and it is shown that they have similar compositions. Two questions arise. Are the two types of rock, which have identical compositions, formed by (a) the diagenetic replacement of limestones, by (b) the replacement of exposed limestones by surficial processes, or by (c) the weathering and concentration of a mudstone phosphorite? Did they form penecontemporaneously during Cambrian times or more recently?

Large areas of Australia are lateritized by weathering cycles which extend back to the early Cenozoic. Drilling shows that below the laterite cappings a pallid zone extends to depths of 100 m or more, the depth of weathering depending on the rock types, geology, and the resultant land form. Much of the laterite has been eroded along the eastern edge of the Georgina Basin leaving the pallid zone exposed. Variation in the chemistry of a lateritized pelletal phosphorite capping has been demonstrated by Cook (1972), whereas the present study illustrates the progressive leaching of mudstone phosphorite below the capping. Evidence presented earlier, however, shows that the mudstone phosphorite was also exposed to subaerial weathering during the Cambrian. At Galah Creek such weathering produced a ferruginous and manganiferous surface layer a few centimeters thick which is directly analogous to the Cenozoic laterite described by Cook (1972) in terms of process but not of intensity.

Field observations and core from drill holes at D Tree show that neither enriched residual concentrations of phosphorites nor surficial replacement of phosphorites are developed from or in mudstones below erosion surfaces.

It is only where phosphorite is high grade that "brain-type" dissolution surfaces become notable and white crusts up to 1 cm thick cover the outcrop, filling joint planes of the phosphorite and the rocks immediately beneath, including those of the Precambrian basement. Additionally, the crusts cement surface rubble adjacent to the outcrop. All evidence indicates that these crusts or phoscrete are Cenozoic to Recent in age and are forming today, as evidenced by the coating of rubble. Such phoscrete crusts can be seen capping high-grade mudstone phosphorite at Replacement Hill, Lady Annie, and numerous occurrences of high-grade pelletal phosphorite (de Keyser, 1969) and replacement phosphorite at D Tree. The occurrence at Ardmore, referred to by Cook (1972), is not in contact with phosphorite and could be either residual surficial crust or replace-

ment phosphorite. In this paper and in Rogers and Keevers (1976) phoscrete refers to these minor crusts.

By comparison, the phoscrete-crusted high-grade replacement phosphorites at D Tree and that at Lady Annie are substantial bodies which have formed by the replacement of carbonate rocks in Cambrian times. At D Tree the rocks are diagenetically replaced micritic and calcarenitic limestones and dolomites. The favored depositional environment is a shallow depression to the east of an ill-defined north-trending line of submerged basement hillocks (Fig. 2a). Cross-bedded and scoured skeletal sands developed in shoaling conditions over the basement high, and to the east burrowed micritic carbonates indicate a gradation to an intertidal mudbank environment. The total diagenetic replacement of these beds in such a small, restricted area and their geochemical impoverishment suggest that the replacement was effected by highly fractionated solutions derived from the surficial weathering of spatially related phosphorites or phosphatic limestones which were being constantly fed into the depression during deposition.

In summary, replacement phosphorite at D Tree is of diagenetic origin and formed in Cambrian times. The replacement phosphorites at Lady Annie (Cook, 1972) and Rogers and Keevers (1976) are contained in karst or collapse structures within the Thorntonia Limestone, and evidence suggests a postdiagenetic replacement of carbonate rocks during the Cambrian. It is possible that replacement phosphorites formed in a range of Cambrian environments from surficial replacement to shallow-water diagenetic replacement of carbonate rocks. Phoscrete on the other hand is a minor surficial solution and replacement effect on the surface of high-grade phosphorites during Cenozoic to Recent times.

Literature and evidence of replacement origin: Excellent papers have been written on the origin of pelletal and mudstone phosphorites of the Georgina Basin as a whole by de Keyser and Cook (1972) and Cook (1972), on the Duchess deposit by Russell and Trueman (1971), on the Lady Annie deposit by Rogers and Keevers (1976), and lastly a comparative study on Duchess and Lady Annie deposits was produced by Fleming (1977). The last two papers have contributed much new data, especially Fleming (1977) who presented the sedimentary petrology of the facies, supporting his descriptions with pertinent photographic evidence. In the past the origin of the pellets which comprise the Georgina Basin pelletal phosphorites has been much debated, the frame of reference being the only well-described deposit, Duchess (Russell and Trueman, 1971), until the recent papers. Although there was general agreement that the pellets were allochems, the question of their origin was left open. The size and degree of sorting of the pellets indicate that they were distributed by current transport, but their structureless form provided no evidence as to whether they were formed by replacement of carbonate pellets, diagenetic alteration of fecal pellets or the comminution of a precursor phosphorite bed. In his study, Fleming (1977) found that in the calcareous phosphorites at Duchess there were micritic pellets in all stages of replacement from unreplaced to completely phosphatized carbonate. He could also identify 5 to 10 percent of the pellets as feces, but the remainder were structureless. However, at Lady Annie where pelletal phosphorites are common, Rogers and Keevers (1976) and Fleming (1977) estimated that the pelletal phosphorites were composed of well-sorted sand-sized grains, 50 percent or more of which were phosphatized skeletal fragments and the remainder featureless apatite. No fecal pellets could be recognized. In view of the fact that this is true also at D Tree where thin pelletal phosphorite beds are spatially related to thin beds of totally phosphatized coquina, it is but a small step to accept that all the pellets were derived from the comminution of coquina and that the structureless pellets are skeletal grains which have been micritized by endolithic algae (Selley, 1976; Bathurst, 1971) prior to phosphatization. At D Tree the pelletal phosphorite and the replacement phosphorite after coquina are wholly contained within mudstone phosphorite which formed in a subtidal lagoon and an estuary, both of which became very shallow during periods of sea-level fluctuations and developed marginal tidal flats. The coquinas are interpreted as having formed on banks or bars and the skeletal carbonate sands to have been derived from them during periodic, but rare, times of high energy. The apparently non-systematic distribution of pelletal phosphorite and phosphatized coquina is a measure of the changing environment as shoals migrated to and fro with tidal scour and perhaps were subjected to wave action. Core holes show that some pelletal phosphorite beds are coincident with ferruginous outwash horizons, suggesting that a lowered sea level led not only to reworking of shell debris but also to an increased terrigenous input because of the lowering of the base level of erosion.

The mudstone phosphorites show little evidence of their origin. Fleming (1977) recorded a single example of an algal structure in position of growth at Lady Annie and also an example of cross-bedding which he speculated might be algal laminae. Progressive changes in the nature of mudstone phosphorite from Duchess through Lady Annie to D Tree can be recognized. Thus at Duchess mudstone phosphorite is minor and consists of 1- to 2-cm-thick high-grade finely laminated beds with abruptly undu-

latory surfaces (Russell and Trueman, 1971; de Keyser, 1969), whereas at D Tree it consists of thick (1–15 m) medium-grade beds (19% P_2O_5) of microcrystalline carbonate fluorapatite set in a matrix of terrigenous silt.

Single major-ion composition of interstitial waters can deviate significantly from sea-water composition (Atlas, 1975). It would be expected, therefore, that geochemical differences would be discernible between a primary carbonate fluorapatite precipitate and/or ones formed by an interstitial replacement process. However, they would presumably not be discernible if the replacement process were taking place progressively at the sediment-water interface as carbonate mud was being deposited. Evidence to prove the origin of the mudstone phosphorite as a chemical or biochemical precipitate versus one of progressive replacement of lime muds during their depositions is lacking. However, it is logical that if bottom waters could replace all carbonates which are macroscopically and microscopically identifiable as fossil debris, then it follows that they could replace the carbonate muds in which they are interbedded. This was pointed out by Cook (1972) and Fleming (1977) and is the interpretation favored in this study.

Source and synthesis of features: The source of the Georgina Basin phosphate has been much debated. Russell and Trueman (1971) proposed oceanic currents as the source, but other authors, de Keyser (1969), de Keyser and Cook (1972), Cook (1972), Howard (1972), and Fleming (1977), believed that the shallow epicontinental sea and the depositional environments indicated by the sedimentary section leave no scope for applying the up-welling oceanic-water hypothesis originally proposed by Kazakov (1937) and developed by modern workers. It is beyond the scope of this paper to review phosphate genesis, which has been ably done by Gulbrandsen (1969), Bushinski (1966), Tooms et al. (1969), Burnett (1977), Atlas (1975), and Cook (1976b). However, data on the phosphorite types of the Georgina Basin epicontinental sea are synthesized below for comparative purposes.

1. Phosphate formed in restricted and shallow to very shallow water environments ranging from subtidal to intertidal.

2. The contained faunas in different areas are very different in overall composition, and it appears that they developed independently of each other (Fleming, 1977). In this study, the geochemical data indicate that there were discernible differences in the chemistry of the waters of these depressions.

3. Outside of the restricted areas, phosphogenesis declined rapidly and ceased basinward, even though shallow open-marine conditions persisted. Figure 1 illustrates the extent of phosphogenesis[10] in a portion of the basin systematically drilled during exploration. Section A-A′ (Fig. 1) from a restricted paleodepression containing phosphorites into the open basin, illustrates a change to phosphatic siltstones and limestones with sharp tops and bottoms and a maximum known thickness of 43 m which progressively feathers and tapers out to zero.

4. Phosphogenesis was confined to a specific faunal time zone (Xystridura zone).

Of key importance is the fact that ocean water was probably near equilibrium or saturated relative to carbonate fluorapatite. That its concentration was small compared to carbonate, resulting in a dominant calcium carbonate and a subordinate apatite equilibrium, would be offset by specific local environmental conditions in terms of concentrating apatite (Gulbrandsen, 1969). These, for the deposits under study, would be the constant addition of phosphate to the water from streams (Bushinski, 1964; Youssef, 1965) into coastal lagoons and estuaries, leading to inorganic precipitation or the replacement of carbonate debris at the sediment-water interface as distinct from interstitial water. In the latter case, replacement of carbonate by apatite ceases once the pore solution becomes saturated in both phases. Without a mechanism for recirculating the pore water, complete phosphatization of carbonate could take place only where it comprises but a few percent of the sediment, as demonstrated by the studies of D'Anglejan (1968) and Manheim et al. (1975). The same limitations apply to the replacement of carbonate debris at the sediment-water interface during sedimentation unless a high concentration of phosphate is maintained in respect to $CaCO_3$.

The favored interpretation to account for the four characteristic features of the Georgina Basin phosphorites enumerated above is that there was a set of circumstances which coincided to form a phosphate "pump." These were normal sea water saturated in carbonate fluorapatite but supplemented by phosphate from coastal streams in areas of lagoons, estuaries, or more open but restricted embayments, and a rapid concentrating mechanism which could maintain a high bottom-water concentration. It is favored that the concentrating agent was a prolific phytoplankton population which on death sank and released phosphate in the oxidizing environment at the sediment-water interface. This and other hypotheses proposed as concentrating mechanisms are ably reviewed by Trudinger (1976).

It is not suggested that this model of diagenetic replacement by phosphorus of coquinas, carbonate sands, and muds at the sediment-water interface is

[10] As determined from analytical data of tens of thousands of samples.

necessarily applicable to all phosphorite types in all Georgina Basin deposits. Progressive changes can be recognized in the relative proportions of the phosphorite types and in their petrology, in the order of Duchess, Lady Annie, and the group under study in this paper, namely, D Tree, Wonarah, and Sherrin Creek. These changes coincide with progressive changes in the depositional environment and possibly changes in the mechanism of formation.

Acknowledgments

The analytical data collection was made possible by grants from Macquarie University and the Australian Research Grants Commission. Thanks are owed to the Phosphate Co-operative Company of Australia, Ltd., for fluorine analyses and to D. L. Everhart and P. W. Pritchard of the International Minerals and Chemical Development Corporation for supplying the samples, analytical data, and appropriate reports. We also thank P. J. Cook, F. de Keyser, P. J. G. Fleming, R. Gulbrandsen, and G. McClellan for their constructive criticism, acknowledging that some omissions and differences of opinion will only be resolved by further studies.

P. F. H.
SCHOOL OF EARTH SCIENCES
MACQUARIE UNIVERSITY
NORTH RYDE, N.S.W. 2113, AUSTRALIA
M. J. H.
MINERAL RESEARCH LABORATORIES
C.S.I.R.O.
DELHI ROAD
NORTH RYDE, N.S.W. 2113, AUSTRALIA
October 6, 1978

REFERENCES

Atlas, E. L., 1975, Phosphate equilibria in seawater and interstitial waters: Ph.D. dissert., Oregon State Univ., Corvallis, 154 p.

Bathurst, R. G. C., 1971, Carbonate sediments and their diagenesis: Amsterdam, Elsevier Pub. Co., 620 p.

Brown, G., 1961, The X-ray identification and crystal structure of clay minerals, 2nd ed.: London, Mineralog. Soc. (Clay Mineral Group), 544 p.

Burnett, W. C., 1977, Geochemistry and origin of phosphorite deposits from off Peru and Chile: Geol. Soc. America Bull., v. 88, p. 813–823.

Bushinski, G. I., 1964, Shallow water origin of phosphorite sediments, *in* van Straaten, L. M. U., ed., Deltaic and shallow marine deposits: Amsterdam, Elsevier Pub. Co., p. 62–70.

—— 1966, The origin of marine phosphorites: Lithology and Mineral Resources, v. 3, p. 292–311. (Translation of Lithologiya i Poleznye Iskopaemye).

Chappell, B. W., Compston, W., Arriens, P. A., and Vernon, M. J., 1969, Rubidium and strontium determinations by X-ray spectrometry and isotope dilution below the part per million level: Geochim. et Cosmochim. Acta, v. 33, p. 1002–1006.

Conover, W. J., 1971, Practical nonparametric statistics: New York, John Wiley and Sons, 462 p.

Cook, P. J., 1972, Petrology and geochemistry of the phosphate deposits of northwest Queensland, Australia: ECON. GEOL., v. 67, p. 1193–1213.

—— 1976a, Georgina Basin phosphatic province, Queensland and Northern Territory—Regional geology, *in* Knight, C. L., ed., Economic geology of Australia and Papua New Guinea: Australasian Inst. Mining Metallurgy Mon. 5, v. 4, p. 245–250.

—— 1976b, Sedimentary phosphate deposits, *in* Wolf, K. H., ed., Handbook of stratabound and stratiform ore deposits: Amsterdam, Elsevier Pub. Co., v. 7, p. 505–535.

D'Anglejan, B. F., 1968, Phosphate diagenesis of carbonate sediments as a mode of *in situ* formation of marine phosphorites: Observations in a core from the Eastern Pacific: Canadian Jour. Earth Sci., v. 5, p. 81–87.

de Keyser, F., 1968, The Cambrian of the Burke River Outlier: Australia Bur. Mineral Resources, Geology Geophysics, Rec. 1968/67 (unpub.).

—— 1969, On the genesis of the Georgina Basin phosphorites, northwest Queensland: Australia Bur. Mineral Resources, Geology Geophysics, Rec. 1969/79 (unpub.), 20 p.

—— 1973, A review of the Middle Cambrian stratigraphy in the Queensland portion of the Georgina Basin: Australia Bur. Mineral Resources, Geology Geophysics Bull., v. 139, p. 13–28.

de Keyser, F., and Cook, P. J., 1972, The geology of the Middle Cambrian phosphorites and associated sediments of north-west Queensland: Australia Bur. Mineral Resources, Geology Geophysics Bull. 138, 79 p.

Fenner, P., and Hagner, A. F., 1967, Correlation of variations in trace element and mineralogy of Esopus Formation, Kingston, New York: Geochim. et Cosmochim. Acta, v. 31, p. 237–261.

Fleming, P. J. G., 1974, Origin of some Cambrian bedded cherts, and other aspects of silicification in the Georgina Basin, Queensland: Queensland Geol. Survey Pubs., v. 358, 9 p.

—— 1977, Faunas, lithologies, and the origin of phosphorites in parts of the Middle Cambrian Beetle Creek Formation of Northwest Queensland: Queensland Geol. Survey Pubs., v. 364, 21 p.

Gulbrandsen, R. A., 1966, Chemical composition of phosphorites of the Phosphoria Formation: Geochem. et Cosmochim. Acta, v. 30, p. 769–778.

—— 1967, Some compositional features of phosphorites of the Phosphoria Formation, *in* Hale L. A., ed., Anatomy of the Western Phosphate Field: Intermountain Assoc. Geol., 15th Field Conf., p. 99–102.

—— 1969, Physical and chemical factors in the formation of marine apatite: ECON. GEOL., v. 64, p. 365–382.

Howard, P. F., 1971, The discovery of phosphorites in northern Australia: Soc. Mining Engineers AIME Trans., v. 250, p. 269–275.

—— 1972, Exploration for phosphorite in Australia—a case history: ECON. GEOL., v. 67, p. 1180–1292.

Howard, P. F., and Cooney, A. M., 1976, D Tree phosphate deposit, Georgina Basin, Queensland, *in* Knight, C. L., ed., Economic geology of Australia and Papua New Guinea: Australasian Inst. Mining Metallurgy Mon. 5, v. 4, p. 265–273.

Howard, P. F., and Perrino, F. A., 1976, Wonarah phosphate deposit, Georgina Basin, Northern Territory, *in* Knight, C. L., ed., Economic geology of Australia and Papua New Guinea: Australasian Inst. Mining Metallurgy Mon. 5, v. 4, p. 273–277.

Kazakov, A. V., 1937, The phosphorite facies and the genesis of phosphorites, *in* Geological investigations of agricultural ores: Sci. Inst. Fertilizers and Insectofungicides Trans., no. 142, p. 95–113. (Published for the 17th Internat. Geol. Cong., Leningrad).

Manheim, F., Rowe, G. T., and Jipa, D., 1975, Marine phosphorite formation off Peru: Jour. Sed. Petrology, v. 45, p. 243–251.

McArthur, J. M., 1978, Systematic variations in the contents of Na, Sr, CO_3, and SO_4 in marine carbonate-fluorapatite and their relation to weathering: Chem. Geology, v. 21, p. 89–112.

McClellan, G. H., and Lehr, J. R., 1969, Crystal chemical investigation of natural apatites: Am. Mineralogist, v. 54 p. 1374–1391.

McConnell, D., 1973, Apatite, its crystal chemistry, mineralogy, utilization, and geologic and biologic occurrences: New York, Springer-Verlag, 111 p.

McKelvey, V. E., 1956, Uranium in phosphate rock: U. S. Geol. Survey Prof. Paper 300, p. 477.

Norrish, K., 1975, Geochemistry and mineralogy of trace elements, *in* Nicholas, D. J. G., and Egens, A. R., Trace elements in soil-plant-animal system: New York, Academic Press, p. 55–81.

Norrish, K., and Chappell, B. W., 1967, X-ray fluorescence spectrography, *in* Zussman, J., Physical methods of determinative Mineralogy: New York, Academic Press, p. 161–214.

Norrish, K., and Hutton, J. T., 1969, An accurate X-ray spectrographic method for the analysis of a wide range of geological samples: Geochim. et Cosmochim. Acta, v. 33, p. 431–453.

Rankama, K., and Sahama, Th. G., 1950, Geochemistry: Chicago, Univ. of Chicago Press, 912 p.

Rogers, J. K., and Keevers, R. E., 1976, Lady Annie—Lady Jane phosphate deposits, Georgina Basin, Queensland, *in* Knight, C. L., ed., Economic geology of Australia and Papua New Guinea: Australasian Inst. Mining Metallurgy Mon. 5, v. 4, p. 251–265.

Russell, R. T., 1967, Discovery of major phosphate deposits in northwest Queensland: Queensland Govt. Mining Jour., v. 68, p. 153–157.

Russell, R. T., and Trueman, N. A., 1971, The geology of the Duchess phosphate deposits, northwestern Queensland, Australia: Econ. Geol., v. 66, p. 1186–1214.

Selley, R. C., 1976, An introduction to sedimentology: London, Academic Press, 408 p.

Smith, J. P., and Lehr, J., 1966, An X-ray investigation of carbonate apatites: Jour. Agr. Food Chemistry, v. 14, p. 342–349.

Thomson, L. D., and Russell, R. T., 1971, Discovery, exploration and investigations of phosphate deposits in Queensland: Australasian Inst. Mining Metallurgy Proc., no. 240, p. 1–14.

Thorez, J., 1975, Phyllosilicates and clay minerals: a laboratory handbook for their X-ray diffraction analysis: Dison, Belgium, Lelotte, 579 p.

Till, R., 1974, Statistical methods for the earth scientist: London, McMillan, 154 p.

Tooms, J. S., Summerhayes, C. P., and Cronan, D. S., 1969, Geochemistry of marine phosphate and manganese deposits: Oceanography Marine Biology Ann. Rev. [London], v. 7, p. 49–100.

Trudinger, P. A., 1976, Microbiological processes in relation to ore genesis, *in* Wolf, K. H., Handbook of stratabound and stratiform ore deposits, v. 1, Principles and general studies: Amsterdam, Elsevier Pub. Co., p. 135–190.

Wedepohl, K. H., 1969, Handbook of geochemistry: Berlin, Springer-Verlag.

Youssef, M. I., 1965, Genesis of bedded phosphates: Econ. Geol., v. 60, p. 590–600.